



Nonlinear impairments aware resource allocation for cognitive satellite systems

Arthur Louchart

► To cite this version:

Arthur Louchart. Nonlinear impairments aware resource allocation for cognitive satellite systems. Information Theory [math.IT]. Institut Polytechnique de Paris, 2021. English. NNT : 2021IPPAT031 . tel-03485181

HAL Id: tel-03485181

<https://theses.hal.science/tel-03485181>

Submitted on 17 Dec 2021

HAL is a multi-disciplinary open access archive for the deposit and dissemination of scientific research documents, whether they are published or not. The documents may come from teaching and research institutions in France or abroad, or from public or private research centers.

L'archive ouverte pluridisciplinaire **HAL**, est destinée au dépôt et à la diffusion de documents scientifiques de niveau recherche, publiés ou non, émanant des établissements d'enseignement et de recherche français ou étrangers, des laboratoires publics ou privés.



INSTITUT
POLYTECHNIQUE
DE PARIS



Nonlinear impairments aware resource allocation for cognitive satellite systems

Thèse de doctorat de l'Institut Polytechnique de Paris
préparée à Télécom Paris

École doctorale n°626 École doctorale de l'Institut Polytechnique de Paris (EDIPP)
Spécialité de doctorat : Information, communications, électronique

Thèse présentée et soutenue à Palaiseau, le 7 décembre 2021, par

ARTHUR LOUCHART

Composition du Jury :

Jean-Marie Gorce Professeur des universités, INSA Lyon	Président
Arsenia Chorti Professeure des universités, ENSEA Cergy	Rapporteur
Philippe Mary Maître de conférences, INSA Rennes	Rapporteur
Karine Amis Professeure, IMT Atlantique	Examineur
Marios Kountouris Professeur, EURECOM	Examineur
Philippe Ciblat Professeur, Télécom Paris	Directeur de thèse
Charly Poulliat Professeur des universités, Toulouse INP-ENSEEIH	Co-directeur de thèse
Jean-Baptiste Dupé Docteur, Thales Alenia Space	Invité

Remerciements

Ces premiers propos tendent à remercier toutes les personnes qui ont participé à l'aboutissement de ce manuscrit de thèse, tout en clôturant cette belle période de doctorant, qui, soit dit en passant, fût parsemée d'incertitude par la pandémie.

En premier lieu, je tiens à remercier mon directeur de thèse Philippe Ciblat. Son ouverture d'esprit, ses grandes connaissances ainsi que son habilité à débloquent les situations ont grandement aidé à l'avancement de mes travaux de recherche, surtout lors de ces périodes de confinement si difficile. Je remercie aussi mon co-directeur de thèse Charly Poulliat pour son regard extérieur et expert, mais aussi pour sa grande disponibilité dans les moments importants, notamment lors de l'application de la méthode *Agile* pour la rédaction du manuscrit.

Je souhaite ensuite remercier les membres de mon jury de thèse, en commençant par Jean-Marie Gorce qui a présidé ma soutenance, Arsenia Chorti et Philippe Mary pour la dure tâche de relecture, et enfin Karine Amis et Marios Kountouris pour leur travail d'examen. Je remercie aussi Jean-Baptiste Dupé qui a accepté l'invitation à participer au jury de thèse.

Mes derniers remerciements vont à ma famille et mes amis. Leurs présences ont été une source de réussite pour mes travaux de recherche. Je renouvelle l'expression de mes sentiments envers ma compagne Morgane ; son inébranlable support, sa douceur et ses petites attentions ont bonifié les heures passées à ne pas écrire ce manuscrit, et de facto, contribué à ma réussite.

Résumé

Les communications par satellite sont une technologie prometteuse pour la connectivité omniprésente, étant donné la demande croissante des débits de données due aux nouvelles applications et aux nouveaux services. Les normes de communication par satellite existantes, telles que DVB-S2X et sa liaison retour DVB-RCS2, peuvent déjà fournir des débits de données élevés. Néanmoins, de nouveaux services et applications sont envisagés, tels que les communications par satellite à haut débit de nouvelle génération, l'internet des objets (IoT) et les communications de machine à machine (M2M). Compte tenu du manque de techniques à fort impact pour augmenter les débits de données et de la rareté croissante du spectre, une stratégie pour améliorer les débits de données consiste à occuper une bande passante supplémentaire, ce qui entraîne un partage du spectre sous licence avec d'autres systèmes. En effet, la majorité des systèmes existants utilisent des bandes de fréquences exclusives qui ne sont pas partagées avec d'autres entités. C'est pourquoi la *World Radiocommunication Conference* (WRC) et des organisations similaires comme l'*European Telecommunications Standards Institute* (ETSI) et l'*International Telecommunication Union-Radiocommunication* (ITU-R) ont validé l'utilisation de nouvelles fréquences telles que 17.7-19.7 GHz (liaison descendante par satellite) et 27.5-29.5 GHz (liaison montante par satellite). Cependant, ces fréquences sont déjà occupées par les systèmes terrestres en place, appelés *Fixed Service* (FS) et les systèmes par satellite doivent coexister avec eux de manière cognitive.

L'objectif de cette thèse est de se concentrer sur la liaison montante du satellite, afin de fournir de nouvelles solutions pour étendre le débit de données, en utilisant une bande passante supplémentaire non exclusive de 2 GHz autour des fréquences 28 GHz, déjà utilisées par les systèmes terrestres. **Cet objectif conduit à la proposition de techniques d'allocation de ressources pour un système cognitif satellitaire de type sous-couche.** Dans le paradigme de la radio cognitive de type sous-couche, les utilisateurs cognitifs doivent s'assurer que l'impact des interférences sur le système primaire en place ne dépasse pas les limites réglementaires d'interférence. Dans cette thèse, les utilisateurs primaires sont le réseau terrestre en place (appelé FS) et les utilisateurs secondaires sont les terminaux satellitaires, appelés *Fixed-Satellite Service* (FSS). **Le problème abordé dans cette thèse est l'allocation des ressources (puissance et sous-bande) afin de satisfaire les contraintes de la radio cognitive.** Les travaux proposés dans cette thèse couvrent cette problématique de liaison montante et permettent d'encourager le déploiement massif de terminaux cognitifs dans la bande 28 GHz. Plus précisément, la thèse se concentrera sur le scénario de liaison montante suivant.

Nous considérons un système de communication par satellite cognitif avec un opérateur et

plusieurs terminaux satellitaires, avec des schémas d'accès orthogonaux et une réutilisation de fréquence à une seule couleur (c'est-à-dire en utilisant toute la bande de fréquence de 2 GHz pour chaque faisceau). Les terminaux satellitaires transmettent des données sur la liaison montante et interfèrent avec les récepteurs primaires terrestres voisins, car les lobes secondaires des antennes des terminaux ne peuvent pas être négligés. Il est à noter qu'à l'intérieur d'un faisceau, les terminaux utilisent un schéma orthogonal basé sur *Multi-Frequency Time-Division Multiple Access* (MF-TDMA), comme dans la norme DVB-RCS2.

Dans ce scénario, le système de communication cognitif par satellite doit adapter sa puissance de transmission et l'allocation des sous-bandes, pour optimiser une fonction objective spécifique (par exemple, le débit, l'équité, ...), tout en satisfaisant les contraintes d'interférence concernant les systèmes primaires. Comme mentionné ci-dessus, le but de cette thèse est d'améliorer le débit des utilisateurs secondaires tout en limitant les interférences causées aux utilisateurs primaires. En général, l'allocation des sous-bandes et des puissances est entreprise, afin de limiter les interférences avec les utilisateurs primaires.

En outre, les *High-Power Amplifier* (HPA) à large bande sont utilisés à bord des satellites en raison des contraintes de puissance/masse, et une multitude de sous-bandes (ou porteuses) sont amplifiées conjointement par un HPA. Le HPA est intrinsèquement non linéaire et l'amplification de plusieurs sous-bandes provoque des distorsions dans la bande et hors de la bande. Cela réduit le *Signal-to-Interference-plus-Noise Ratio* (SINR) de la sous-bande, ce qui entraîne une baisse du débit.

Un back-off plus élevé ou un espacement plus important entre les sous-bandes sont nécessaires pour réduire les distorsions susmentionnées, ce qui entraîne une efficacité spectrale et un rendement moins bons. Ainsi, la prise en compte du HPA ajoute des sources supplémentaires de complexité, lorsqu'on cherche à optimiser la conception du système. L'allocation traditionnelle des ressources, basée sur des canaux d'interférence linéaires, peut ne pas convenir à de tels canaux d'interférence non linéaires, ce qui nécessite une étude plus approfondie. Le principal défi de cet exercice comprend l'évaluation des effets non linéaires sur le débit des utilisateurs, lorsque le HPA est modélisé par des séries de Volterra.

Par conséquent, l'objectif principal de la thèse est d'effectuer l'allocation des ressources (puissance et sous-bande) afin de maximiser le débit total du système (ou d'autres fonctions objectives pertinentes), tout en satisfaisant les limites d'interférence concernant les systèmes primaires, en prenant en compte les dégradations non linéaires dues aux composants du satellite modélisés par des séries de Volterra.

Cette thèse est composée de six chapitres. Les principales contributions sont présentées dans les chapitres 3, 4, 5 et 6, tandis que le chapitre 1 présente le contexte de la recherche et le chapitre 2 donne un aperçu des outils d'optimisation utilisés tout au long de la thèse.

Dans le chapitre 1, nous avons présenté le modèle de notre système de communication par satellite, de l'utilisateur terrestre jusqu'à la passerelle, en passant par le satellite. Nous avons décrit également le réseau primaire et la contrainte d'interférence associée, que le réseau satellitaire cognitif ne doit surtout pas dépasser. Ensuite, le problème général d'optimisation a été énoncé et nous avons ouvert la discussion concernant les objectifs de la thèse.

Dans le chapitre 2, nous avons introduit le concept d'optimisation convexe et donné des

méthodes conventionnelles de programmation non linéaire pour résoudre les problèmes non convexes. Nous nous sommes concentrés également sur une branche de l'optimisation, appelée *Geometric Programming* (GP) et son extension non-convexe *Signomial Programming* (SP). En particulier, nous avons présenté une méthode générique pour résoudre le problème non convexe SP. Les outils présentés dans ce chapitre ont largement été utilisés dans les chapitres suivants, qui traitent des problèmes d'allocation de ressources.

Dans le chapitre 3, nous avons abordé le problème d'optimisation avec l'hypothèse d'un HPA linéaire, en se focalisant sur l'allocation de puissance. Même si ce scénario semblait basique, les problèmes d'optimisation rencontrés ont dû tout de même prendre en compte l'interférence inter-faisceaux, conduisant à des problèmes non convexes. Cela nous a permis d'appliquer et de comprendre les procédures de résolution des problèmes non convexes, présentées dans le chapitre 2. Nous avons proposé également deux méthodes d'allocation pour l'attribution des sous-bandes et l'allocation de puissance.

Dans le chapitre 4, nous avons exprimé le débit de données des utilisateurs en présence d'effets non linéaires générés par le HPA, à partir de l'expression de l'information mutuelle dans le cas d'un canal non linéaire. Le HPA a été modélisé comme un polynôme sans mémoire, conduisant à des séries de Volterra. Nous avons obtenu deux expressions du débit de données des utilisateurs, liées à deux récepteurs différents. Le premier, appelé *nonlinearity-aware receiver*, exploitait les effets non linéaires comme information supplémentaire. L'autre, appelé *nonlinearity-agnostic receiver*, considérait les non-linéarités comme un bruit additionnel. Enfin, nous avons mis l'accent sur les propriétés mathématiques des expressions du débit de données.

Dans le chapitre 5, nous avons abordé le problème de l'optimisation en présence d'effets non linéaires et en utilisant le récepteur voyant les non-linéarités comme de l'interférence. Sur la base de l'expression du débit de données correspondante, nous avons montré que les problèmes rencontrés ont pu être exprimés sous forme GP ou *Complementary Geometric Programming* (CGP) et nous avons présenté une méthode de résolution utilisant les outils donnés dans le chapitre 2.

Dans le chapitre 6, nous avons considéré le problème d'optimisation en présence d'effets non linéaires et en utilisant le récepteur exploitant les non-linéarités. À partir de l'expression du débit évaluée avec ce récepteur, on a obtenu des problèmes de la forme CGP ou SP. Pour résoudre ces problèmes non convexes, nous avons présenté des méthodes de résolution utilisant les outils donnés dans le chapitre 2.

Contents

List of acronyms	11
General introduction	13
1 Problem statement	17
1.1 System model of satellite communication	18
1.2 Transmission chain of satellite communication	19
1.3 General statement of the optimization problem	21
1.4 Conclusion	23
2 Overview of optimization: from Convex to Signomial Programming	25
2.1 General statement of an optimization problem	25
2.2 Convex optimization	26
2.3 Non-convex optimization	29
2.4 Geometric programming and extensions	34
2.5 Conclusion	38
3 Cognitive satellite system resource allocation using ideal power amplifier	41
3.1 Problem formulation	42
3.2 Solution for neglected inter-beam interference	43
3.3 Extended work for subband assignment	45
3.4 Solution for the non-convex problem with successive convex approximation	49
3.5 Fairness	53
3.6 Numerical results	56
3.7 Conclusion	59
4 Closed-form expression of the data rate in presence of nonlinearities	61
4.1 Data rate expression in presence of nonlinearities	62
4.2 Closed-form expressions for the involved terms in data rate	65
4.3 Numerical results	77
4.4 Conclusion	79
5 Resource allocation for nonlinearity-agnostic receiver	81

5.1	Problem formulation	82
5.2	Solution for the maximization of the sum-rate	82
5.3	Maximization of the minimum per-user rate	85
5.4	Minimization of the sum-power	86
5.5	Numerical results	87
5.6	Conclusion	91
6	Resource allocation for nonlinearity-aware receiver	93
6.1	Problem formulation	94
6.2	Solution for the maximization of the sum-rate	94
6.3	Maximization of the minimum per-user rate	99
6.4	Minimization of the sum-power	101
6.5	Numerical results	104
6.6	Conclusion	108
	Conclusions and perspectives	111
	Bibliography	115

List of acronyms

AO	Alternating Optimization
AWGN	Additive White Gaussian Noise
CGP	Complementary Geometric Programming
CR	Cognitive Radio
DC	Difference of Concave
FDMA	Frequency-Division Multiple Access
FS	Fixed Service
FSS	Fixed-Satellite Service
GP	Geometric Programming
HPA	High-Power Amplifier
IP	Integer Programming
IPM	Interior-Point Method
KKT	Karush-Kuhn-Tucker
LDC	Logarithm of Difference of Concave
LHS	Left-Hand Side
LP	Linear Programming
MF-TDMA	Multi-Frequency Time-Division Multiple Access
RHS	Right-Hand Side
SCA	Successive Convex Approximation
SINR	Signal-to-Interference-plus-Noise Ratio
SP	Signomial Programming
SRRC	Square-Root-Raised-Cosine

General introduction

Context and objectives of the thesis

Satellite-based communication is a promising technology for ubiquitous connectivity, given the increasing demand for data rate due to new applications (3DTV/ UHDTV, broadband internet) and services (aeronautical / maritime). Existing satellite communications standards, such as DVD-S2X (and its return link DVB-RCS2), can already deliver high data rates for TV and broadband applications. Yet, new services and applications are envisioned: for instance, one can mention SES-17 and Eutelsat QUANTUM, both providing enhanced flexibility, capacity, coverage, and service quality for the highly competitive mobility market, as well as other fast growing enterprise markets. Next generation high throughput broadband satellite communications, internet of things (IoT), and machine to machine (M2M) communications are also examples. However, the majority of existing systems use exclusive spectrum bands that are not shared with other entities. With a lack of high-impact techniques to increase data rates and increasing spectrum scarcity, one proposed strategy to improve data rates is to occupy additional bandwidth, resulting in a share of licensed spectrum with other systems. Therefore *World Radiocommunication Conference*, and similar organizations like European Telecommunications Standards Institute (ETSI), and International Telecommunication Union-Radiocommunication Sector (ITU-R) have validated the use of new frequencies such as 17.7-19.7 GHz (satellite downlink) and 27.5-29.5 GHz (satellite uplink). However, these frequencies are already occupied by incumbent terrestrial systems, called *Fixed Service (FS)* systems, and the satellite-based systems must coexist with them in a cognitive manner.

The aim of this thesis is to focus on the satellite uplink in order to provide new solutions for extending the data rate by using additional non-exclusive 2 GHz bandwidth in 28 GHz, and consequently opening new areas of applications and services in satellite communications on frequencies already used by terrestrial systems. **This goal leads to the proposed resource allocation techniques for an underlay satellite cognitive systems** [1]. Indeed, the initial studies of the European Project CoRaSat showed that the cognitive underlay paradigm suits well for deployment of cognitive satellite terminals in uplink [2, 3]. These studies have shown that employing cognitive radio paradigm in satellite communications can increase the uplink system throughput. In an underlay cognitive radio, the cognitive users have to ensure that the impact of interference on the incumbent system does not exceed the regulatory interference limitations. As in [2, 4, 5], the cognitive radio principle applied in this thesis corresponds to the

case where the primary user is the incumbent terrestrial network (i.e., the FS) and the secondary users are the satellite terminals of interest, so called *Fixed-Satellite Service (FSS)*. **The issue addressed in this thesis is the allocation of resources (power and subband) in order to fulfill the cognitive radio constraints.** Within the CoRaSat project, efficient techniques have been developed for resource allocation for cognitive downlink satellite communications [3, 6, 7]. However, as it will be discussed later, cognitive uplink satellite communications still is in its infancy and some works were proposed in [3, 8]. The work proposed in this thesis covers that uplink issue and allows to encourage mass deployment of cognitive uplink terminals in 28 GHz band. More specifically, the thesis will focus on the following relevant uplink scenario.

We consider a cognitive radio network with one operator and multiple satellite terminals with orthogonal access schemes and single color frequency reuse (i.e. using the whole 2 GHz frequency band for each beam). The satellite terminals transmit data on the uplink and interfere with their neighboring incumbent terrestrial receivers since the sidelobes of the terminal can not be neglected. Note that within a beam, the terminals employ an orthogonal scheme based on *Multi-Frequency Time-Division Multiple Access (MF-TDMA)* as in DVB-RCS2 standard [3].

In that scenario, the cognitive radio satellite system has to adapt its power and the subband allocation to optimize a specific objective function (e.g. throughput, fairness, etc.) while satisfying the interference temperature constraints regarding the primary systems. As mentioned above, the aim of this thesis is to enhance the throughput of the secondary users while limiting the interference to the primary users within acceptable limits. Typically, subband and power allocation is undertaken, based on available information, to limit interference to the primary users.

Additionally, wideband *High-Power Amplifier (HPA)* are being used on-board of satellite due to power/mass constraints and a multitude of subbands (or carriers) are jointly amplified by a HPA. The HPA is intrinsically nonlinear and amplification of multiple subbands causes in-band and out-of-band distortions. This reduces the *Signal-to-Interference-plus-Noise Ratio (SINR)* of the subband leading to lower throughput and is affected by resource allocation (especially subband and power allocation).

Higher back-off or higher subband spacing are needed to reduce the aforementioned distortions, leading to poorer HPA efficiency and spectral use. Poorer HPA efficiency affects payload dimensioning due to scarce power on-board and increases operational costs of the uplink terminal, the inefficient spectral efficiency belies the cognitive paradigm. Thus including the HPA adds additional sources of complexity when aiming for optimized system design. Traditional resource allocation based on linear interference channels may not be suitable for such nonlinear interference channels leading to further investigation. The key challenge in this exercise includes the evaluation of nonlinear effects on user throughput, when the HPA is modeled by Volterra series.

Therefore, the main objective of the thesis is to perform resource allocation (power and subband) to maximize the system sum-rate (or other relevant objective functions), while satisfying the interference temperature limits regarding the primary systems, by taking into account nonlinear impairments due to satellite components modeled by Volterra series.

Outline of the manuscript and contributions

This thesis is composed of six chapters. The main contributions are presented in Chapters 3, 4, 5 and 6, while Chapter 1 presents the context of the research and Chapter 2 provides an overview of the optimization tools used throughout the thesis.

In Chapter 1, the system model of the satellite communication is presented, from the terrestrial user to the gateway, by passing through the satellite. We also describe the primary network and the relevant constraint of interference-temperature, that the cognitive satellite network has to not exceed. Then the general optimization problem is stated and finally we open the discussion regarding the goals of the thesis.

In Chapter 2, we introduce the concept of convex optimization and give conventional nonlinear programming methods to solve non-convex problems. We also focus on a branch of optimization, which is called *Geometric Programming (GP)* and its non-convex extension *Signomial Programming (SP)*. In particular, we present a generic method to solve non-convex SP problem. The tools presented in this chapter are widely used in the following chapters dealing with resource allocation problems.

In Chapter 3, we address the optimization problem with the assumption of a linear HPA focusing on power allocation. Even if this scenario seems basic, the optimization problems encountered must still take into account the inter-beam interference, leading to non-convex problems. This allows us to apply and understand the resolution procedures for non-convex problems presented in Chapter 2. We also propose two allocation methods for subband assignment and power allocation.

In Chapter 4, we express the user data rate in the presence of nonlinear effects generated by the HPA, from the expression of the mutual information in the case of a nonlinear channel. The HPA is modeled as a memoryless polynomial, leading to Volterra series. We obtain two expressions of the user data rate, related to two different receivers. The first one, called *nonlinearity-aware receiver*, exploiting the nonlinear effects as additional information. The other one, called *nonlinearity-agnostic receiver*, considering the nonlinearities as additional noise. We finally emphasize the mathematical properties of data rate expressions.

In Chapter 5, we address the optimization problem in the presence of nonlinear effects and using the nonlinearity-agnostic receiver. Based on the corresponding data rate expression, we show that the problems encountered can be expressed in GP or *Complementary Geometric Programming (CGP)* form and we present a tailored resolution method derived from the general framework as given in Chapter 2.

In Chapter 6, we consider the optimization problem in the presence of nonlinear effects and using the nonlinearity-aware receiver. From the expression of the data rate evaluated with this receiver, we obtain problems of the form CGP or SP. To solve these non-convex problems, we present tailored resolution methods derived from the general framework as given in Chapter 2.

List of publications

The research work during the thesis has produced the following publications.

Peer-reviewed journal

- J1.** A. Louchart, P. Ciblat, and C. Poulliat, "Power Allocation for Uplink Multiband Satellite Communications With Nonlinear Impairments," in *IEEE Communications Letters*, vol. 25, no. 8, pp. 2713-2717, Aug. 2021.
- J2.** A. Louchart, E. Tohidi, P. Ciblat, D. Gesbert, E. Lagunas, and C. Poulliat, "Power allocation for multi-operator and multi-beam cognitive uplink satellite systems," *To be submitted for IEEE Transactions on Cognitive Communications and Networking*.

International conference

- C1.** A. Louchart, P. Ciblat, and P. de Kerret, "Resource Optimization for Cognitive Satellite Systems with Incumbent Terrestrial Receivers," *European Signal Processing Conference (EUSIPCO)*, A Coruña, Spain, 2019, pp. 1-5.
- C2.** A. Louchart, P. Ciblat, and C. Poulliat, "Sum-capacity of Uplink Multiband Satellite Communications with Nonlinear Impairments," *IEEE International Conference on Communications (ICC)*, Montreal, Canada, 2021, pp. 1-6.
- C3.** A. Louchart, P. Ciblat, and C. Poulliat, "Power allocation in Uplink Multiband Satellite System with Nonlinearity-Aware Receiver," *IEEE Signal Processing Advances in Wireless Communications (SPAWC)*, Lucca, Italy, 2021, pp. 1-5.
- C4.** A. Louchart, P. Ciblat, and C. Poulliat, "Power Allocation for Multibeam Satellite Communications with Nonlinear Impairments," *ITG Workshop on Smart Antennas (WSA)*, Sophia Antipolis, France, 2021, pp. 1-6.

French conference

- C5.** A. Louchart, P. de Kerret, and P. Ciblat, "Allocation de ressources pour des réseaux satellitaires cognitifs," *GRETSI*, Lille, France, 2019, pp. 1-4.

Problem statement

Traditionally, most of the existing communication systems operate on exclusive spectrum bands which are not shared with other entities. Due to spectrum scarcity and the dearth of high-impact techniques to enhance data rate, a promising approach is to extend the usable spectrum by considering operation in the non-exclusive bands. In that context, *World Radiocommunication Conference*, European Telecommunications Standards Institute (ETSI), and International Telecommunication Union-Radiocommunication Sector (ITU-R) have validated the co-primary use of certain spectrum portions in the Ka-band, i.e., 27.5-29.5 GHz for the satellite uplink [9]. These frequencies are already occupied by incumbent terrestrial systems, called *Fixed Service (FS)* systems, which implies that the upcoming satellite-based systems will have to coexist with them in an underlay *Cognitive Radio (CR)* manner.

The cognitive users have thus to ensure that the impact of interference on the incumbent system does not exceed the regulatory interference limitations. In the particular instance of the satellite communication *CR* system, the primary user is the incumbent terrestrial network, i.e. the *FS*, and the secondary users are the satellite terminals of interest, so-called *Fixed-Satellite Service (FSS)* users. As in more traditional terrestrial *CR* systems, one central issue to facilitate the coexistence between the *CR* devices and the incumbent is the *power allocation* in order to fulfill the cognitive radio constraints and to increase the data rate of the secondary systems. The satellite communication *CR* systems described in Fig. 1.1 consider orthogonal access schemes within multiple beams, single color frequency reuse (i.e. all the beams use the same bandwidth) and take into account *High-Power Amplifier (HPA)* at the Geostationary (GSO) satellite side. Moreover, the created interference from satellite terminals due to antenna sidelobes can affect multiple *FS* receivers, which are not mobile.

This first chapter presents the system model and the considered transmission chain and formalizes the main optimization problem to be solved. All the notions and notations presented in this chapter constitute the foundations for the rest of this thesis.

The rest of the chapter is organized as follows. In Section 1.1, we describe the cognitive satellite communication system model. In Section 1.2, we give the mathematical writing of the transmission chain of the considered system. In Section 1.3, the main optimization problem is formulated, and the constraints of the problem are made explicit. Finally, Section 1.4 concludes this chapter.

1.1 System model of satellite communication

As in DVB-RCS2 standard for uplink satellite communication, we consider a *Multi-Frequency Time-Division Multiple Access* (MF-TDMA). It allows a group of user terminals on the Earth to communicate with the gateway (through the satellite) by means of a time-frequency resource grid. Essentially, a set of carrier frequencies is considered, each of which is divided into time-slots. For the sake of synchronization aspects, fixed-slot MF-TDMA is usually considered, where the bandwidth and duration of successive traffic slots used by a particular terminal are fixed. In this thesis, we work on the power allocation within one time-slot assuming that the subband assignment has been already fixed. We consider a frequency reuse factor between each beam equal to one. Each beam of the satellite uses the same MF-TDMA scheme synchronized between them. If not synchronized, we may add a random time but the way to write the interference power between beams will be similar and does not modify the structure of the optimization problem, just its numerical evaluation. Therefore, for the sake of simplicity, we assume perfect synchronization.

We consider a multibeam satellite system where N terrestrial users are spread over B beams using the same band, so there are $K := N/B$ users in a beam. This band is split into M subbands. In each beam, we assume a *Frequency-Division Multiple Access* (FDMA) preventing the intra-beam interference, where the number of users K is equal to the number of subband, so $M = K$. User using subband m in beam b will transmit a symbol sequence $\{a_{b,m,n}\}_n$, where n is the symbol index. All users have the same shaping filter with an impulse response of $p_T(t)$. This shaping filter $p_T(t)$ is an *Square-Root-Raised-Cosine* (SRRC) with a roll-off of 0.25. The DVB-RCS2 standard allows to use others values.

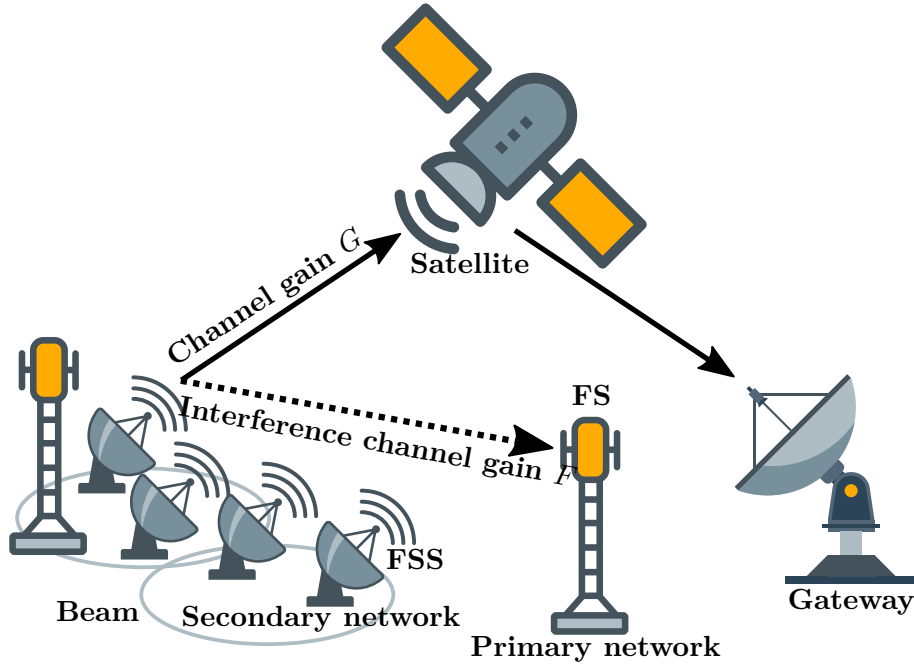


Figure 1.1: Scenario of the satellite communication system which creates interference on the primary network.

1.2 Transmission chain of satellite communication

In Fig. 1.2, we display a diagram of the transmission chain of our satellite communication system.

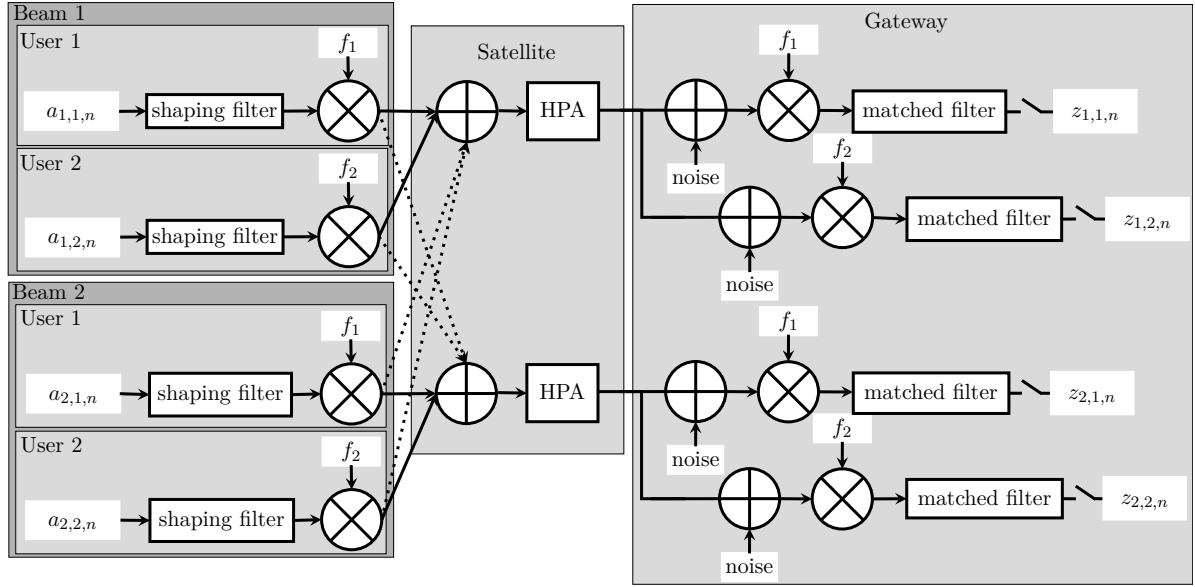


Figure 1.2: Transmission chain of our satellite communication system with $B = 2$ beams and $M = 2$ users per beam. The dotted lines represent the inter-beam interference.

The baseband signal emitted by the user belonging to beam b using subband m , denoted by $x_{b,m}(t)$, is

$$x_{b,m}(t) = \sum_{n \in \mathbb{Z}} a_{b,m,n} p_T(t - nT_s). \quad (1.1)$$

Each signal $x_{b,m}(t)$ is transposed around the frequency f_m . The difference between two adjacent frequencies is denoted ΔF .

The antenna b associated with beam b receives the sum of the M transposed signals of this beam and the inter-beam interference. This received analytic signal is denoted by $x_a^{(b)}(t)$,

$$x_a^{(b)}(t) = \sum_{m=1}^M \sqrt{G_m^{(b)}} x_{b,m}(t) e^{2i\pi f_m t} + x_{\text{IB}}^{(b)}(t), \quad (1.2)$$

where $x_{\text{IB}}^{(b)}(t)$ is the inter-beam interference,

$$x_{\text{IB}}^{(b)}(t) = \sum_{\substack{b'=1 \\ b' \neq b}}^B \sum_{m=1}^M \sqrt{G_m^{(b',b)}} x_{b',m}(t) e^{2i\pi f_m t}, \quad (1.3)$$

with

- $G_m^{(b)}$ the channel gain between user using subband m of beam b and antenna b ,
- $G_m^{(b',b)}$ the channel gain between user using subband m of beam b' and antenna b .

Let $y_a^{(b)}(t)$ be the received analytic signal at the gateway coming from the antenna b . From the received signal at the antenna b $x_a^{(b)}(t)$, the received signal at the gateway passes through a

dedicated [HPA](#) modeled as nonlinear memoryless device and an [Additive White Gaussian Noise \(AWGN\)](#) channel between the satellite and the gateway. Consequently, we get

$$y_a^{(b)}(t) = \gamma_1 x_a^{(b)}(t) + \gamma_3 x_a^{(b)}(t) \overline{x_a^{(b)}(t)} + w_a(t), \quad (1.4)$$

where $\overline{\cdot}$ stands for the complex-conjugate, and $w_a(t)$ is a complex-valued circularly-symmetric zero-mean [AWGN](#) with variance \mathcal{P}_W . The coefficients γ_1 and γ_3 are positive parameters and characterize the nonlinear distortion of the [HPA](#) [10]. Notice that the input-output relationship of the [HPA](#) is expressed as a power series truncated at third order, which is commonly used in satellite communication context [10, 11]. Moreover, we assume a perfect link between the satellite and the gateway, because the downlink uses a different frequency and involves broadcast to a single gateway.

Let us now consider the demodulation for user belonging to beam b using subband m . We first go back in baseband,

$$y_{b,m}(t) = y_a^{(b)}(t) e^{-2i\pi f_m t}, \quad (1.5)$$

we then apply the matched filter $p_R(t) := \overline{p_T}(-t)$,

$$z_{b,m}(t) = \int_{\mathbb{R}} p_R(\tau) y_{b,m}(t - \tau) d\tau. \quad (1.6)$$

Finally, the signal is sampled at the symbol rate T_s resulting in the sequence $z_{b,m,n}$,

$$z_{b,m,n} = z_{b,m}(nT_s). \quad (1.7)$$

To conduct the derivations of $z_{b,m,n}$, we first write $z_{b,m}(t)$ according to the symbol sequences,

$$\begin{aligned} z_{b,m}(t) = & \gamma_1 \sum_{m'=1}^M \sum_{n' \in \mathbb{Z}} \sqrt{G_{m'}^{(b)}} a_{b,m',n'} e^{2i\pi(f_{m'} - f_m)t} \int_{\mathbb{R}} p_T(t - \tau - n'T_s) p_R(\tau) e^{-2i\pi(f_{m'} - f_m)\tau} d\tau \\ & + \gamma_1 \sum_{\substack{b'=1 \\ b' \neq b}}^B \sum_{m'=1}^M \sum_{n' \in \mathbb{Z}} \sqrt{G_{m'}^{(b',b)}} a_{b',m',n'} e^{2i\pi(f_{m'} - f_m)t} \int_{\mathbb{R}} p_T(t - \tau - n'T_s) p_R(\tau) e^{-2i\pi(f_{m'} - f_m)\tau} d\tau \\ & + \gamma_3 \sum_{b_1, b_2, b_3=1}^B \sum_{m_1, m_2, m_3=1}^M \sum_{n_1, n_2, n_3 \in \mathbb{Z}} \sqrt{G_{m_1}^{(b_1,b)} G_{m_2}^{(b_2,b)} G_{m_3}^{(b_3,b)}} \\ & \times a_{b_1, m_1, n_1} a_{b_2, m_2, n_2} \overline{a_{b_3, m_3, n_3}} e^{2i\pi(f_{m_1} + f_{m_2} - f_{m_3} - f_m)t} \\ & \times \int_{\mathbb{R}} p_T(t - \tau - n_1 T_s) p_T(t - \tau - n_2 T_s) p_T(t - \tau - n_3 T_s) p_R(\tau) e^{-2i\pi(f_{m_1} + f_{m_2} - f_{m_3} - f_m)\tau} d\tau \\ & + \int_{\mathbb{R}} p_R(\tau) w_a(t - \tau) e^{-2i\pi f_m(t - \tau)} d\tau. \end{aligned} \quad (1.8)$$

Notice that the perfect synchronization between beams is assumed. This hypothesis is realistic because the beams are collocated at the satellite.

In order to simplify the writing of $z_{b,m}(t)$, two Volterra kernels of first-order and third-order respectively are introduced:

$$h_1(t_1, \ell) = \int_{\mathbb{R}} p_T(t_1 - \tau) p_R(\tau) e^{-2i\pi \ell \Delta F \tau} d\tau, \quad (1.9)$$

$$h_3(t_1, t_2, t_3, \ell) = \int_{\mathbb{R}} p_T(t_1 - \tau) p_T(t_2 - \tau) p_T(t_3 - \tau) p_R(\tau) e^{-2i\pi \ell \Delta F \tau} d\tau. \quad (1.10)$$

Therefore,

$$\begin{aligned}
z_{b,m}(t) = & \gamma_1 \sum_{m'=1}^M \sum_{n' \in \mathbb{Z}} \sqrt{G_{m'}^{(b)}} a_{b,m',n'} e^{2i\pi(m'-m)\Delta F t} h_1(t - n'T_s, m' - m) \\
& + \gamma_1 \sum_{\substack{b'=1 \\ b' \neq b}}^B \sum_{m'=1}^M \sum_{n' \in \mathbb{Z}} \sqrt{G_{m'}^{(b',b)}} a_{b',m',n'} e^{2i\pi(m'-m)\Delta F t} h_1(t - n'T_s, m' - m) \\
& + \gamma_3 \sum_{b_1, b_2, b_3=1}^B \sum_{m_1, m_2, m_3=1}^M \sum_{n_1, n_2, n_3 \in \mathbb{Z}} \sqrt{G_{m_1}^{(b_1,b)} G_{m_2}^{(b_2,b)} G_{m_3}^{(b_3,b)}} \\
& \times a_{b_1, m_1, n_1} a_{b_2, m_2, n_2} \overline{a_{b_3, m_3, n_3}} e^{2i\pi(m_1+m_2-m_3-m)\Delta F t} \\
& \times h_3(t - n_1 T_s, t - n_2 T_s, t - n_3 T_s, m_1 + m_2 - m_3 - m) \\
& + \int_{\mathbb{R}} p_R(\tau) w_a(t - \tau) e^{-2i\pi f_m(t-\tau)} d\tau.
\end{aligned} \tag{1.11}$$

Consequently, after sampling the signal $z_{b,m}(t)$ at nT_s , the term $z_{b,m,n}$ can be decomposed into four parts:

$$z_{b,m,n} = z_{b,m,n}^{(L)} + z_{b,m,n}^{(I)} + z_{b,m,n}^{(NL)} + w_{b,m,n}, \tag{1.12}$$

where $z_{b,m,n}^{(L)}$ is the part depending on the current symbol, $z_{b,m,n}^{(I)}$ the part depending linearly on the symbols $\{a_{b,m,n}\}$ except the current one, and $z_{b,m,n}^{(NL)}$ the part depending non-linearly on the symbols $\{a_{b,m,n}\}$.

As $h_1(nT_s, m)$ is equal to zero for any $n \neq 0$ or any $m \neq 0$ (orthogonality in time and frequency between users thanks to the [SRRC](#) shaping filter which fulfills the Nyquist criterion), and equal to one otherwise, we force $m' = m$ and $n' = n$ to obtain the linear part as follows

$$z_{b,m,n}^{(L)} = \gamma_1 \sqrt{G_m^{(b)}} a_{b,m,n}, \tag{1.13}$$

$$z_{b,m,n}^{(I)} = \gamma_1 \sum_{\substack{b'=1 \\ b' \neq b}}^B \sqrt{G_m^{(b',b)}} a_{b',m,n}. \tag{1.14}$$

The non-linear part takes the following form

$$\begin{aligned}
z_{b,m,n}^{(NL)} = & \gamma_3 \sum_{b_1, b_2, b_3=1}^B \sum_{m_1, m_2, m_3=1}^M \sum_{n_1, n_2, n_3 \in \mathbb{Z}} \sqrt{G_{m_1}^{(b_1,b)} G_{m_2}^{(b_2,b)} G_{m_3}^{(b_3,b)}} \\
& \times a_{b_1, m_1, n-n_1} a_{b_2, m_2, n-n_2} \overline{a_{b_3, m_3, n-n_3}} e^{2i\pi(m_1+m_2-m_3-m)\Delta F n T_s} \\
& \times h_3(n_1 T_s, n_2 T_s, n_3 T_s, m_1 + m_2 - m_3 - m).
\end{aligned} \tag{1.15}$$

Throughout the thesis, we will assume that the received samples sequence of user belonging to beam b using subband m follows (1.12)-(1.15). When we assume a perfect [HPA](#), so only linearity is considered as done in Chapter 3, we set the [HPA](#) coefficient to $\gamma_1 = 1$ and $\gamma_3 = 0$. Otherwise in Chapters 4, 5 and 6, we have $\gamma_1 \neq 1$ and $\gamma_3 \neq 0$.

1.3 General statement of the optimization problem

We consider that the satellite communication [CR](#) system adjusts its transmission strategy, i.e. its transmit power, with the goal of maximizing its own sum data rate while not causing harmful

interference to the primary services [3, 12]. The reason behind this approach is that spectrum-hungry applications for satellite communication are broadband services, which demand higher data rate. As a consequence, the main optimization problem to be solved in this thesis is the maximization of the system sum rate.

It is well-known that maximizing data rate ignores fairness among different users. Fairness objectives have been proposed in the literature to avoid such undesirable situations. Most of the works have considered fairness by focusing on maximizing the minimum per-user data rate or the sum-log data rate of the cognitive user [13, 8]. This is why the fairness between users is additionally addressed, as well as other figures of merit will be considered from time to time.

Before focusing on the cost function to maximize, we first study the constraints. First of all, we need to limit the interference power received at each terrestrial incumbent (FS) receivers. We assume L primary FS receivers. As in [3], we assume that each primary receiver works on a set of band intervals where each band interval corresponds to the set of S adjacent subbands of the satellite communication CR system. We put $T = M/S$ the number of FS subbands. For the sake of simplicity, we force T to be an integer. We define $\mathcal{S}_{m'} = \{(m' - 1)S + 1, \dots, m'S\}$ the set of FSS subbands inside the FS subband m' . On each band interval $m' \in \{1, \dots, T\}$ for each FS receiver $\ell \in \{1, \dots, L\}$, we have to satisfy the following interference-temperature constraints:

$$\sum_{b=1}^B \sum_{m \in \mathcal{S}_{m'}} F_{b,m}^{(\ell)} P_{b,m} \leq I_{th}^{(\ell)}(m'), \quad \forall \ell, m', \quad (1.16)$$

with

- $I_{th}^{(\ell)}(m')$ the interference-temperature at FS ℓ on band interval m' that the satellite communication CR system has to satisfy,
- $P_{b,m} := \mathbb{E} [|a_{b,m,n}|^2]$ the power of user belonging to beam b using subband m ,
- $F_{b,m}^{(\ell)}$ the channel gain between user belonging to beam b using subband m to FS receiver ℓ .

In addition, for each user, we have a peak power constraint, i.e.,

$$0 \leq P_{b,m} \leq P_{\max}, \quad \forall b, m, \quad (1.17)$$

where P_{\max} is the maximum transmit power.

We now move the general optimization problem corresponding to maximize the sum data rate of the whole satellite communication CR systems, while satisfying the interference-temperature and individual power constraints. So we have Problem 1.1 where $\mathbf{P} = (P_{b,m})_{1 \leq b \leq B, 1 \leq m \leq M}$ is the matrix formed by the transmit power of users, and $R_{b,m}$ is the data rate for user using subband m belonging to beam b .

Problem 1.1 (Main Problem).

$$\begin{aligned} \mathbf{P}^* &= \arg \max_{\mathbf{P}} \sum_{b=1}^B \sum_{m=1}^M R_{b,m} \\ \text{s.t. } & (1.16) \text{ and } (1.17). \end{aligned} \quad (1.18)$$

The way to express the data rate $R_{b,m}$ depends on the chapter, since it is based on the assumptions made about the HPA (linear or nonlinear regime), as well as on the way the nonlinear effects are treated at the receiver.

Notice that the optimal solution is seldom full power $P_{b,m} = P_{\max}$ since the interference-temperature constraints as well as the linear and nonlinear interference (of the satellite on itself) usually prevent this solution.

As we will see later, the involved functions in Problem 1.1 depend on the channel gains $G_m^{(b',b)}$ and $F_{b,m}^{(\ell)}$. From the satellite communication system side, we assume that all channel gains are known. The channel gains for links from the secondary terrestrial users to the satellite are easily available, since they depend on the user location which can be obtained through GPS and the position of the satellite which is known in advance [14, 15]. The gains for the links between the satellite terminals and the terrestrial devices can be listed into a database [3]. Nevertheless, these values may be affected by strong fading in adverse weather conditions [14]. If these events are short in time, they can be overcome using conventional higher-layer protocols like re-transmission of missing data and buffering. If the impairments last longer, this information can be updated to the network manager computing the power allocation when it is appropriate and so not so often.

1.4 Conclusion

In this chapter, we have presented the model of the satellite communication system. The transmission chain has been explained as well as the modeling of the HPA, in order to obtain the output sample sequence according to the symbols at the input of the link.

The main optimization problem has been formulated, and its constraints related to the cognitive radio paradigm have been made explicit. This problem constitutes the main thread of this thesis.

In Chapter 3, we give solutions to this problem under the assumption of a perfectly linear HPA. In Chapter 4 is devoted to the expression of the data rate in the presence of nonlinearity, then in Chapters 5 and 6 we focus on our optimization problem when the HPA generates nonlinear effects.

Overview of optimization: from Convex to Signomial Programming

In this chapter, we introduce the optimization framework which is used in next Chapters 3, 5 and 6. In particular, we present classes of non-convex problems that are currently used in the field of resource allocation for communication systems [16, 17], but also more general problems [18] that find application in our context.

The rest of the chapter is organized as follows. In Section 2.1, the general framework for optimization is presented as well as the inherent notations and definitions. In Section 2.2, the basic notions and properties on convex sets and functions are reviewed and the concepts of convex optimization problem are presented. In Section 2.3, we introduce two procedures to find a suboptimal solution of general non-convex problems, as well as two non-convex problems having a form facilitating the implementation of these procedures. In Section 2.4, we address *Geometric Programming* (GP), which is easily convertible into a convex problem, and its non-convex extensions to which we can nevertheless easily apply the non-convex resolution methods. Finally, Section 2.5 concludes this chapter. The concepts presented in this chapter are, for the most part, basic results in optimization theory that can be found in most of the standard introductory literature [19, 20, 17, 18].

2.1 General statement of an optimization problem

A general formulation for an optimization problem can be stated as follows,

Problem 2.1.

$$\begin{aligned} & \min_{\mathbf{x}} f_0(\mathbf{x}) \\ \text{s.t.} \quad & f_k(\mathbf{x}) \leq 0, \quad \forall k \in \{1, \dots, K\}, \\ & h_j(\mathbf{x}) = 0, \quad \forall j \in \{1, \dots, J\}, \end{aligned}$$

meaning that we want to find an $\mathbf{x} \in \mathbb{R}^n$ that minimizes $f_0(\mathbf{x})$ among all \mathbf{x} , while satisfying the conditions $f_k(\mathbf{x}) \leq 0$, $k \in \{1, \dots, K\}$, and $h_j(\mathbf{x}) = 0$, $j \in \{1, \dots, J\}$. The function $f_0 : \mathbb{R}^n \rightarrow \mathbb{R}$ is called *objective function* of the Problem. The functions $f_k : \mathbb{R}^n \rightarrow \mathbb{R}$, $k \in \{1, \dots, K\}$, are

called *inequality constraints*. The function $h_j : \mathbb{R}^n \rightarrow \mathbb{R}$, $j \in \{1, \dots, J\}$, are called *equality constraints*. The inequality and equality constraints form the *constraint set*. We suppose that the above mentioned functions are continuous and differentiable.

Definition 2.1. The constraint set \mathcal{F} is defined as

$$\mathcal{F} = \{\mathbf{x} \in \mathbb{R}^n \mid f_k(\mathbf{x}) \leq 0, h_j(\mathbf{x}) = 0, \quad \forall k \in \{1, \dots, K\}, \forall j \in \{1, \dots, J\}\}. \quad (2.1)$$

In the following, we omit the equality constraints because they will not be present in the considered optimization problems.

2.2 Convex optimization

In this section, we address a class of problems, called *convex problems*. From basic definitions related to convex set and convex function with illustrative examples, we state the writing of a convex optimization problem and give the optimality conditions. The convex optimization has been deeply addressed in [19].

2.2.1 Definitions of convex sets and convex functions

A set $\mathcal{C} \subseteq \mathbb{R}^n$ is said to be convex if it contains all the line segments connecting any two points in the set. Because the line connecting the points \mathbf{x}_1 and \mathbf{x}_2 can be written as $\theta\mathbf{x}_1 + (1 - \theta)\mathbf{x}_2$ for parameter $\theta \in [0, 1]$, this can be expressed mathematically as follows.

Definition 2.2. A set $\mathcal{C} \subseteq \mathbb{R}^n$ is convex if

$$\theta\mathbf{x}_1 + (1 - \theta)\mathbf{x}_2 \in \mathcal{C}, \quad \forall \mathbf{x}_1, \mathbf{x}_2 \in \mathcal{C}, \forall \theta \in [0, 1]. \quad (2.2)$$

From a geometric point of view, this definition means that the line segment between \mathbf{x}_1 and \mathbf{x}_2 is inside the set, as illustrated in Fig. 2.1.

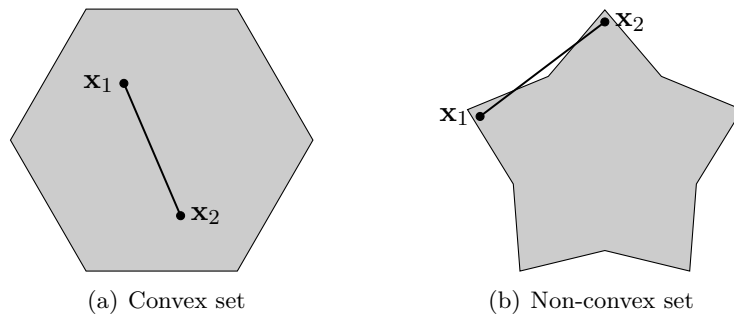


Figure 2.1: Illustration of convex and non-convex set.

It is worth noting that a discrete set is never convex (unless when it consists of a single point) because it does not satisfy Definition 2.2. Instead, the convex hull of a discrete set, denoted $\mathbf{conv} \mathcal{C}$, is by definition the smallest convex set that contains \mathcal{C} . The set $\mathcal{C} = \{0, 1, 2, 3\}$ is not convex, whereas the integer-relaxed set $\mathbf{conv} \mathcal{C} = [0, 3]$ is convex.

A function $f : \mathbb{R}^n \rightarrow \mathbb{R}$ is said to be convex if its domain $\mathbf{dom} f$ is convex, and if all the chords connecting any two points in the graph of f lies above the graph of f . This can be expressed mathematically as follows.

Definition 2.3. A function $f : \mathbb{R}^n \rightarrow \mathbb{R}$ is convex if its domain $\mathbf{dom} f$ is convex and

$$f(\theta \mathbf{x}_1 + (1 - \theta) \mathbf{x}_2) \leq \theta f(\mathbf{x}_1) + (1 - \theta) f(\mathbf{x}_2), \quad \forall \mathbf{x}_1, \mathbf{x}_2 \in \mathbb{R}^n, \forall \theta \in [0, 1]. \quad (2.3)$$

A function which is not convex is called non-convex. Conversely, if the sign of inequality in (2.3) is reversed, the function is concave. Similarly, if the function f is convex, then $-f$ is concave and if f is concave, then $-f$ is convex.

From a geometric point of view, the inequality (2.3) means that the line segment between $(\mathbf{x}_1, f(\mathbf{x}_1))$ and $(\mathbf{x}_2, f(\mathbf{x}_2))$ is above the graph of function f , illustrated in Fig. 2.2.

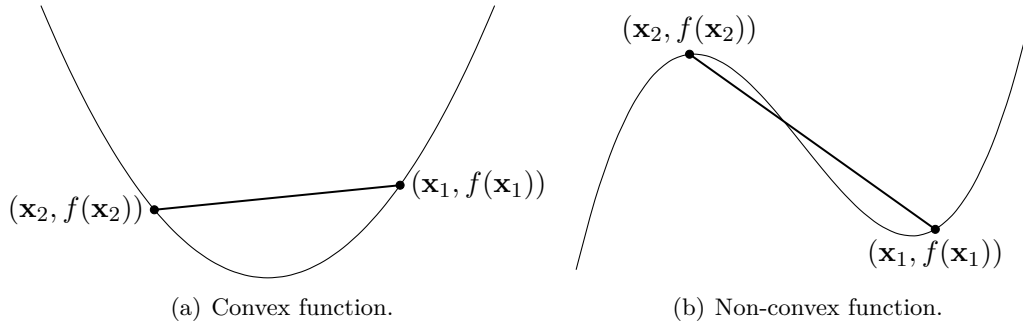


Figure 2.2: Graph of a convex and non-convex function.

Remark 2.1. An affine function f is convex and concave.

In the following, we introduce theorems that will be useful in this manuscript.

Theorem 2.1. Let $f : \mathbb{R}^n \rightarrow \mathbb{R}$ be a differentiable function. Then f is convex if and only if $\mathbf{dom} f$ is convex and

$$f(\mathbf{x}) \geq f(\mathbf{x}_i) + \nabla f(\mathbf{x}_i)^T (\mathbf{x} - \mathbf{x}_i), \quad \forall \mathbf{x}, \mathbf{x}_i \in \mathbb{R}^n. \quad (2.4)$$

The affine function $\tilde{f}(\mathbf{x}) = f(\mathbf{x}_i) + \nabla f(\mathbf{x}_i)^T (\mathbf{x} - \mathbf{x}_i)$ is the first-order Taylor approximation of f near \mathbf{x}_i . The inequality (2.4) states that for a convex function f , the first-order Taylor approximation \tilde{f} is in fact a *global underestimator* of the function f . Conversely, if the sign of inequality in (2.4) is reversed, the function is concave.

Theorem 2.2. Let $f : \mathbb{R}^n \rightarrow \mathbb{R}$ be a twice differentiable function. Then f is convex if and only if $\mathbf{dom} f$ is convex and its Hessian is positive semidefinite,

$$\mathbf{y}^T \mathbf{H}(f) \mathbf{y} \geq 0, \quad \forall \mathbf{y} \in \mathbb{R}^n, \quad (2.5)$$

where

$$\mathbf{H}_{ij}(f) = \frac{\delta^2 f}{\delta x_i \delta x_j}. \quad (2.6)$$

Theorem 2.3. If f_1, \dots, f_n are convex functions and w_1, \dots, w_n are nonnegative real coefficients, then the weighted sum of convex functions

$$f = w_1 f_1 + w_2 f_2 + \dots + w_n f_n \quad (2.7)$$

is convex.

The set of convex functions is closed under addition and positive scaling, i.e., the sum of convex functions is convex.

Theorem 2.4. If f is a convex function, then the perspective of f , denoted by $g : \mathbb{R}^{n+1} \rightarrow \mathbb{R}$ defined as

$$g(\mathbf{x}, t) = t f\left(\frac{\mathbf{x}}{t}\right), \quad t > 0, \quad (2.8)$$

is convex in (\mathbf{x}, t) .

Theorem 2.5. If $f : \mathbb{R}^n \rightarrow \mathbb{R}$ is a convex function, then the function $g : \mathbb{R}^m \rightarrow \mathbb{R}$ defined as

$$g(\mathbf{x}) = f(\mathbf{A}\mathbf{x} + \mathbf{b}), \quad \mathbf{A} \in \mathbb{R}^{n \times m}, \mathbf{b} \in \mathbb{R}^n, \quad (2.9)$$

is convex.

Theorem 2.6. Let $f : \mathbb{R}^n \rightarrow \mathbb{R}^m$ and $g : \mathbb{R}^m \rightarrow \mathbb{R}$. By denoting the composition $h = g \circ f$, then

- h is convex if g is convex and nondecreasing, and f is convex,
- h is convex if g is convex and nonincreasing, and f is concave,
- h is concave if g is concave and nondecreasing, and f is concave,
- h is concave if g is concave and nonincreasing, and f is convex.

2.2.2 Convex optimization problems

Reminding the general optimization Problem 2.1, we introduce the following definition and property.

Definition 2.4. If the objective function f_0 and the constraint set \mathcal{F} of a problem are convex, then the problem is a convex optimization problem.

Property 2.1. If the functions $f_k : \mathbb{R}^n \rightarrow \mathbb{R}$ constituting the constraint set \mathcal{F} are convex, then the constraint set \mathcal{F} is convex.

Arising from the two above mentioned definition and property, a convex optimization problem is one of the form

Problem 2.2.

$$\begin{aligned} & \min_{\mathbf{x}} f_0(\mathbf{x}) \\ \text{s.t.} \quad & f_k(\mathbf{x}) \leq 0, \quad \forall k \in \{1, \dots, K\}, \end{aligned}$$

where $f_k, k \in \{0, K\}$, are convex.

The following problem also boils down to a convex optimization problem,

Problem 2.3.

$$\begin{aligned} & \max_{\mathbf{x}} f_0(\mathbf{x}) \\ \text{s.t.} \quad & f_k(\mathbf{x}) \leq 0, \quad \forall k \in \{1, \dots, K\}, \end{aligned}$$

where the objective function f_0 is concave and the functions f_k , $k \in \{1, \dots, K\}$, are convex.

A fundamental property of convex optimization problems is the following,

Property 2.2. Any locally optimal point of a convex optimization problem is globally optimal.

Conditions for optimality

In order to find the optimal solution \mathbf{x}^* of a convex optimization problem, the so-called *Karush-Kuhn-Tucker* (KKT) conditions are necessary and sufficient. The KKT conditions associated to the Problem 2.2, assuming that the functions f_k are differentiable, $k \in \{0, \dots, K\}$, are

$$\nabla f_0(\mathbf{x}^*) + \sum_{k=1}^K \lambda_k^* \nabla f_k(\mathbf{x}^*) = 0, \quad (2.10)$$

$$f_k(\mathbf{x}^*) \leq 0, \quad \forall k \in \{1, \dots, K\}, \quad (2.11)$$

$$\lambda_k^* \geq 0, \quad \forall k \in \{1, \dots, K\}, \quad (2.12)$$

$$\lambda_k^* f_k(\mathbf{x}^*) = 0, \quad \forall k \in \{1, \dots, K\}, \quad (2.13)$$

where \mathbf{x}^* is the optimal solution of Problem 2.2 and λ_k^* , $k \in \{1, \dots, K\}$, is the non-negative optimal value of the Lagrangian multiplier associated to constraint $f_k(\mathbf{x}) \leq 0$. The set of equalities (2.13) are called *complementary slackness conditions*.

Solving the KKT conditions consists in finding the optimal solution \mathbf{x}^* and the optimal Lagrangian multipliers λ_k^* , $k \in \{1, \dots, K\}$, which simultaneously satisfy (2.10)-(2.13). The difficulty lies in solving the KKT conditions, which can be done in two ways, namely,

- Using analytical methods, which are dependent on the writing of the problem. When the KKT conditions are written in a function of a single Lagrangian multiplier, the problem is then considered to be solved analytically.
- Using numerical procedures, which are more complex but independent of the writing of the problem. These procedures use the *Interior-Point Method* (IPM) and its variants [21], as well as Newton's method to solve numerically the KKT conditions.

Notice that the analytical methods are preferred, but sometimes they are not possible. In this case, numerical procedures are used to solve the problem.

2.3 Non-convex optimization

When the general Problem 2.1 is non-convex, i.e., the objective function is non-convex or the constraint set is non-convex, the optimal solution of the problem becomes complex to determine.

Indeed, the [KKT](#) conditions are no longer sufficient to guarantee a global minimum. The search for the optimal solution is then of exponential complexity. In this section, we introduce two procedures for finding a local optimum of a non-convex problem with affordable complexity [\[22, 23\]](#).

2.3.1 Alternating optimization

The following notation is used for a possibly non-convex problem,

Problem 2.4.

$$\begin{aligned} & \min_{\mathbf{x}_1, \dots, \mathbf{x}_T} h_0(\mathbf{x}_1, \dots, \mathbf{x}_T) \\ \text{s.t.} \quad & h_k(\mathbf{x}_1, \dots, \mathbf{x}_T) \leq 0, \quad \forall k \in \{1, \dots, K\}. \end{aligned}$$

The [Alternating Optimization \(AO\)](#) method is an iterative procedure. For a given iteration, there is T steps since only one variable \mathbf{x}_t , $t \in \{1, \dots, T\}$ is considered in the problem, the others being fixed. Then we solve the following problem,

Problem 2.5. At iteration i , for a given $t \in \{1, \dots, T\}$,

$$\begin{aligned} \mathbf{x}_t^{*,(i)} &= \arg \min_{\mathbf{x}_t} h_0(\mathbf{x}_1^{(i)}, \dots, \mathbf{x}_{t-1}^{(i)}, \mathbf{x}_t, \mathbf{x}_{t+1}^{(i-1)}, \dots, \mathbf{x}_T^{(i-1)}) \\ \text{s.t.} \quad & h_k(\mathbf{x}_1^{(i)}, \dots, \mathbf{x}_{t-1}^{(i)}, \mathbf{x}_t, \mathbf{x}_{t+1}^{(i-1)}, \dots, \mathbf{x}_T^{(i-1)}) \leq 0, \quad \forall k \in \{1, \dots, K\}. \end{aligned}$$

The alternating optimization method is interesting when the optimal solving of Problem 2.5 is easier than finding the optimal solution of Problem 2.4. The [AO](#) procedure depicted in Algorithm 2.1 converges towards a stationary point [\[23\]](#). Notice that the obtained solution is suboptimal and determining a feasible initial solution of Problem 2.4 can be difficult.

Algorithm 2.1 [AO](#) based procedure for solving Problem 2.4

```

1: Set  $\epsilon > 0$ ,  $E = \epsilon + 1$ ,  $i = 0$ 
2: Find  $(\mathbf{x}_1^{(0)}, \dots, \mathbf{x}_T^{(0)})$  a feasible solution of Problem 2.4
3: while  $E > \epsilon$  do
4:    $i = i + 1$ 
5:   for  $t = 1, \dots, T$  do
6:     Find  $\mathbf{x}_t^{*,(i)}$  the optimal solution of Problem 2.5
7:     Set  $\mathbf{x}_t^{(i)} = \mathbf{x}_t^{*,(i)}$ 
8:   end for
9:   Compute the Euclidean distance  $E = \left\| [\mathbf{x}_1^{(i)}, \dots, \mathbf{x}_T^{(i)}] - [\mathbf{x}_1^{(i-1)}, \dots, \mathbf{x}_T^{(i-1)}] \right\|_2$ 
10: end while
11: return  $(\mathbf{x}_1^*, \dots, \mathbf{x}_T^*) = (\mathbf{x}_1^{(i)}, \dots, \mathbf{x}_T^{(i)})$ 

```

2.3.2 Successive convex approximation

The [Successive Convex Approximation \(SCA\)](#) method is an iterative procedure to solve the [KKT](#) conditions for non-convex problems. For a given iteration, the non-convex functions of the problem are approximated by convex functions around a feasible point. The resulting problem is

naturally convex and optimally solved. The resulting optimal solution then acts as a feasible point for the next iteration.

The following notation is used for a non-convex problem,

Problem 2.6.

$$\begin{aligned} & \min_{\mathbf{x}} h_0(\mathbf{x}) \\ \text{s.t.} \quad & h_k(\mathbf{x}) \leq 0, \quad \forall k \in \{1, \dots, K\}. \end{aligned}$$

The functions $h_k(\mathbf{x})$, $k \in \{0, \dots, K\}$, are supposed to be continuous and differentiable. At iteration i , the resulting convex optimization problem is the following.

Problem 2.7. *At iteration i ,*

$$\begin{aligned} \mathbf{x}_i^* &= \min_{\mathbf{x}} \tilde{h}_0^{(i-1)}(\mathbf{x}) \\ \text{s.t.} \quad & \tilde{h}_k^{(i-1)}(\mathbf{x}) \leq 0, \quad \forall k \in \{1, \dots, K\}, \end{aligned}$$

where $\tilde{h}_k^{(i-1)}(\mathbf{x})$, $k \in \{0, \dots, K\}$, is the convex approximation of $h_k(\mathbf{x})$ around the point \mathbf{x}_{i-1} .

The [SCA](#) procedure converges toward a local optimum if the convex approximation satisfies the following conditions [\[22\]](#).

Hypothesis 2.1. *The convex approximation $\tilde{h}_k^{(i)}(\mathbf{x})$, $k \in \{0, \dots, K\}$, of $h_k(\mathbf{x})$ around the point \mathbf{x}_i satisfies the [SCA](#) conditions if*

- $\tilde{h}_k^{(i)}(\mathbf{x}) \geq h_k(\mathbf{x})$, the convex approximation upper-bound the non-convex function,
- $\tilde{h}_k^{(i)}(\mathbf{x}_i) = h_k(\mathbf{x}_i)$, the convex approximation is locally tight,
- $\nabla \tilde{h}_k^{(i)}(\mathbf{x}_i) = \nabla h_k(\mathbf{x}_i)$, the gradient of the convex approximation is consistent with the gradient of the non-convex function.

The difficulty of the [SCA](#) procedure lies in writing an approximation that respects the conditions mentioned above. The [SCA](#) procedure depicted in [Algorithm 2.2](#) converges towards a local optimum. Notice that determining a feasible initial solution of [Problem 2.6](#) can be difficult.

Algorithm 2.2 [SCA](#) based procedure for solving [Problem 2.6](#)

- 1: Set $\epsilon > 0$, $E = \epsilon + 1$, $i = 0$
 - 2: Find \mathbf{x}_0 a feasible solution of [Problem 2.4](#)
 - 3: **while** $E > \epsilon$ **do**
 - 4: $i = i + 1$
 - 5: Compute the convex approximation $\tilde{h}_k^{(i-1)}(\mathbf{x})$ around the point \mathbf{x}_{i-1}
 - 6: Find $\mathbf{x}_i^{*,(i)}$ the optimal solution of [Problem 2.7](#)
 - 7: Compute the Euclidean distance $E = \|\mathbf{x}_i - \mathbf{x}_{i-1}\|_2$
 - 8: **end while**
 - 9: **return** $\mathbf{x}^* = \mathbf{x}_i$
-

2.3.3 Difference of concave

In some applications, the objective function of a non-convex problem can be explicitly written as a *Difference of Concave* (DC) functions. In that case, the writing of the convex approximation is closed-form, allowing a straightforward application of the SCA procedure to find a local optimum.

The general problem of the maximization of a DC can be written as follows,

Problem 2.8.

$$\begin{aligned} & \max_{\mathbf{x}} f(\mathbf{x}) - g(\mathbf{x}) \\ \text{s.t.} \quad & f_k(\mathbf{x}) \leq 0, \quad \forall k \in \{1, \dots, K\}, \end{aligned}$$

where $f(\mathbf{x})$ and $g(\mathbf{x})$ are concave function, whereas $f_k(\mathbf{x})$, $k \in \{1, \dots, K\}$, are convex functions.

This type of problem can be handled by the SCA method. As previously discuss in Section 2.3.2, the difficulty lies in the writing of a concave approximation of the objective function. We denote by h the difference of concave functions, which has to be approximated, as follows,

$$h(\mathbf{x}) = f(\mathbf{x}) - g(\mathbf{x}). \quad (2.14)$$

Theorem 2.7. If $h(\mathbf{x}) = f(\mathbf{x}) - g(\mathbf{x})$ is a difference of concave functions, then

$$\tilde{h}^{(i)}(\mathbf{x}) = f(\mathbf{x}) - \tilde{g}^{(i)}(\mathbf{x}), \quad (2.15)$$

is the concave approximation of $h(\mathbf{x})$ around the point \mathbf{x}_i that satisfies the SCA conditions, where

$$\tilde{g}^{(i)}(\mathbf{x}) = g(\mathbf{x}_i) + \nabla g(\mathbf{x}_i)^T (\mathbf{x} - \mathbf{x}_i) \quad (2.16)$$

is the first-order Taylor approximation of $g(\mathbf{x})$.

Proof. Let us focus on the second concave function $g(\mathbf{x})$. Thanks to Theorem 2.1, we have

- $\tilde{g}^{(i)}(\mathbf{x}) \geq g(\mathbf{x})$, the Taylor approximation upper-bound the concave function,
- $\tilde{g}^{(i)}(\mathbf{x}_i) = g(\mathbf{x}_i)$, the Taylor approximation is locally tight,
- $\nabla \tilde{g}^{(i)}(\mathbf{x}_i) = \nabla g(\mathbf{x}_i)$, the gradient of the Taylor approximation is consistent,
- $\tilde{g}^{(i)}(\mathbf{x})$ is an affine function.

Since $\tilde{h}^{(i)}(\mathbf{x}) = f(\mathbf{x}) - \tilde{g}^{(i)}(\mathbf{x})$, the approximation is concave thanks to Theorem 2.3 and satisfies the SCA conditions given in Section 2.3.2, namely

- $\tilde{h}^{(i)}(\mathbf{x}) = f(\mathbf{x}) - \tilde{g}^{(i)}(\mathbf{x}) \leq f(\mathbf{x}) - g(\mathbf{x})$ and finally $\tilde{h}^{(i)}(\mathbf{x}) \leq h(\mathbf{x})$,
- $\tilde{h}^{(i)}(\mathbf{x}_i) = f(\mathbf{x}_i) - \tilde{g}^{(i)}(\mathbf{x}_i) = f(\mathbf{x}_i) - g(\mathbf{x}_i)$ and finally $\tilde{h}^{(i)}(\mathbf{x}_i) = h(\mathbf{x}_i)$,
- $\nabla \tilde{h}^{(i)}(\mathbf{x}_i) = \nabla f(\mathbf{x}_i) - \nabla \tilde{g}^{(i)}(\mathbf{x}_i) = \nabla f(\mathbf{x}_i) - \nabla g(\mathbf{x}_i)$ and finally $\nabla \tilde{h}^{(i)}(\mathbf{x}_i) = \nabla h(\mathbf{x}_i)$. \square

By replacing $g(\mathbf{x})$ with $\tilde{g}^{(i)}(\mathbf{x})$ in Problem 2.8, the resulting optimization problem is

Problem 2.9.

$$\begin{aligned} \mathbf{x}_i^* &= \arg \max_{\mathbf{x}} f(\mathbf{x}) - \tilde{g}^{(i-1)}(\mathbf{x}) \\ \text{s.t.} \quad & f_k(\mathbf{x}) \leq 0, \quad \forall k \in \{1, \dots, K\}. \end{aligned}$$

Result 2.1. *Problem 2.9 is convex since it maximizes a concave function over a convex set.*

Since the concave approximation satisfies the [SCA](#) conditions, the [SCA](#) procedure depicted in Algorithm 2.3 converges towards a stationary point. The obtained solution is suboptimal.

Algorithm 2.3 [SCA](#) based procedure for solving [DC](#) Problem 2.8

- 1: Set $\epsilon > 0$, $E = \epsilon + 1$, $i = 0$
 - 2: Find \mathbf{x}_0 a feasible solution of Problem 2.8
 - 3: **while** $E > \epsilon$ **do**
 - 4: $i = i + 1$
 - 5: Compute the convex approximation $\tilde{h}^{(i)}(\mathbf{x})$ around the point \mathbf{x}_{i-1} , using (2.15)
 - 6: Find \mathbf{x}_i^* the optimal solution of Problem 2.9
 - 7: Compute the Euclidean distance $E = \|\mathbf{x}_i - \mathbf{x}_{i-1}\|_2$
 - 8: **end while**
 - 9: **return** $\mathbf{x}^* = \mathbf{x}_i$
-

Remark 2.2. *The presented method is also valid for a sum of [DC](#).*

2.3.4 Logarithm of difference of concave

In some applications, the objective function of a non-convex problem can be explicitly written as a [Logarithm of Difference of Concave \(LDC\)](#) functions. In that case, the writing of the convex approximation is also closed-form, allowing a straightforward application of the [SCA](#) procedure to find a local optimum.

The general problem of the maximization of the [LDC](#) can be written as follows,

Problem 2.10.

$$\begin{aligned} \max_{\mathbf{x}} & \log(f(\mathbf{x}) - g(\mathbf{x})) \\ \text{s.t.} \quad & f_k(\mathbf{x}) \leq 0, \quad \forall k \in \{1, \dots, K\}. \end{aligned}$$

Remark 2.3. *Obviously, the logarithm function can be easily removed thanks to its strict increase. However, we keep it since the presented method is also valid for a sum of [LDC](#).*

This type of problem can also be handled by the [SCA](#) method. As previously discuss in Section 2.3.2, the difficulty lies in the writing of a convex approximation of the objective function. We denote by h the difference of concave functions, which has to be approximated, as follows,

$$h(\mathbf{x}) = f(\mathbf{x}) - g(\mathbf{x}). \quad (2.17)$$

Theorem 2.8. *If $\log h(\mathbf{x}) = \log(f(\mathbf{x}) - g(\mathbf{x}))$ is a logarithm of difference of concave functions, then*

$$\log \tilde{h}^{(i)}(\mathbf{x}) = \log \left(f(\mathbf{x}) - \tilde{g}^{(i)}(\mathbf{x}) \right), \quad (2.18)$$

is the concave approximation of $\log h(\mathbf{x})$ around the point \mathbf{x}_i that satisfies the [SCA](#) conditions, where $\tilde{g}^{(i)}(\mathbf{x})$ is the first-order Taylor approximation of $g(\mathbf{x})$ given by (2.16).

Proof. We suppose that $\tilde{h}^{(i)}(\mathbf{x})$ is the concave approximation at the point \mathbf{x}_i of $h(\mathbf{x})$, a difference of concave functions, that satisfies the [SCA](#) conditions. This approximation is given by Theorem 2.7. Then $\log \tilde{h}^{(i)}(\mathbf{x})$ is concave, thanks to Theorem 2.6, and approximates $\log h(\mathbf{x})$ around the point \mathbf{x}_i while satisfying [SCA](#) conditions,

- $\log \tilde{h}^{(i)}(\mathbf{x}) \leq \log h(\mathbf{x})$, thanks to the monotonically increase of the logarithm function,
- $\log \tilde{h}^{(i)}(\mathbf{x}_i) = \log h(\mathbf{x}_i)$, thanks to the bijectivity of logarithm function,
- $\nabla \log \tilde{h}^{(i)}(\mathbf{x}_i) = \frac{\nabla \tilde{h}^{(i)}(\mathbf{x}_i)}{\tilde{h}^{(i)}(\mathbf{x}_i)} = \frac{\nabla h(\mathbf{x}_i)}{h(\mathbf{x}_i)}$, and finally $\nabla \log \tilde{h}^{(i)}(\mathbf{x}_i) = \nabla \log h(\mathbf{x}_i)$. □

By replacing $g(\mathbf{x})$ with $\tilde{g}^{(i)}(\mathbf{x})$ in Problem 2.10, the resulting optimization problem is

Problem 2.11.

$$\begin{aligned} \mathbf{x}_i^* &= \arg \max_{\mathbf{x}} \log \left(f(\mathbf{x}) - \tilde{g}^{(i-1)}(\mathbf{x}) \right) \\ \text{s.t.} \quad & f_k(\mathbf{x}) \leq 0, \quad \forall k \in \{1, \dots, K\}. \end{aligned}$$

Result 2.2. Problem 2.11 is convex since it maximizes a concave function over a convex set.

Since the convex approximation satisfies the [SCA](#) conditions, the [SCA](#) procedure depicted in Algorithm 2.4 converges towards a stationary point. The obtained solution is suboptimal.

Algorithm 2.4 [SCA](#) based procedure for solving [LDC](#) Problem 2.10

- 1: Set $\epsilon > 0$, $E = \epsilon + 1$, $i = 0$
 - 2: Find \mathbf{x}_0 a feasible solution of Problem 2.10
 - 3: **while** $E > \epsilon$ **do**
 - 4: $i = i + 1$
 - 5: Compute the convex approximation $\log \tilde{h}^{(i)}(\mathbf{x})$ around the point \mathbf{x}_{i-1} , using (2.18)
 - 6: Find \mathbf{x}_i^* the optimal solution of Problem 2.11
 - 7: Compute the Euclidean distance $E = \|\mathbf{x}_i - \mathbf{x}_{i-1}\|_2$
 - 8: **end while**
 - 9: **return** $\mathbf{x}^* = \mathbf{x}_i$
-

2.4 Geometric programming and extensions

In this section, we review a family of non-convex problems having a form that facilitates the implementation of non-convex solution methods. Starting from the definition of a [GP](#) and its natural conversion into a convex problem, we give non-convex extensions that find applications in some domains.

2.4.1 Geometric programming

In this section, we present a class of optimization problems, called **GP**, which are not convex in their natural form [20]. However, by changing variables and transforming the objective and constraint functions, it can be turned into convex optimization problems. Before giving the form of a **GP**, let us first introduce the two following definitions.

Definition 2.5. *A monomial function takes the following form,*

$$m(\mathbf{x}) = c \prod_{n=1}^N x_n^{b_n}$$

with $c \in \mathbb{R}^{+*}$ and $b_n \in \mathbb{R}$.

Monomials are closed under multiplication and division.

Definition 2.6. *A posynomial function takes the following form,*

$$p(\mathbf{x}) = \sum_{k=1}^K m_k(\mathbf{x})$$

where $\{m_k\}_{k=1,\dots,K}$ are monomial functions.

Posynomials are closed under addition, multiplication, and nonnegative scaling. If a posynomial is multiplied by a monomial, the result is a posynomial. Similarly, a posynomial can be divided by a monomial, the result is also a posynomial.

The following notation is used for **GP**,

Problem 2.12.

$$\begin{aligned} & \min_{\mathbf{x}} p_0(\mathbf{x}) \\ \text{s.t. } & p_k(\mathbf{x}) \leq 1, \quad \forall k \in \{1, \dots, K\}, \end{aligned}$$

where $\{p_k\}_{k=1,\dots,K}$ are posynomial functions.

Notice that equality constraints can be present in the Problem, written as monomial functions equal to one. We omit these equality constraints because they will not be present in the considered optimization problems. There is also an implicit constraint that the variables are positive, i.e., $x_n > 0$.

Problems in **GP** form are in general non-convex. However, they can be easily converted into convex optimization problem, by a logarithmic change of variable $y_n = \log(x_n)$ and logarithmic transformation of the objective and constraint functions.

Property 2.3. *The log-sum-exp function, $f : \mathbb{R}^n \rightarrow \mathbb{R}$, defined as*

$$f(\mathbf{x}) = \log \sum_{k=1}^n (\exp(x_k)), \quad (2.19)$$

is convex.

Combining this property of the *log-sum-exp* function and Theorem 2.5, the **GP** becomes a convex optimization problem.

2.4.2 Complementary Geometric Programming

In this section, we present the *Complementary Geometric Programming* (CGP). Note that this category is not well defined [18, 17], as the boundary between CGP and *Signomial Programming* (SP), presented in the next section, is very thin. In this thesis, we consider that a CGP is an optimization problem of the following form [18],

Problem 2.13.

$$\begin{aligned} & \min_{\mathbf{x}} \frac{p_0(\mathbf{x})}{q_0(\mathbf{x})} \\ \text{s.t. } & \frac{p_k(\mathbf{x})}{q_k(\mathbf{x})} \leq 1, \quad \forall k \in \{1, \dots, K\}, \end{aligned} \quad (2.20)$$

where $p_k(\mathbf{x})$ and $q_k(\mathbf{x})$, $k \in \{0, \dots, K\}$, are posynomial functions.

Problem 2.13 is non-convex since it involves ratios of posynomial functions in the objective function and constraint set. This type of problem can be handled by the SCA method. In order to apply this method, the goal is now to find a tight upper-bound for the ratios of posynomials, which is either directly convex or GP.

Theorem 2.9. *If $q(\mathbf{x}) := \sum_{k=1}^K m_k(\mathbf{x})$ is a posynomial function, then*

$$\tilde{q}^{(i)}(\mathbf{x}) = \prod_{k=1}^K \left(\frac{m_k(\mathbf{x})}{\delta_k} \right)^{\delta_k} \quad (2.21)$$

is the lower-bound monomial approximation of $q(\mathbf{x})$ around the point \mathbf{x}_i that satisfies the SCA conditions, where

$$\delta_k = m_k(\mathbf{x}_i)/q(\mathbf{x}_i). \quad (2.22)$$

Proof. Let us start with the comparison between arithmetic and geometric mean,

$$\sum_{k=1}^K \delta_k y_k \geq \prod_{k=1}^K y_k^{\delta_k}, \quad (2.23)$$

with $\delta_k \geq 0$ and $\sum_{k=1}^K \delta_k = 1$. Then we consider that $y_k = \frac{m_k(\mathbf{x})}{\delta_k}$ and $\delta_k = m_k(\mathbf{x}_i)/q(\mathbf{x}_i)$. Thus, we get that

- $q(\mathbf{x}) \geq \tilde{q}^{(i)}(\mathbf{x}) := \prod_{k=1}^K \left(\frac{m_k(\mathbf{x})}{\delta_k} \right)^{\delta_k}$, the monomial approximation is a lower-bound of the posynomial function,
- $\tilde{q}^{(i)}(\mathbf{x}_i) = \prod_{k=1}^K (q(\mathbf{x}_i))^{m_k(\mathbf{x}_i)/q(\mathbf{x}_i)} = (q(\mathbf{x}_i))^{\sum_{k=1}^K \frac{m_k(\mathbf{x}_i)}{q(\mathbf{x}_i)}} = q(\mathbf{x}_i)$, the monomial approximation is locally tight,
- $\nabla \log q(\mathbf{x}_i) = \frac{\sum_{k=1}^K \nabla m_k(\mathbf{x}_i)}{q(\mathbf{x}_i)}$ and $\nabla \log \tilde{q}^{(i)}(\mathbf{x}_i) = \sum_{k=1}^K \delta_k \frac{\nabla m_k(\mathbf{x}_i)}{m_k(\mathbf{x}_i)} = \frac{\sum_{k=1}^K \nabla m_k(\mathbf{x}_i)}{q(\mathbf{x}_i)}$. Therefore, we have $\nabla \log q(\mathbf{x}_i) = \nabla \log \tilde{q}^{(i)}(\mathbf{x}_i)$.

Moreover, we can show that $\nabla \log \tilde{q}^{(i)}(\mathbf{x}_i) = \frac{\nabla \tilde{q}^{(i)}(\mathbf{x}_i)}{\tilde{q}^{(i)}(\mathbf{x}_i)} = \frac{\nabla \tilde{q}^{(i)}(\mathbf{x}_i)}{q(\mathbf{x}_i)}$ (thanks to the locally tightness of the monomial approximation).

Thus, we obtain $\nabla \tilde{q}^{(i)}(\mathbf{x}_i) = \nabla q(\mathbf{x}_i)$, so the gradient of the monomial approximation is consistent with the gradient of the original posynomial function.

Finally, the monomial approximation satisfies the three [SCA](#) conditions, seen in [Section 2.3.2](#). \square

By replacing $q_k(\mathbf{x})$ with its lower-bound monomial approximation $\tilde{q}_k^{(i)}(\mathbf{x})$, $k \in \{0, \dots, K\}$, in [Problem 2.13](#), the resulting optimization problem is

Problem 2.14.

$$\begin{aligned} \min_{\mathbf{x}} \quad & \frac{p_0(\mathbf{x})}{\tilde{q}_0^{(i-1)}(\mathbf{x})} \\ \text{s.t.} \quad & \frac{p_k(\mathbf{x})}{\tilde{q}_k^{(i-1)}(\mathbf{x})} \leq 1, \quad \forall k \in \{1, \dots, K\}. \end{aligned} \quad (2.24)$$

Remark 2.4. If a posynomial is multiplied or divided by a monomial, the result is a posynomial.

Result 2.3. [Problem 2.14](#) is [GP](#) since it minimizes a posynomial function over a set in [GP](#) form.

Since the monomial approximation satisfies the [SCA](#) conditions, the [SCA](#) procedure depicted in [Algorithm 2.5](#) converges towards a stationary point. The obtained solution is suboptimal.

Algorithm 2.5 [SCA](#) based procedure for solving [CGP](#) [Problem 2.13](#)

- 1: Set $\epsilon > 0$, $E = \epsilon + 1$, $i = 0$
 - 2: Find \mathbf{x}_0 a feasible solution of [Problem 2.13](#)
 - 3: **while** $E > \epsilon$ **do**
 - 4: $i = i + 1$
 - 5: Compute the monomial approximation $\tilde{q}^{(i)}(\mathbf{x})$ around the point \mathbf{x}_{i-1} , using [\(2.21\)](#)
 - 6: Find \mathbf{x}_i^* the optimal solution of [Problem 2.14](#)
 - 7: Compute the Euclidean distance $E = \|\mathbf{x}_i - \mathbf{x}_{i-1}\|_2$
 - 8: **end while**
 - 9: **return** $\mathbf{x}^* = \mathbf{x}_i$
-

Remark 2.5. The presented method is also valid for a product of ratios of posynomial functions.

2.4.3 Signomial Programming

In this section, we present the problems of the [Signomial Programming \(SP\)](#) form. We will see that the conversion between [SP](#) and [CGP](#) is easy, this is why the boundary between them is thin. Before giving the form of a [SP](#), let us first introduce the definition of signomial function.

Definition 2.7. A signomial function takes the following form,

$$s(\mathbf{x}) = p(\mathbf{x}) - q(\mathbf{x})$$

where $p(\mathbf{x})$ and $q(\mathbf{x})$ are posynomial functions.

In this thesis, we consider that a [SP](#) is an optimization problem of the following form [\[18\]](#),

Problem 2.15.

$$\begin{aligned} \min_{\mathbf{x}} \quad & \frac{s_0(\mathbf{x})}{r_0(\mathbf{x})} \\ \text{s.t.} \quad & \frac{s_k(\mathbf{x})}{r_k(\mathbf{x})} \leq 1, \quad \forall k \in \{1, \dots, K\}, \end{aligned}$$

where $s_k(\mathbf{x})$ and $r_k(\mathbf{x})$, $k \in \{0, \dots, K\}$, are signomial functions.

The difficulty lies in the negative sign in the signomials. By introducing a new slack variable $t \in \mathbb{R}^{+*}$, the problem becomes

Problem 2.16.

$$\begin{aligned} & \min_{\mathbf{x}, t} t \\ \text{s.t.} \quad & \frac{s_0(\mathbf{x})}{r_0(\mathbf{x})} \leq t, \\ & \frac{s_k(\mathbf{x})}{r_k(\mathbf{x})} \leq 1, \quad \forall k \in \{1, \dots, K\}. \end{aligned}$$

We still have ratios of signomial functions, but they are all located in the constraint set.

Property 2.4. *A ratio of signomials less or equal to one,*

$$\frac{a(\mathbf{x}) - b(\mathbf{x})}{c(\mathbf{x}) - d(\mathbf{x})} \leq 1, \quad (2.25)$$

can be rewritten as a ratio of posynomials less or equal to one, if $c(\mathbf{x}) - d(\mathbf{x})$ is positive for some feasible \mathbf{x} [18], as follows

$$\frac{a(\mathbf{x}) + d(\mathbf{x})}{b(\mathbf{x}) + c(\mathbf{x})} \leq 1. \quad (2.26)$$

The signomial functions are decomposed as a difference of posynomials, thus $s_k(\mathbf{x}) = a_k(\mathbf{x}) - b_k(\mathbf{x})$ and $r_k(\mathbf{x}) = c_k(\mathbf{x}) - d_k(\mathbf{x})$, $k \in \{0, \dots, K\}$. Using the above Property 2.4 and assuming a constant positive sign of $r_k(\mathbf{x})$ in the feasible set, we obtain

Problem 2.17.

$$\begin{aligned} & \min_{\mathbf{x}, t} t \\ \text{s.t.} \quad & \frac{a_0(\mathbf{x}) + td_0(\mathbf{x})}{b_0(\mathbf{x}) + tc_0(\mathbf{x})} \leq 1, \\ & \frac{a_k(\mathbf{x}) + d_k(\mathbf{x})}{b_k(\mathbf{x}) + c_k(\mathbf{x})} \leq 1, \quad \forall k \in \{1, \dots, K\}. \end{aligned}$$

Result 2.4. *Problem 2.17 is CGP since it involves ratios of posynomial functions less or equal to one in the constraint set.*

Finally, solving a problem in SP form requires the conversion into a CGP problem. The solution of a CGP problem was presented in Section 2.4.2.

2.5 Conclusion

In this chapter, we introduced the optimization framework which is used in Chapters 3, 5 and 6. More precisely, we addressed the notion of convex sets and functions, as well as the general writing and optimal resolution of a convex optimization problem. Then, two suboptimal procedures were proposed for solving non-convex problems. We also focused on two non-convex problems with a particular form, allowing for easy implementation of suboptimal solution methods. Finally, we reviewed the non-convex optimization problems belonging to the class of GPs, and proposed suboptimal procedures for solving CGP and SP.

A summary of the addressed problems along with the proposed solutions is presented in Table 2.1.

Problem	Solution
Convex	Optimal solution in an analytical or numerical way
GP	Transformation into convex form
DC	SCA – Algorithm 2.3
LDC	SCA – Algorithm 2.4
CGP	SCA – Algorithm 2.5
SP	Transformation into CGP form
Non-convex	AO – Algorithm 2.1 or SCA – Algorithm 2.2

Table 2.1: Addressed problems and proposed solutions.

Cognitive satellite system resource allocation using ideal power amplifier

In the context of uplink cognitive satellite systems using an ideal linear *High-Power Amplifier* (HPA), solutions for sum-rate maximization have been proposed in [3, 8] mainly based on power optimization. In both papers, the authors propose to overcome the main technical difficulty, which lies in the presence of multiple interference-temperature constraints, by introducing two different heuristic approaches enabling to manage in an easier way these constraints.

In this chapter, we propose, on the one hand, to optimize the power allocation by keeping all the interference-temperature constraints as they stand, and on the other hand, we propose a novel heuristic approach for power optimization by handling in an other way the multiple interference-temperature constraints. Moreover, we extend our work to jointly optimize the subband assignment and the power allocation.

Actually, the power allocation problem raised by the cognitive satellite systems is close to allocation problems encountered in multi-cell Orthogonal Frequency Division Multiple Access (OFDMA) system or in Cloud Radio Access Network (CRAN), where a beam can be seen as a cell and the beam antenna as a base station. Nevertheless in most works, there is one system, and the multiple interference-temperature constraints vanish (see [24, 25, 26] and references therein). When interference-temperature constraints exist, typically in cognitive radio context or multi-tier system or energy-harvesting system [27, 28, 29, 30, 31], the optimization problem can not be solved in closed-form due to the multiple constraints. Indeed, in [27, 28, 29], the optimization problem is written in the dual domain and the dual variables are optimized through gradient descent algorithm. For instance, in [30, 31], the proposed algorithm is iterative and requires a grid search of dimension N , where N is the number of constraints in the optimization problem. Unlike these papers, we propose for the power allocation a simple algorithm in closed-form with fixed number of iterations.

The rest of the chapter is organized as follows. In Section 3.1, we give the mathematical writing of the optimization problem when linear HPA is considered. In Section 3.2, we propose a solution for the presented problem under inter-beam interference free assumption. In Section 3.3, we extend our work to assignment and power allocation. In Section 3.4, we exhibit a way to deal with the non-convex optimization problem. In Section 3.5, we quickly address fairness among

users by formulating two other optimization problems. In Section 3.6, we present the numerical results of our proposed solutions to solve optimization problems. Finally, Section 3.7 concludes this chapter.

3.1 Problem formulation

Let us focus on the closed-form expression for $R_{b,m}$. Assuming an independent and identically distributed complex-valued circularly-symmetric Gaussian random process as the channel input, we consider a separate inter-beam decoder where each beam is decoded by having only its own observations and by assuming the inter-beam interference as a noise. Consequently, the data rate writes as

$$R_{b,m} = \log_2 \left(1 + \frac{G_m^{(b)} P_{b,m}}{\mathcal{P}_W + \sum_{\substack{b'=1 \\ b' \neq b}}^B G_m^{(b',b)} P_{b',m}} \right), \quad (3.1)$$

where we recall that

- $P_{b,m}$ is the power of the user belonging to beam b using subband m ,
- $G_m^{(b)}$ the channel gain between user using subband m of beam b and antenna b ,
- $G_m^{(b',b)}$ the channel gain between user using subband m of beam b' and antenna b ,
- \mathcal{P}_W is the power of the [AWGN](#).

By putting (3.1) in the main Problem 1.1, the resulting power optimization problem is

Problem 3.1.

$$\mathbf{P}^* = \arg \max_{\mathbf{P}} \sum_{b=1}^B \sum_{m=1}^M \log_2 \left(1 + \frac{G_m^{(b)} P_{b,m}}{\mathcal{P}_W + \sum_{\substack{b'=1 \\ b' \neq b}}^B G_m^{(b',b)} P_{b',m}} \right) \quad (3.2)$$

s.t. (1.16) and (1.17).

Consequently, the powers of the users sharing the same subband are coupled through the utility function (3.1) and the interference-temperature constraint (1.16). The general optimization of Problem 3.1 described above leads to two concerns,

- the utility function, due to the *Signal-to-Interference-plus-Noise Ratio (SINR)*, is non-convex, and
- the number of interference temperature constraints is huge since the number of primary *Fixed Service (FS)* users may be huge.

For satellite communication CR systems, the first idea comes from the possibility of neglecting the inter-beam interference in order to simplify the utility function [3, 8] in order to render the objective function convex. In general, the inter-beam interference will be weak when the users sharing the same subband are far away from each other (and subband assignment not treated in this section may force this property) or when the beams are well separate to each other (i.e., offer a negligible overlap). In Sections 3.2 and 3.3, we use this assumption to simplify our optimization problem and focus on the huge number of constraints to propose relevant resolution method. In Section 3.4, we keep the non-convex objective function in the problem and we are looking at the resolution of non-convex problems.

3.2 Solution for neglected inter-beam interference

In the case where the inter-beam interference vanishes, the figure of merit associated with the data rate of (3.1) is replaced with (3.3) as stated in Problem 3.2.

Problem 3.2.

$$P_{b,m}^* = \arg \max_{P_{b,m}} \sum_{b=1}^B \sum_{m=1}^M \log_2 \left(1 + \frac{G_m^{(b)} P_{b,m}}{\mathcal{P}_W} \right) \quad (3.3)$$

s.t. (1.16) and (1.17).

Result 3.1. *Problem 3.2 is convex since it maximizes a concave function over a convex set.*

Proof. The objective function is concave thanks to the composition rule of the logarithm function, which is concave, and $1 + \frac{G_m^{(b)} P_{b,m}}{\mathcal{P}_W}$, which is affine. Finally the sum of concave functions is also concave. \square

Since the problem is concave, its solution can be evaluated numerically by efficient solution algorithms, such as the *Interior-Point Method* (IPM) [19, 21]. So the difficulty does not lie in the nature of the optimization problem but in the potential huge number of interference-temperature coupling constraints (1.16). To circumvent the use of standard toolboxes which converge slowly when the number of constraints is huge [21], some papers propose simplified algorithms [3, 8] by managing the coupling constraints in different ways.

In [3], the interference-temperature constraints are written beam-per-beam which decouples the optimization problem and enables the transformation of the power allocation problem into a closed-form expression. This approach really makes sense when the number of FS receivers is small, but is poor if the FS receivers becomes dense as expected in the future, since the interference level is not exploited to the maximum allowed.

Here, we propose another way by taking into account the interference-temperature constraints one by one. The idea is to consider only one interference constraint i in the problem, and going through all interference constraints one by one. Indeed we can easily write the Karush-Kuhn-Tucker (KKT) conditions and find closed-form expression of the solution for one coupling constraint. The obtained transmit power will define the maximum power constraint of the next step $i + 1$. By separating the problem for each FS band interval m' , and then introducing the interference-temperature constraints one by one L -times, the final solution satisfies all interference

constraints. So, considering the constraint $i \in \{1, \dots, L\}$ and the **FS** subband m' , we wish to solve

Problem 3.3. For a given $i \in \{1, \dots, L\}$, a given $m' \in \{1, \dots, T\}$ and $P_{b,m}^{(0)} = P_{\max} \forall b, m$,

$$\begin{aligned} \left\{ P_{b,m}^{\star,(i)} \right\}_{\substack{b=1,\dots,B \\ m \in \mathcal{S}_{m'}}} = \arg \max_{\substack{\{P_{b,m}\}_{b=1,\dots,B} \\ m \in \mathcal{S}_{m'}}} \sum_{b=1}^B \sum_{m \in \mathcal{S}_{m'}} \log_2 \left(1 + \frac{G_m^{(b)} P_{b,m}}{\mathcal{P}_W} \right) \\ \text{s.t.} \quad \sum_{b=1}^B \sum_{m \in \mathcal{S}_{m'}} F_{b,m}^{(i)} P_{b,m} \leq I_{th}^{(i)}(m'), \end{aligned} \quad (3.4)$$

$$0 \leq P_{b,m}, \quad \forall b, m \in \mathcal{S}_{m'}, \quad (3.5)$$

$$P_{b,m} \leq P_{b,m}^{\star,(i-1)}, \quad \forall b, m \in \mathcal{S}_{m'}. \quad (3.6)$$

Remark 3.1. The sequence $\left\{ P_{b,m}^{\star,(i)} \right\}_i$ is decreasing since at each step i , the maximum transmit power constraint (3.6) is modified by taking into account the solution of the previous step.

Because of the concavity of Problem 3.3, we know that the KKT conditions are necessary and sufficient to find the optimal solution of the problem. We define $\lambda_{m'}^{(i)}$, $\{\mu_{b,m}\}_{b=1,\dots,B}^{m \in \mathcal{S}_{m'}}$ and $\{\nu_{b,m}\}_{b=1,\dots,B}^{m \in \mathcal{S}_{m'}}$ the Lagrangian multipliers associated with constraints (3.4), (3.5) and (3.6) respectively. The KKT conditions of Problem 3.3 are

$$\frac{-G_m^{(b)}}{\ln 2 \left(\mathcal{P}_W + G_m^{(b)} P_{b,m} \right)} + \lambda_{m'}^{(i)} F_{b,m}^{(i)} - \mu_{b,m} + \nu_{b,m} = 0 \quad \forall b, m \in \mathcal{S}_{m'}. \quad (3.7)$$

In addition, the following complementary slackness conditions hold at the optimum:

$$\lambda_{m'}^{(i)} \sum_{b=1}^B \sum_{m \in \mathcal{S}_{m'}} \left(F_{b,m}^{(i)} P_{b,m} - I_{th}^{(i)}(m') \right) = 0, \quad (3.8)$$

$$-\mu_{b,m} P_{b,m} = 0, \quad \forall b, m \in \mathcal{S}_{m'}, \quad (3.9)$$

$$\nu_{b,m} \left(P_{b,m} - P_{b,m}^{\star,(i-1)} \right) = 0, \quad \forall b, m \in \mathcal{S}_{m'}. \quad (3.10)$$

Notice that the **FSS** subband m , which is inside $\mathcal{S}_{m'}$, is linked to the Lagrangian multiplier $\lambda_{\lceil \frac{m}{S} \rceil}^{\star,(i)}$, where $\lceil \cdot \rceil$ denotes the round toward positive. To solve the optimality conditions (3.7)-(3.10), we first express the optimal value as a function of $\lambda_{m'}^{(i)}$. We split the space defined by (3.5) and (3.6) in three cases:

- $P_{b,m}^{\star,(i)} \neq P_{b,m}^{\star,(i-1)}$ and $P_{b,m}^{\star,(i)} \neq 0$. In that case, $P_{b,m} = \frac{1}{\ln 2 \lambda_{m'}^{\star,(i)} F_{b,m}^{(i)}} - \frac{\mathcal{P}_W}{G_m^{(b)}}$.
- $P_{b,m}^{\star,(i)} = 0$. In that case, $\lambda_{m'}^{\star,(i)} \geq \frac{G_m^{(b)}}{\ln 2 \mathcal{P}_W F_{b,m}^{(i)}}$.
- $P_{b,m}^{\star,(i)} = P_{b,m}^{\star,(i-1)}$. In that case, $\lambda_{m'}^{\star,(i)} \leq \frac{G_m^{(b)}}{\ln 2 F_{b,m}^{(i)} \left(\mathcal{P}_W + G_m^{(b)} P_{b,m}^{\star,(i-1)} \right)}$.

A waterfilling-like solution can be obtained for Problem 3.3, we get

$$P_{b,m}^{*,(i)} = \left[\frac{1}{\ln 2 \lambda_{\lceil \frac{m}{S} \rceil}^{*,(i)} F_{b,m}^{(i)}} - \frac{\mathcal{P}_W}{G_m^{(b)}} \right]_{0}^{P_{b,m}^{*,(i-1)}} \quad (3.11)$$

with $[x]_a^b = \min(b, \max(a, x))$, $a \leq b$, and $\lambda_{m'}^{*,(i)}$ the optimal waterlevel chosen to fulfill the interference temperature constraint of FS subband m' at iteration i . It remains to find the appropriate waterlevel, which is the solution of the following problem,

Problem 3.4. For a given $i \in \{1, \dots, L\}$ and a given $m' \in \{1, \dots, T\}$,

$$\begin{aligned} \lambda_{m'}^{*,(i)} &= \arg \min_{\lambda} \lambda \\ \text{s.t. } &\sum_{b=1}^B \sum_{m \in \mathcal{S}_{m'}} F_{b,m}^{(i)} \min \left(P_{b,m}^{*,(i-1)}, \max \left(0, \frac{1}{\ln 2 \lambda F_{b,m}^{(i)}} - \frac{\mathcal{P}_W}{G_m^{(b)}} \right) \right) \leq I_{th}^{(i)}(m'). \end{aligned} \quad (3.12)$$

This problem is very easily solved by a search method since there is only one dimension to search. The procedure depicted in Algorithm 3.1 allows to obtain a solution of the problem in a very efficient way. Indeed, this approach is scalable into the number of FS since we have only LT waterfilling-like solutions to compute in parallels since the problem is separable in the FS subband m' . Notice that the obtained solution is sub-optimal and the order in which the constraints are introduced plays a role in the final solution. We show in Section 3.6 that the proposed algorithm outperforms the existing ones and is close to the optimal solution in the context of satellite communication CR systems.

Algorithm 3.1 Simplified procedure for solving Problem 3.2 by taking one by one the interference-temperature constraints

- 1: Set $i = 1$, $P_{b,m}^*(0) = P_{\max}$
 - 2: **while** $i \leq L$ **do**
 - 3: Compute the optimal waterlevel $\lambda_{m'}^{*,(i)}$ of Problem 3.4 using line search
 - 4: Compute the optimal solution $P_{b,m}^*(i)$ of Problem 3.3 using (3.11)
 - 5: $i = i + 1$
 - 6: **end while**
 - 7: **return** $P_{b,m}^* = P_{b,m}^*(i)$
-

3.3 Extended work for subband assignment

In this section, we still use the assumption of inter-beam interference free, and we propose to extend our study to jointly optimize the power allocation and the subband assignment. The notations introduced in this section are completely independent of the rest of the manuscript. We assume that the matching between users and beams is prefixed, based on the user location.

The purpose of this section is to optimize the sum-rate of our system, under the following parameters:

- $\mathbf{A}(b) = (A_{b,k,m})_{\substack{1 \leq k \leq K \\ 1 \leq m \leq M}}$, which corresponds to subband assignment. If subband m is assigned to user k in beam b , then $A_{b,k,m} = 1$, else 0,

- $\mathbf{P} = (P_{b,k})_{\substack{1 \leq b \leq B, \\ 1 \leq k \leq K}}$, where $P_{b,k}$ corresponds to the transmit power of user k in beam b .

Actually, allocating the subband is an assignment problem where for each beam, each user must be allocated to a single subband. Within a beam, as we assume that there are as many users as subbands, the mapping between user and subband is a permutation problem, i.e.,

$$\sum_{k=1}^K A_{b,k,m} = 1, \quad \forall b, m, \quad (3.13)$$

$$\sum_{m=1}^M A_{b,k,m} = 1, \quad \forall b, k, \quad (3.14)$$

$$A_{b,k,m} \in \{0, 1\}, \quad \forall b, k, m, \quad (3.15)$$

where constraint (3.13) deals with *Frequency-Division Multiple Access (FDMA)* per beam, and (3.14) means that one user has only one subband. This last constraint ensures that each user will be served and guarantees a certain level of fairness between users. The binary constraint (3.15) is completely related to the assignment problem.

The interference-temperature constraint, related to the primary network, is always present in the problem and is written

$$\sum_{b=1}^B \sum_{k=1}^K \sum_{m \in \mathcal{S}_{m'}} F_{b,k,m}^{(\ell)} A_{b,k,m} P_{b,k} \leq I_{th}^{(\ell)}(m'), \quad \forall \ell, m', \quad (3.16)$$

where $F_{b,k,m}^{(\ell)}$ is the interference channel gain between user k of beam b on subband m and the primary FS ℓ .

Moreover, we still have the mask constraint for the transmit power of user k in beam b ,

$$0 \leq P_{b,k} \leq P_{\max}, \quad \forall b, k. \quad (3.17)$$

Finally, the optimization problem to solve is written

Problem 3.5.

$$\begin{aligned} & \max_{\{\mathbf{A}^{(b)}\}_b, \mathbf{P}} \sum_{b=1}^B \sum_{k=1}^K \sum_{m=1}^M \log_2 \left(1 + \frac{G_{k,m}^{(b)} A_{b,k,m} P_{b,k}}{\mathcal{P}_W} \right) \\ & \text{s.t. (3.13), (3.14), (3.15), (3.16) and (3.17),} \end{aligned} \quad (3.18)$$

where $G_{k,m}^{(b)}$ is the channel gain of user k in beam b using subband m .

Remark 3.2. By noting that $\log(1 + ax) = a \log(1 + x)$ for a binary variable a , the objective function can also be written by $A_{b,k,m} \log_2 \left(1 + \frac{G_{k,m}^{(b)} P_{b,k}}{\mathcal{P}_W} \right)$.

Problem 3.5 is not jointly convex in \mathbf{A} and \mathbf{P} . Indeed, the non-convexity comes from the binary set and the product between \mathbf{A} and \mathbf{P} .

In [3], this problem has been treated in a sub-optimal manner. Actually, in [3], the beams were assumed not to use the same band. But the main idea – dealing with a simpler way to manage the multiple interference-temperature constraints (3.16) – can be straightforwardly extended to

our case. The authors uncouple the interference-temperature constraints beam by beam and subband by subband, by replacing (3.16) with

$$\sum_{k=1}^K F_{b,k,m}^{(\ell)} A_{b,k,m} P_{b,k} \leq \frac{I_{th}^{(\ell)}(\lceil \frac{m}{S} \rceil)}{BS}, \quad \forall b, m, \ell. \quad (3.19)$$

As FDMA is applied on each beam, only one term is active in (3.19). If user k in beam b is active on subband m , then we have,

$$P_{b,k}(m) = \min \left(P_{\max}, \frac{I_{th}^{(1)}(\lceil \frac{m}{S} \rceil)}{F_{b,k,m}^{(1)} BS}, \dots, \frac{I_{th}^{(L)}(\lceil \frac{m}{S} \rceil)}{F_{b,k,m}^{(L)} BS} \right). \quad (3.20)$$

Once the power is obtained through (3.20), the subband assignment can be solved with the Hungarian method since the cost function (3.18) is insensitive to inter-beam interference.

In this section, we propose an alternative approach while maintaining the coupling constraint (3.16). In order to overcome the two sources of non-convexity of Problem 3.5, we propose to apply a change of variable or *Alternating Optimization (AO)* to manage the product, and relax the binary set. These two approaches are detailed in the following subsections.

3.3.1 Joint optimization with change of variable

We rewrite the Problem 3.5 using the Remark 3.2 as follow

Problem 3.6.

$$\begin{aligned} \max_{\{\mathbf{A}(b)\}_b, \mathbf{P}} \quad & \sum_{b=1}^B \sum_{k=1}^K \sum_{m=1}^M A_{b,k,m} \log_2 \left(1 + \frac{G_{k,m}^{(b)} P_{b,k}}{\mathcal{P}_W} \right) \\ \text{s.t.} \quad & (3.13), (3.14), (3.15), (3.16) \text{ and } (3.17). \end{aligned} \quad (3.21)$$

The first approach is inspired by [32, 25], where we start by relaxing the discrete constraint, following the well-known convex relaxation approach. Then, we apply a change of variables $(A_{b,k,m}, P_{b,k}) \mapsto (A_{b,k,m}, Q_{b,k,m})$ with $Q_{b,k,m} = A_{b,k,m} P_{b,k}$, Problem 3.6 becomes

Problem 3.7.

$$\mathbf{A}^*, \mathbf{Q}^* = \arg \max_{\mathbf{A}, \mathbf{Q}} \sum_{b=1}^B \sum_{k=1}^K \sum_{m=1}^M A_{b,k,m} \log_2 \left(1 + \frac{G_{k,m}^{(b)} Q_{b,k,m}}{A_{b,k,m} \mathcal{P}_W} \right) \quad (3.22)$$

s.t. (3.13), (3.14),

$$\sum_{b=1}^B \sum_{k=1}^K \sum_{m \in \mathcal{S}_{m'}} F_{b,k,m}^{(\ell)} Q_{b,k,m} \leq I_{th}^{(\ell)}(m'), \quad \forall \ell, m', \quad (3.23)$$

$$0 \leq Q_{b,k,m} \leq A_{b,k,m} P_{\max}, \quad \forall b, k, m,$$

$$A_{b,k,m} \in [0, 1], \quad \forall b, k, m.$$

Result 3.2. Problem 3.7 is convex since it maximizes a concave function over a convex set.

Proof. The objective function is concave since the perspective of a concave function preserves concavity. We define the function g as

$$g(Q_{b,k,m}) = \log \left(1 + \frac{G_{k,m}^{(b)} Q_{b,k,m}}{\mathcal{P}_W} \right). \quad (3.24)$$

The function g is concave since $1 + \frac{G_{k,m}^{(b)} Q_{b,k,m}}{\mathcal{P}_W}$ is affine and the logarithm function is concave and increasing. Now, recall that g is concave if and only if the perspective of g is concave. The perspective of g is

$$h(A_{b,k,m}, Q_{b,k,m}) = A_{b,k,m} g\left(\frac{Q_{b,k,m}}{A_{b,k,m}}\right). \quad (3.25)$$

So the function h is concave. \square

Since the problem is convex, we can use numerical solution tools to find the optimal solutions of the problem [33]. Obviously the subband assignment solution \mathbf{A}^* is not a binary vector, and we perform a projection on the binary set while satisfying the assignment constraints (3.13), (3.14), in order to obtain a valid subband assignment.

Once the subband assignment is fixed, it is mandatory to determine a new power allocation. Indeed, the transition from the relaxed form to the binary form no longer guarantees the interference-temperature constraints (3.16).

Therefore, the Problem 3.5 must be solved again, by fixing the assignment optimization variable. It is also possible to use the trick presented in Section 3.2 to quickly determine a power allocation.

Yet, bounding the losses due to the convex relaxation of (3.15) for that problem is, to the best of our knowledge, an open problem.

3.3.2 Joint optimization with Alternating Optimization

The second approach is based on alternating optimization method. Actually, the Problem 3.5 is convex when the assignment \mathbf{A} is fixed (power optimization) and *Integer Programming* (IP) when the power \mathbf{P} is fixed (assignment optimization). So the idea is to alternate optimization between subband assignment and power allocation.

Subband assignment

Now we focus only on assignment optimization by assuming a predefined power allocation for user k belonging to beam b , $P_{b,k}$. By using Remark 3.2, the resulting problem is

Problem 3.8.

$$\begin{aligned} \{\mathbf{A}^*(b)\}_b &= \arg \max_{\{\mathbf{A}^{(b)}\}_b} \sum_{b=1}^B \sum_{k=1}^K \sum_{m=1}^M A_{b,k,m} \log_2 \left(1 + \frac{G_{k,m}^{(b)} P_{b,k}}{\mathcal{P}_W} \right) \\ &\text{s.t. (3.13), (3.14), (3.15) and (3.16).} \end{aligned}$$

Problem 3.8 is IP, and by using the well-known binary relaxation, we obtain the following problem

Problem 3.9.

$$\begin{aligned} \{\mathbf{A}^*(b)\}_b &= \arg \max_{\{\mathbf{A}(b)\}_b} \sum_{b=1}^B \sum_{k=1}^K \sum_{m=1}^M A_{b,k,m} \log_2 \left(1 + \frac{G_{k,m}^{(b)} P_{b,k}}{\mathcal{P}_W} \right) \\ \text{s.t. } & (3.13), (3.14), (3.16), \\ & A_{b,k,m} \in [0, 1], \quad \forall b, k, m. \end{aligned}$$

Result 3.3. *Problem 3.9 is Linear Programming (LP) since it maximizes an affine function over a set in LP form.*

Then numerical tools, such as simplex method or IPM [34], give optimal solution of the LP problem. However this solution is composed of real values, and a dedicated algorithm transforms it into a binary vector, while satisfying the assignment constraints (3.13), (3.14), to obtain a solution. The algorithm finds the highest value in the matrix $\mathbf{A}(b)$, set it to 1 and clear the corresponding row and column, then iterates until the assignment constraints are satisfied. When applying this algorithm, we cannot guarantee that the constraints (3.16) are still satisfied and we have to perform a power allocation in order to overcome this issue.

Notice that we obtain a sub-optimal solution of the original Problem 3.8, and the distance to the optimal is unknown.

Power allocation

The power optimization problem, when the subband assignment is fixed, has already been treated in Section 3.2. We can therefore reuse the same solution methods to obtain the power allocation.

Finally, we have proposed in this section two solutions that address the optimization problem of subband assignment and power allocation jointly. This section is the only one that deals with the subband assignment problem.

In the next section, we consider again our power allocation Problem 3.1, but taking into account the inter-beam interference.

3.4 Solution for the non-convex problem with successive convex approximation

In this section, we focus on the original Problem 3.1, which is non-convex. The concerns of Section 3.2 still exist, namely the large number of constraints, however we focus here on methods for solving the non-convex problem.

The management of a non-convex problem is often done using the *Successive Convex Approximation* (SCA) method, presented in Section 2.3.2.

Here we propose two different methods, based on the SCA procedure. The first one exploits the particular shape of the objective function. The second one relies on the underlying mathematical properties of the objective function.

3.4.1 Using the Difference of Concave form

In this section, we focus on the non-convex Problem 3.1. By rewriting the objective function, a *Difference of Concave (DC)* appears as follows

Problem 3.10.

$$\mathbf{P}^* = \arg \max_{\mathbf{P}} \sum_{b=1}^B \sum_{m=1}^M \left(\log_2 \left(\mathcal{P}_W + \sum_{b'=1}^B G_m^{(b',b)} P_{b',m} \right) - \log_2 \left(\mathcal{P}_W + \sum_{\substack{b'=1 \\ b' \neq b}}^B G_m^{(b',b)} P_{b',m} \right) \right) \quad (3.26)$$

s.t. (1.16), (1.17).

The resulting problem is non-convex but the objective function is in the form of DC. We treat the non-convex problem with the SCA procedure. The problem is approximated several times by a convex problem. If the convex approximation satisfies the SCA conditions, then this procedure converges to a local optimum. The difficulty lies in writing a convex approximation that satisfies the SCA convergence conditions.

However, when a non-convex problem can be written as a DC problem, then the computation of the convex approximation respecting the SCA conditions is straightforward, as seen in Section 2.3.3. The idea is to replace the second term, which is concave, by its first Taylor approximation, at a given feasible point which is a solution of Problem 3.10. By definition, the first Taylor approximation of a concave function is an affine function which satisfies the SCA conditions. Then, the nature of the objective function is now concave and the problem is solvable by numerical tools, which gives us a new solution of Problem 3.10. Finally, the algorithm iterates until convergence. Notice that the final solution is not optimal.

We denote the second concave function by

$$g_{b,m}(\mathbf{P}) = \log_2 \left(\mathcal{P}_W + \sum_{\substack{b'=1 \\ b' \neq b}}^B G_m^{(b',b)} P_{b',m} \right). \quad (3.27)$$

The affine approximation at the point \mathbf{P}_i is denoted by $\bar{g}_{b,m}^{(i)}$. This affine function is built using the first Taylor approximation at the point \mathbf{P}_i , which satisfies naturally the SCA conditions if $g_{b,m}$ is concave. The obtained expression is as follows,

$$\bar{g}_{b,m}^{(i)}(\mathbf{P}) = g_{b,m}(\mathbf{P}_i) + \sum_{\substack{b'=1 \\ b' \neq b}}^B \frac{\partial g_{b,m}}{\partial P_{b',m}} \Big|_{\mathbf{P}_i} (P_{b',m} - P_{b',m}^{(i)}) \geq g_{b,m}(\mathbf{P}), \quad (3.28)$$

where the derivative of $g_{b,m}$ is given by

$$\frac{\partial g_{b,m}}{\partial P_{i,j}}(\mathbf{P}) = (1 - \delta_{i,b}) \delta_{j,m} \frac{1}{\ln 2} \frac{G_j^{(i,b)}}{\left(\mathcal{P}_W + \sum_{\substack{b'=1 \\ b' \neq b}}^B G_j^{(b',b)} P_{b',j} \right)}, \quad (3.29)$$

with $\delta_{k,l}$ the Kronecker delta function.

The resulting approximated optimization problem is

Problem 3.11.

$$\mathbf{P}_i^* = \arg \max_{\mathbf{P}} \sum_{b=1}^B \sum_{m=1}^M \left(\log_2 \left(\mathcal{P}_W + \sum_{b'=1}^B G_m^{(b',b)} P_{b',m} \right) - \bar{g}_{b,m}^{(i-1)}(\mathbf{P}) \right) \quad (3.30)$$

s.t. (1.16) and (1.17).

Result 3.4. *Problem 3.11 is convex since it maximizes a concave function over a set which can be easily rewrite in convex form.*

Since the affine approximation satisfies the SCA conditions, the SCA procedure depicted in Algorithm 3.2 converges towards a stationary point. The obtained solution is sub-optimal.

Algorithm 3.2 SCA based procedure for solving Problem 3.1

- 1: Set $\epsilon > 0$, $E = \epsilon + 1$, $i = 0$
 - 2: Find \mathbf{P}_0 a feasible solution of Problem 3.1
 - 3: Compute the sum-rate R_0 using (3.1)
 - 4: **while** $E > \epsilon$ **do**
 - 5: $i = i + 1$
 - 6: Compute the affine approximation $\bar{g}_{b,m}^{(i-1)}$ around the point \mathbf{P}_{i-1} , using (3.28)
 - 7: Find \mathbf{P}_i^* the optimal solution of Problem 3.11
 - 8: Compute the sum-rate R_i and $E = |R_i - R_{i-1}|$
 - 9: **end while**
 - 10: **return** $\mathbf{P}^* = \mathbf{P}_i$
-

To sum up, this procedure is useful for refining a solution obtained with neglected inter-beam interference in Section 3.2. Indeed, we use the obtained solution as starting point of the SCA.

3.4.2 Using the ratio of posynomial form

In this section, we still focus on the non-convex Problem 3.1, but another approximation method is used. Thanks to the monotonic growth of the logarithm function, Problem 3.1 is equivalent to the following one.

Problem 3.12.

$$\mathbf{P}^* = \arg \min_{\mathbf{P}} \prod_{b=1}^B \prod_{m=1}^M \frac{\mathcal{P}_W + \sum_{\substack{b'=1 \\ b' \neq b}}^B G_m^{(b',b)} P_{b',m}}{\mathcal{P}_W + \sum_{b'=1}^B G_m^{(b',b)} P_{b',m}} \quad (3.31)$$

s.t. (1.16) and (1.17).

The difficulty is still located in the objective function, where we have a ratio of posynomial functions, so the problem boils down to *Complementary Geometric Programming (CGP)*, presented in Section 2.4.2. Since the objective function of the problem is already a ratio of posynomials, we can directly use the SCA procedure with monomial approximation of the denominator.

We denote the denominator by

$$D_{b,m}(\mathbf{P}) = \mathcal{P}_W + \sum_{b'=1}^B G_m^{(b',b)} P_{b',m}. \quad (3.32)$$

The monomial approximation at the point \mathbf{P}_i is denoted by $\tilde{D}_{b,m}^{(i)}$. This approximation is built in such a way that it satisfies the [SCA](#) conditions, presented in [Section 2.4.2](#),

$$\tilde{D}_{b,m}^{(i)}(\mathbf{P}) = \left(\frac{\mathcal{P}_W}{\nu_{b,m}} \right)^{\nu_{b,m}} \times \prod_{b'=1}^B \left(\frac{G_m^{(b',b)} P_{b',m}}{\lambda_{b,m}(b')} \right)^{\lambda_{b,m}(b')}, \quad (3.33)$$

where

$$\nu_{b,m} = \frac{\mathcal{P}_W}{D_{b,m}(\mathbf{P}_i)}, \quad (3.34)$$

$$\lambda_{b,m}(b') = \frac{G_m^{(b',b)} P_{b',m}^{(i)}}{D_{b,m}(\mathbf{P}_i)}. \quad (3.35)$$

The resulting approximated optimization problem is

Problem 3.13.

$$\mathbf{P}_i^* = \arg \min_{\mathbf{P}} \prod_{b=1}^B \prod_{m=1}^M \left(\tilde{D}_{b,m}^{(i-1)}(\mathbf{P}) \right)^{-1} \left(\mathcal{P}_W + \sum_{\substack{b'=1 \\ b' \neq b}}^B G_m^{(b',b)} P_{b',m} \right) \quad (3.36)$$

s.t. [\(1.16\)](#) and [\(1.17\)](#).

Result 3.5. *Problem 3.13 is [Geometric Programming \(GP\)](#) since it minimizes a posynomial function over a set in [GP](#) form and can be efficiently solved by numerical algorithms.*

Since the monomial approximation satisfies the [SCA](#) conditions, the [SCA](#) procedure depicted in [Algorithm 3.3](#) converges towards a stationary point. The obtained solution is sub-optimal.

Algorithm 3.3 [SCA](#) based procedure for solving [Problem 3.1](#)

- 1: Set $\epsilon > 0$, $E = \epsilon + 1$, $i = 0$
 - 2: Find \mathbf{P}_0 a feasible solution of [Problem 3.1](#)
 - 3: Compute the sum-rate R_0 using [\(3.1\)](#)
 - 4: **while** $E > \epsilon$ **do**
 - 5: $i = i + 1$
 - 6: Compute the monomial approximation $\tilde{D}_{b,m}^{(i-1)}$ around the point \mathbf{P}_{i-1} , using [\(3.33\)](#)
 - 7: Find \mathbf{P}_i^* the optimal solution of [Problem 3.13](#)
 - 8: Compute the sum-rate R_i and $E = |R_i - R_{i-1}|$
 - 9: **end while**
 - 10: **return** $\mathbf{P}^* = \mathbf{P}_i$
-

To conclude this section, we have proposed two different methods for solving the non-convex [Problem 3.1](#), based on the [SCA](#) procedure. It is interesting to note that the two methods of resolution by [SCA](#) do not approximate the same part of the function.

3.5 Fairness

In this section, we address the fairness issue between users. Indeed, with the rise of heterogeneous networks, fairness between users, along with issues for high throughput, has become critical. Because there are numerous definitions of *fairness* in the optimization literature [35], no agreement on a single definition has been reached yet. Here, we consider the two most used definitions of fairness, namely *max-min fairness* and *proportional fairness*.

3.5.1 Maximization of the minimum per-user data rate

Here we address the maximization of the minimum per-user data rate. The max-min fairness is reached when the allocation of available resources is feasible and any attempt to increase the data rate of any user necessarily leads to a fall in the data rate of some other users with the lowest rate. In other words, it maximizes the minimum of per-user data rate. The related problem writes as follow

Problem 3.14.

$$\mathbf{P}^* = \arg \max_{\mathbf{P}} \min_{b,m} \log_2 \left(1 + \frac{G_m^{(b)} P_{b,m}}{\mathcal{P}_W + \sum_{\substack{b'=1 \\ b' \neq b}}^B G_m^{(b',b)} P_{b',m}} \right) \quad (3.37)$$

s.t. (1.16) and (1.17).

The obtained problem is not convex due to the minimum operator and the ratio inside the cost function. In [8], the authors uses the assumption of inter-beam interference free. They propose to optimize the power by managing the worst case, i.e., the worst FS receiver receiving the maximum interference temperature when users are at full power, and then they fix the power of the most interfering user for this FS receiver by assuming that other users are full power, and so on.

We propose another approach by rewriting Problem 3.14. As the logarithmic function is monotonically increasing, Problem 3.14 has the following equivalent formulation

Problem 3.15.

$$\mathbf{P}^* = \arg \max_{\mathbf{P}} \min_{b,m} \frac{G_m^{(b)} P_{b,m}}{\mathcal{P}_W + \sum_{\substack{b'=1 \\ b' \neq b}}^B G_m^{(b',b)} P_{b',m}} \quad (3.38)$$

s.t. (1.16) and (1.17).

We introduce a new variable $t \in \mathbb{R}^{+*}$ in order to remove the minimum operator of the objective function. The problem becomes

Problem 3.16.

$$\mathbf{P}^* = \arg \max_{\mathbf{P}, t} t \quad (3.39)$$

s.t. (1.16) and (1.17),

$$t \leq \frac{G_m^{(b)} P_{b,m}}{\mathcal{P}_W + \sum_{\substack{b'=1 \\ b' \neq b}}^B G_m^{(b',b)} P_{b',m}}, \quad \forall b, m. \quad (3.40)$$

Remark 3.3. We notice that $\max t$ is equivalent to $\min t^{-1}$ since $t \in \mathbb{R}^{+*}$.

The difficulty is located in the constraint (3.40), where we have ratios of monomial function over posynomial function. However, this inequality can be rewritten as

$$\left(G_m^{(b)} P_{b,m}\right)^{-1} t \left(\mathcal{P}_W + \sum_{\substack{b'=1 \\ b' \neq b}}^B G_m^{(b',b)} P_{b',m}\right) \leq 1, \quad \forall b, m. \quad (3.41)$$

Lemma 3.1. The constraint (3.41) has the form of a posynomial less than or equal to one, leading to a valid constraint for GP.

Proof. The term $\left(G_m^{(b)} P_{b,m}\right)^{-1}$ is a monomial function. Thanks to the addition rule of posynomial, the rest of the *Left-Hand Side (LHS)* is a posynomial function. Finally, thanks to multiplication rule between a monomial and a posynomial function, the *LHS* is a posynomial function. \square

The resulting optimization problem writes as:

Problem 3.17.

$$\mathbf{P}^* = \arg \min_{\mathbf{P}, t} t^{-1} \quad (3.42)$$

s.t. (1.16), (1.17) and (3.41).

Result 3.6. Problem 3.17 is GP since it minimizes a monomial function over a set written in GP form.

Since the Problem 3.17 is GP, numerical tools can solve it [33] and the obtained solution is optimal. Finally, we succeeded to rewrite the non-convex Problem 3.14 into the equivalent Problem 3.17 which is GP.

3.5.2 Proportional fairness

Now we focus on the Proportional Fairness (PF) problem. Proportional fairness is reached when the allocation of available resources is feasible and a transfer of resources between two users is accepted when the percentage increase in data rate of one user is greater than the percentage decrease in data rate of the other user. It is proved in [36] that maximizing the sum of logarithmic utility functions yields a proportionally fair allocation of data rates. As a result, in our case, the problem can be stated as

Problem 3.18.

$$\mathbf{P}^* = \arg \max_{\mathbf{P}} \sum_{b=1}^B \sum_{m=1}^M \log \left(\log_2 \left(1 + \frac{G_m^{(b)} P_{b,m}}{\mathcal{P}_W + \sum_{\substack{b'=1 \\ b' \neq b}}^B G_m^{(b',b)} P_{b',m}} \right) \right) \quad (3.43)$$

s.t. (1.16) and (1.17).

We can rewrite the problem in order to obtain a LDC form, which becomes

Problem 3.19.

$$\mathbf{P}^* = \arg \max_{\mathbf{P}} \sum_{b=1}^B \sum_{m=1}^M \log \left(\log_2 \left(\mathcal{P}_W + \sum_{b'=1}^B G_m^{(b',b)} P_{b',m} \right) - \log_2 \left(\mathcal{P}_W + \sum_{\substack{b'=1 \\ b' \neq b}}^B G_m^{(b',b)} P_{b',m} \right) \right) \quad (3.44)$$

s.t. (1.16) and (1.17).

The DC is non-concave, so the LDC is also non-concave. We have detailed in Section 3.4.1 a way to manage the DC problem, by using SCA procedure. Hopefully, the concave approximation presented in Section 3.4.1 can be reused, as seen in Section 2.3.4.

The resulting problem is the following

Problem 3.20.

$$\mathbf{P}_i^* = \arg \max_{\mathbf{P}} \sum_{b=1}^B \sum_{m=1}^M \log \left(\log_2 \left(\mathcal{P}_W + \sum_{b'=1}^B G_m^{(b',b)} P_{b',m} \right) - \bar{g}_{b,m}^{(i-1)} \right) \quad (3.45)$$

s.t. (1.16) and (1.17).

Result 3.7. Problem 3.20 is convex since it maximizes a concave function over a convex set.

Since the concave approximation satisfies the SCA conditions, the SCA procedure depicted in Algorithm 3.4 converges towards a stationary point. The obtained solution is sub-optimal.

Algorithm 3.4 SCA based procedure for solving Problem 3.18

- 1: Set $\epsilon > 0$, $E = \epsilon + 1$, $i = 0$
 - 2: Find \mathbf{P}_0 a feasible solution of Problem 3.18
 - 3: Compute the proportional fairness R_0 using (3.43)
 - 4: **while** $E > \epsilon$ **do**
 - 5: $i = i + 1$
 - 6: Compute the affine approximation $\bar{g}_{b,m}^{(i-1)}$ around the point \mathbf{P}_{i-1} , using (3.28)
 - 7: Find \mathbf{P}_i the optimal solution of Problem 3.20
 - 8: Compute the proportional fairness R_i and $E = |R_i - R_{i-1}|$
 - 9: **end while**
 - 10: **return** $\mathbf{P}^* = \mathbf{P}_i$
-

To conclude this section, we have proposed two solutions to address the fairness issue in our satellite communication CR system. The first solution is optimal since we succeeded to rewrite the problem in GP form. The second solution is sub-optimal since it involved a SCA procedure.

3.6 Numerical results

We consider a multiband multibeam satellite system operating in the Ka-band for the uplink (27.5-29.5 GHz). The satellite is composed of $B = 2$ beams and there are $K = 6$ users per beam (and so $M = K$ subbands). The primary FS subband contains $S = 2$ FSS subbands. The channel gains $\{G_m^{(b',b)}\}_{b,m,b'}$ and $\{F_{b,m}^{(\ell)}\}_{b,m,\ell}$ are computed according to [2, 3, 15, 14]. The maximum power is $P_{\max} = 50\text{W}$ (47dBm). The maximum interference-temperature level is fixed to $I_{th}^{(\ell)}(m') = 1\text{pW}$ (−90dBm) for any ℓ, m' . All numerical results have been averaged over 100 random draws of primary and secondary user positions, leading to different channel gain values. We use the CVX toolbox to solve convex and GP problems [33].

Unless otherwise stated, we use the subband assignment given by the algorithm presented in [3] and detailed in Section 3.3.

We denote the power allocations related to the maximization of the sum-rate by

- P^{sota1} , the power allocation given by [3] where inter-beam interference is neglected, and detailed in Section 3.2,
- P' , the power allocation given by Algorithm 3.1, which is the waterfilling-like solution for Problem 3.2 where inter-beam interference is neglected,
- P^* , the power allocation which is the optimal solution of Problem 3.2 where inter-beam interference is neglected, obtained by numerical solver [33],
- $P^{\text{sca-dc}}$, the power allocation given by Algorithm 3.2 which is the SCA procedure using the DC form for Problem 3.1, where the inter-beam interference is taken in account,
- $P^{\text{sca-gp}}$, the power allocation given by Algorithm 3.3 which is the SCA procedure using the ratio of posynomial form for Problem 3.1, where the inter-beam interference is taken in account.

We denote the power allocations related to the fairness issue by

- P^{sota2} , the power allocation given by [8] where inter-beam interference is neglected, and detailed in Section 3.5,
- P^{maxmin} , the power allocation which is the optimal solution of Problem 3.14 where the inter-beam interference is taken in account, obtained by numerical solver [33],
- P^{Pf} , the power allocation given by Algorithm 3.4 which is the SCA procedure for Problem 3.18 where the inter-beam interference is taken in account.

The data rate of users is then evaluated by applying the considered solution in the expression given by (3.1).

3.6.1 Sum-rate analysis

In Fig. 3.1, we plot the system sum-rate versus the FS density for the eight above mentioned solutions. The data rate is evaluated by (3.1). We show that our proposed allocations related to

sum-rate offer better performance than the state-of-the-art, although the use of **SCA** method for solving non-convex problem. Moreover, the proposed allocation with the simplest algorithm, i.e. P' , performs well since it is near to the optimal solution P^* . More importantly, the gap between our allocations and the state-of-the-art stays stable when the number of **FS** receivers increases, which makes sense since better management of **FS** constraints is necessary and offers by our propositions. The increase in the sum-rate with increasing density of **FS** for some solutions may seem strange. However, it only concerns solutions that do not optimize the expression of the sum-rate given by (3.1). We observe that the two **SCA** procedures for solving Problem 3.1 are almost equivalent. When the **FS** density increases, we notice that the solutions obtained by neglecting the inter-beam interference are close to the solutions taking it into account. So in the context of a high density of **FS**, the optimization neglecting the inter-beam interference is relevant.

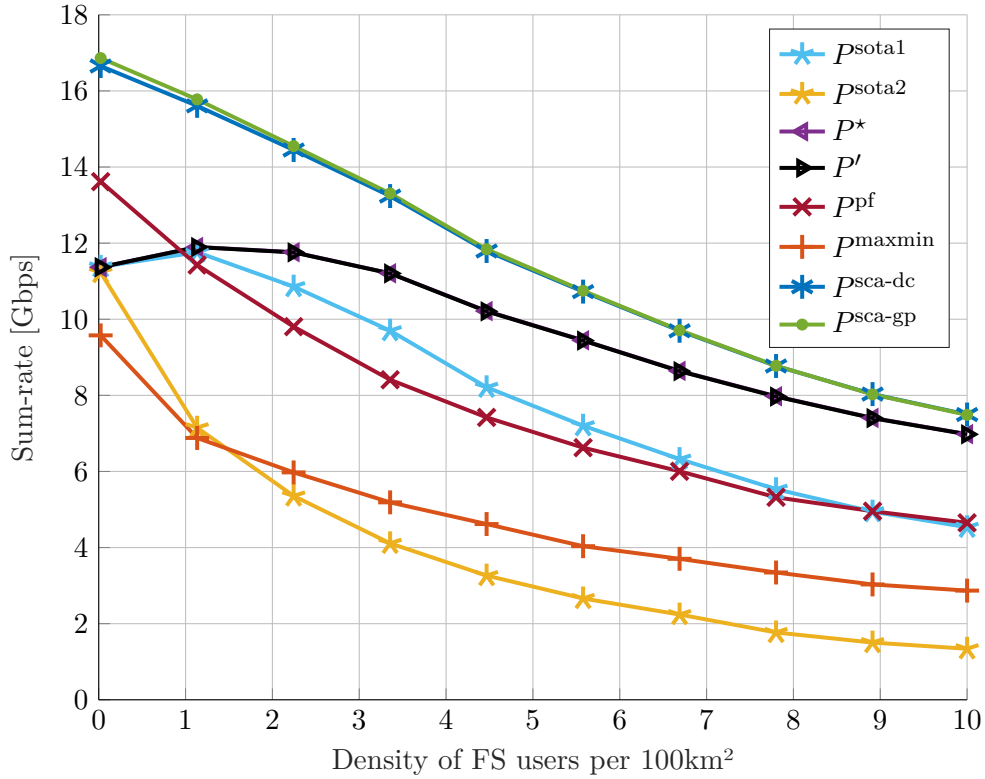


Figure 3.1: Sum-rate vs. **FS** density.

In Fig. 3.2, we plot the sum-rate versus the **FS** density for the six solutions described below.

- A^{sota1}, P^{sota1} , the subband assignment given by [3] and explained in Section 3.3 and the power allocation obtained by Algorithm 3.1,
- A^{sota1}, P^* , the subband assignment given by [3] and explained in Section 3.3 and the power allocation obtained by solving Problem 3.2 with numerical solver [33],
- A^{sota1}, P^{sca-dc} , the subband assignment given by [3] and explained in Section 3.3 and the power allocation obtained by Algorithm 3.2,

- $A^{\text{quant}}, P^{\text{sca-dc}}$, the subband assignment given by joint optimization explained in Section 3.3.1 and the power allocation obtained by Algorithm 3.2,
- $A^{\text{quant}}, P^{\text{quant}}$, the subband assignment and the power allocation given by joint optimization explained in Section 3.3.1,
- $A^{\text{ao}}, P^{\text{ao}}$, the subband assignment and power allocation given by AO explained in Section 3.3.2.

The system sum-rate is then evaluated using (3.1). The proposed allocations all outperform the state-of-the-art. We notice that all solutions related to problem without inter-beam interference provide the same result when the FS density is close to zero. We can explain this behavior because all these algorithms will give the solution P_{max} for all users. Our proposed joint optimization of subband assignment and power allocation is better than AO solution, since we optimize at the same time the resources. In a context of densification of the primary network, the optimization of the subband assignment is essential.

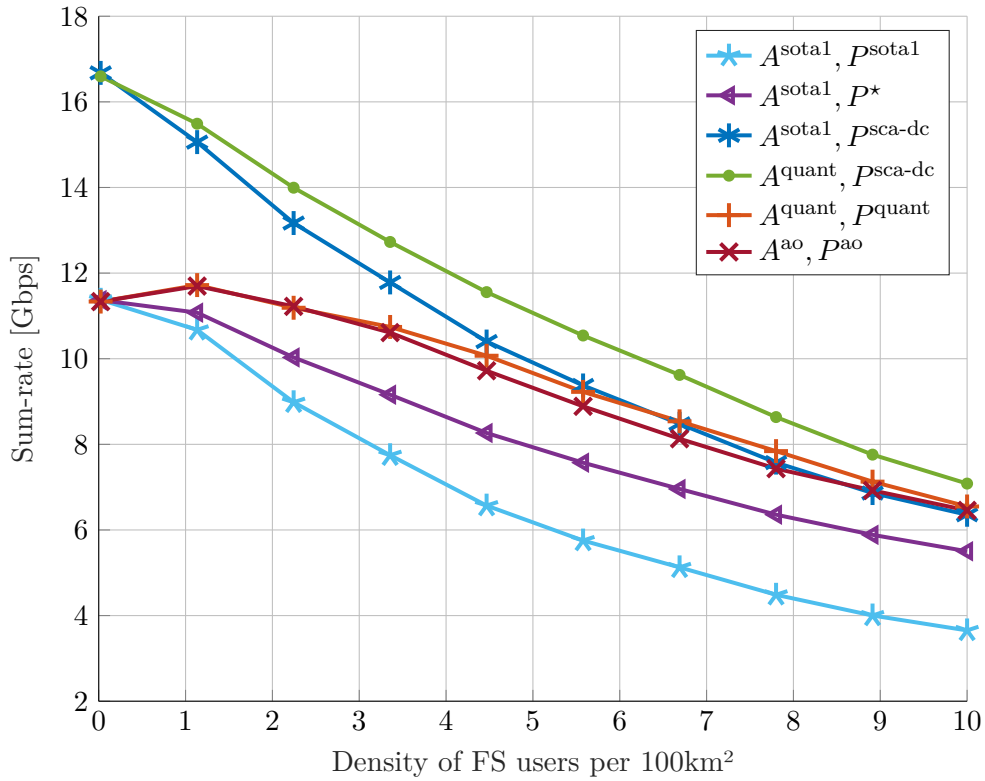


Figure 3.2: Sum-rate vs. FS density.

3.6.2 Fairness analysis

We evaluate the fairness of the proposed solutions versus the FS density. In order to measure the fairness, we observe the minimum per-user data rate and use the Jain's index on the data rate of

users, defined by [37]

$$J = \frac{\left(\sum_{b=1}^B \sum_{m=1}^M R_{b,m}\right)^2}{BM \sum_{b=1}^B \sum_{m=1}^M R_{b,m}^2}. \quad (3.46)$$

It is well known that $J \in [\frac{1}{BM}, 1]$ and the highest index value correspond to the fairest solution.

In Fig. 3.3, we plot the minimum per-user data rate versus the FS density for the eight above mentioned solutions. The solution P^{\maxmin} offers the best minimum per-user data rate, which is consistent since the Problem 3.14 maximizes this criterion. We observe that the proportional fairness does not provide good minimum per-user data rate since it does not optimize that criterion.

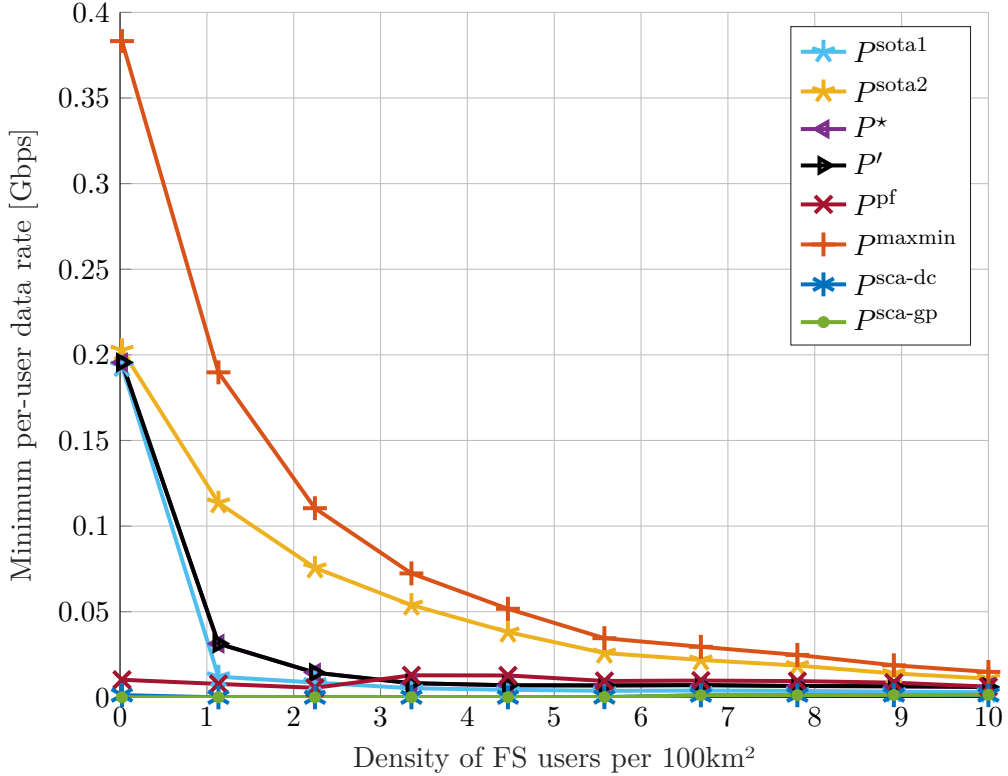


Figure 3.3: Minimum per-user data rate vs. FS density.

In Fig. 3.4, we plot the Jain's index versus the FS density. The solution P^{\maxmin} is better when the FS density is low. The algorithm proposed by the author of [8] is the fairest, regarding Jain's index, for high FS density, because it forces all users to transmit at the same power. In the presence of bottleneck users, however, this algorithm fails miserably for the system sum-rate criterion. If one user has high interference-temperature limits, the others may be unable to improve.

3.7 Conclusion

In this chapter, we have addressed optimization problems in the context of a multibeam satellite with an assumed linear HPA. More precisely, we formalized two power maximization problems. The first one, neglecting the inter-beam interference, is naturally convex and can be solved

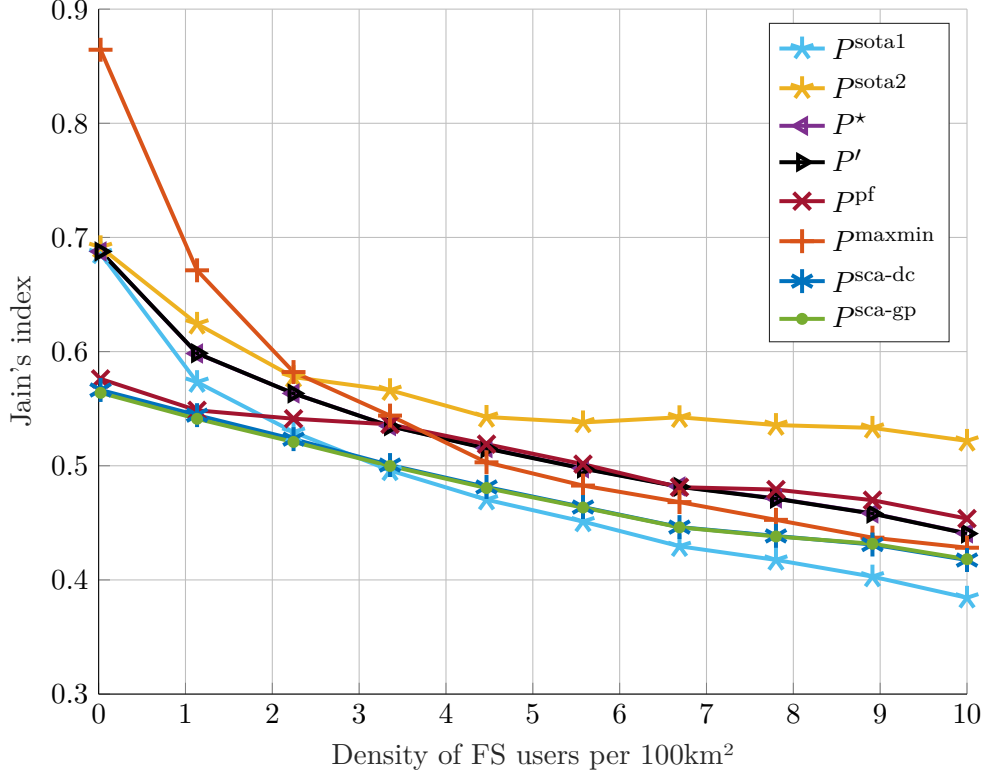


Figure 3.4: Jain index vs. FS density.

by numerical methods. We have proposed a simple algorithm to handle a very large number of primary constraints, which is consistent with the current scenario of network densification. The second problem considered is non-convex because of the consideration of the inter-beam interference. We have proposed two solutions using the SCA procedure. Two issues dealing with fairness among users were also formulated. The first problem maximizing the minimum flow rate has been rewritten in a convex manner and a numerical solver allows to obtain an optimal solution. The second non-convex proportional fairness problem was solved using an SCA procedure. Finally, we are interested in the joint optimization of subband assignment and power allocation. Assuming negligible inter-beam interference, we proposed two solutions. A summary of the addressed problems along with the proposed solutions is presented in Table 3.1.

Issue	Problem	Solution
Sum-rate	Problem 3.2	Waterfilling-like – Algorithm 3.1
		CVX
	Problem 3.1	SCA – Algorithm 3.2
		SCA – Algorithm 3.3
	Problem 3.5	Change of variable – CVX
		AO – CVX
Fairness	Problem 3.14	CVX
	Problem 3.18	SCA – Algorithm 3.4

Table 3.1: Addressed problems and proposed solutions.

Finally, part of the material presented in this chapter has been published in [C1] and [J2].

Closed-form expression of the data rate in presence of nonlinearities

For the uplink to the satellite, the users belonging to the same beam are separated into different subbands and different timeslots, by using the so-called *Multi-Frequency Time-Division Multiple Access (MF-TDMA)*, in order to avoid intra-beam interference. However, the use of the same subbands by other beams creates inter-beam interference.

This paradigm is no longer true when the satellite *High-Power Amplifier (HPA)* operates into the nonlinear regime. Here we assume one *HPA* per beam, such that a *HPA* works on the aggregate signal created by all the subbands. When operating in the nonlinear regime of the *HPA*, in-band and out-of-band distortions are generated causing a loss in performance. Finally, intra-beam interference is created, as well as inter-beam interference from all subbands.

In order to limit these drawbacks, we can proceed in three different ways:

- We force the system to work into the linear regime by applying an Input Back-Off (IBO). However, the energy efficiency of the *HPA* becomes lower. More importantly, the maximum sum-rate of the uplink system is not reached by fixing an operating point preventing nonlinearity to disturb the incoming signal.
- When operating in the non linear regime, pre-compensation methods (see [38] and reference therein) can be applied in order to mitigate nonlinear interference at the receiver side. However, in uplink, this approach can be only implemented in a distributed manner and, thus, it is not optimal anymore. Indeed, the whole cancellation of the nonlinear impairments is impossible since only in-band impairments can be pre-compensated for.
- Assuming the nonlinear regime, post-compensation at the end receiver (i.e. at the gateway in our uplink scenario) can be carried out but cannot increase the data rate according to data processing inequality [39].

In this chapter, we aim to evaluate theoretically the system sum-rate when operating in the nonlinear regime, in order to evaluate clearly the system capacity loss with respect to the case where the nonlinear interference is seen as an additional noise, as well as in order to investigate on the impact of the power allocation among the subbands. To do so, we derive a

closed-form expression for the sum-rate of the uplink multibeam satellite communication system when nonlinearity occurs. We do not assume pre-compensation as well as post-compensation.

The main contributions of this chapter can be summarized as follows:

- First, the impact of the satellite HPA is modeled through the use of Volterra series expansion of the received signal. While this model has been deeply investigated in [10], we propose here an alternative and elegant approach to derive analytically all required terms. Indeed, the proposed derivations for the sum-rate will rely on the closed-form derivations of the autocorrelation of the additional nonlinear term as well as the cross-correlation of this nonlinear term and the linear one. In the context of multiband communications, these terms have been characterized by [10]. Nevertheless, we can propose an alternative path to obtain much more compact and insightful closed-form expressions for these terms. We especially prove that they are all posynomials with respect to the powers. This property is useful for future resource allocation management presented in Chapters 5 and 6.
- Based on these new expressions, we are able to derive closed-form expressions for the sum-rate for two decoding strategies. First, we consider the optimal case for which the decoder takes into account the signal nonlinear structure. Then, we consider the case of a nonlinearity-agnostic decoder, for which any term coming from the nonlinearity is considered as an additional noise.

The rest of the chapter is organized as follows. In Section 4.1, we give the closed-form expression of the data rate when nonlinear effects occur. In Section 4.2, the involved terms in the data rate expression are derived in order to obtain a closed-form and show their properties. In Section 4.3, we present the numerical results of the Volterra coefficients and the sum-rate in nonlinear regime. Finally, Section 4.4 concludes this chapter.

4.1 Data rate expression in presence of nonlinearities

In this section, we provide a closed-form expression of the data rate when nonlinear effects occur. First, we focus on determining the achievable rate for a nonlinear memoryless channel. Then, we apply this expression to our satellite system.

4.1.1 Achievable data rate for nonlinear channel

In order to determine the achievable data rate of a nonlinear memoryless system, we use two different approaches that lead to the same result in our case, namely the *Pinsker's formula* and the *Bussgang decomposition*.

- The Pinsker's formula gives the mutual information between the channel input a and the channel output z [40]. Both of them are assumed to be complex-valued circularly-symmetric Gaussian random variables. In our case, the gaussianity of z can be assumed by the Central Limit Theorem.

- The Bussgang decomposition gives the achievable data rate for a nonlinear memoryless channel [41], where the channel input a and the additive noise are assumed to be Gaussian random variables and uncorrelated.

In Fig. 4.1, we emphasize the difference between a linear Gaussian channel used in Chapter 3 and a nonlinear memoryless channel.

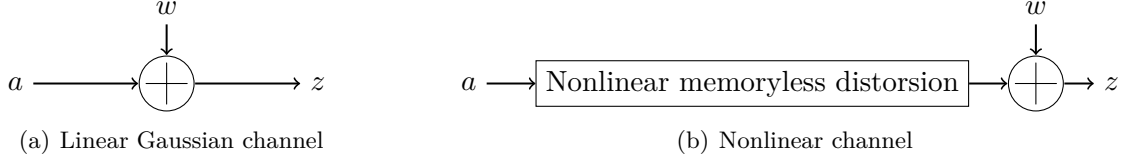


Figure 4.1: Illustration of linear Gaussian channel and nonlinear memoryless channel.

In the same way as a linear Gaussian channel, we have the achievable data rate expression of a nonlinear channel under the above mentioned conditions on a and z , given by [40, 41]

$$R = \log_2 \left(1 + \frac{\mathbb{E}[a\bar{z}] \mathbb{E}[z\bar{a}]}{\mathbb{E}[|a|^2] \mathbb{E}[z\bar{z}] - \mathbb{E}[a\bar{z}] \mathbb{E}[z\bar{a}]} \right). \quad (4.1)$$

4.1.2 Application on multibeam satellite system

We use the achievable data rate as evaluation of the data rate in the remainder of the manuscript, due to the non-optimal assumption on the symbols distribution. For applying (4.1) to our system, we assume that

- the transmitted symbols $\{a_{b,m,n}\}_{b,m,n}$ are independent and identically distributed complex-valued circularly-symmetric Gaussian random processes,
- and that the received sample sequence $z_{b,m,n}$ is an uncorrelated sequence with respect to b, m, n .

Reminding (1.13) and (4.1), the data rate for user belonging to beam b using subband m , denoted by $R_{b,m}$, becomes

$$R_{b,m} = \log_2 \left(1 + \frac{\mathbb{E}[z_{b,m,n}^{(L)} \bar{z}_{b,m,n}] \mathbb{E}[z_{b,m,n} \bar{z}_{b,m,n}^{(L)}]}{\mathbb{E}[|z_{b,m,n}^{(L)}|^2] \mathbb{E}[z_{b,m,n} \bar{z}_{b,m,n}] - \mathbb{E}[z_{b,m,n}^{(L)} \bar{z}_{b,m,n}] \mathbb{E}[z_{b,m,n} \bar{z}_{b,m,n}^{(L)}]} \right). \quad (4.2)$$

In order to go further, we use the decomposition (1.12) of $z_{b,m,n}$, and remind that $\mathbb{E}[z_{b,m,n}^{(L)} \bar{z}_{b,m,n}^{(I)}] = 0$ since the linear interference is not correlated to the current symbol. We introduce several terms to simplify the expression of the data rate,

- $\mathcal{P}_{b,m}^{(L)} = \mathbb{E}[|z_{b,m,n}^{(L)}|^2]$, the autocorrelation of the linear useful part, it can be interpreted as the power of the useful signal,
- $\mathcal{P}_{b,m}^{(I)} = \mathbb{E}[|z_{b,m,n}^{(I)}|^2]$, the autocorrelation of the linear interference part, it can be interpreted as the power of the linear interference,

- $\mathcal{P}_{b,m}^{(\text{NL})} = \mathbb{E} \left[\left| z_{b,m,n}^{(\text{NL})} \right|^2 \right]$, the autocorrelation of the nonlinear part, it can be interpreted as the power of the nonlinear interference,
- $\mathcal{P}_{b,m}^{(\text{LNL})} = \mathbb{E} \left[z_{b,m,n}^{(\text{L})} \bar{z}_{b,m,n}^{(\text{NL})} \right]$, the cross-correlation between the linear useful part and the nonlinear part,
- $\mathcal{P}_{b,m}^{(\text{INL})} = \mathbb{E} \left[z_{b,m,n}^{(\text{I})} \bar{z}_{b,m,n}^{(\text{NL})} \right]$, the cross-correlation between the linear interference part and the nonlinear part,
- $\mathcal{P}_W = \mathbb{E} \left[|w_{b,m,n}|^2 \right]$, the power of the [AWGN](#).

Finally, in the case where the receiver sees the nonlinear effects as an extra signal carrying useful information, called *nonlinearity-aware receiver*, the correlation between the nonlinear part ($z_{b,m,n}^{\text{NL}}$) and the linear part ($z_{k,n}^{\text{L}}$ and $z_{k,n}^{\text{I}}$) can bring additional information. For the nonlinearity-aware receiver, the data rate expression for user belonging to beam b using subband m is

$$R_{b,m} = \log_2 \left(1 + \frac{\mathcal{P}_{b,m}^{(\text{L})^2} + 2\mathcal{P}_{b,m}^{(\text{L})} \Re \left\{ \mathcal{P}_{b,m}^{(\text{LNL})} \right\} + \left| \mathcal{P}_{b,m}^{(\text{LNL})} \right|^2}{\mathcal{P}_{b,m}^{(\text{L})} \mathcal{P}_W + \mathcal{P}_{b,m}^{(\text{L})} \mathcal{P}_{b,m}^{(\text{I})} + \mathcal{P}_{b,m}^{(\text{L})} \mathcal{P}_{b,m}^{(\text{NL})} + 2\mathcal{P}_{b,m}^{(\text{L})} \Re \left\{ \mathcal{P}_{b,m}^{(\text{INL})} \right\} - \left| \mathcal{P}_{b,m}^{(\text{LNL})} \right|^2} \right), \quad (4.3)$$

where $\Re\{\cdot\}$ is the real part.

Remark 4.1. We show that the denominator is positive thanks to Cauchy-Schwarz inequality for complex random variables, which is $\left| \mathbb{E} \left[z_{b,m,n}^{(\text{L})} \bar{z}_{b,m,n}^{(\text{NL})} \right] \right|^2 \leq \mathbb{E} \left[\left| z_{b,m,n}^{(\text{L})} \right|^2 \right] \mathbb{E} \left[\left| z_{b,m,n}^{(\text{NL})} \right|^2 \right]$ and so $\left| \mathcal{P}_{b,m}^{(\text{LNL})} \right|^2 \leq \mathcal{P}_{b,m}^{(\text{L})} \mathcal{P}_{b,m}^{(\text{NL})}$.

Remark 4.2. The cross-correlation between the linear useful part and the nonlinear part plays a significant role in the data rate. If $\Re \left\{ \mathcal{P}_{b,m}^{(\text{LNL})} \right\} > 0$, the data rate is higher than the case $\Re \left\{ \mathcal{P}_{b,m}^{(\text{LNL})} \right\} = 0$. In addition, the data rate does not vanish even if $\mathcal{P}_{b,m}^{(\text{L})} = 0$, since the nonlinear term provides information on the current symbol. Notice that in [10], only the following Mean Square Error (MSE) is analyzed.

$$\mathbb{E} \left[\left| z_{b,m,n} - \gamma_1 \sqrt{G_m^{(b)}} a_{b,m,n} \right|^2 \right] = \mathcal{P}_{b,m}^{(\text{NL})} + \mathcal{P}_W.$$

which does not capture the role of the cross-correlation. Actually, the cross correlation in [10] occurred since the author considered that $h_1(nT_s, m)$ may not vanish for non-zero n or m . But under our orthogonality assumption, the cross-correlation term disappears in the MSE.

Remark 4.3. We can also show that if the [HPA](#) operates in linear regime, i.e. $\gamma_3 = 0$, all the nonlinear terms disappear and only linear terms remain. The data rate for user belonging to beam b using subband m becomes

$$R_{\text{lin. interf.}} = \log_2 \left(1 + \frac{\mathcal{P}_{b,m}^{(\text{L})}}{\mathcal{P}_W + \mathcal{P}_{b,m}^{(\text{I})}} \right). \quad (4.4)$$

The obtained data rate expression is exactly (3.1) used in Chapter 3 where the [HPA](#) is considered linear.

In the case where the receiver sees the nonlinear interference as just additional noise and is not adapted to the presence of nonlinearities, called *nonlinearity-agnostic receiver*, as currently done in most receivers, we just have to calculate the [SINR](#). As a consequence, the data rate of user belonging to beam b using subband m becomes

$$R_{b,m} = \log_2 \left(1 + \frac{\mathcal{P}_{b,m}^{(L)}}{\mathcal{P}_W + \mathcal{P}_{b,m}^{(I)} + \mathcal{P}_{b,m}^{(NL)}} \right). \quad (4.5)$$

Remark 4.4. *The data rate expression of the nonlinearity-agnostic receiver is equivalent to the expression of the nonlinearity-aware receiver when the linear and the nonlinear part are uncorrelated, i.e., when we put $\mathcal{P}_{b,m}^{(LNL)} = 0$ and $\mathcal{P}_{b,m}^{(INL)} = 0$ inside (4.3). It means that the nonlinearity-agnostic receiver supposes that nonlinear effects are not correlated to the linear signal, and they cannot be exploited and bring additional information.*

To sum up this section, two data rate expressions have been given according to the considered receiver. Thus if the cross-correlation between the useful linear part and the nonlinear part vanishes, the nonlinear effects purely corresponds to a degradation. If not, taking into account the cross-correlation at the decoder side is of interest. However, it remains to express in a complete way the terms involved in the data rate expressions, namely $\mathcal{P}_{b,m}^{(L)}$, $\mathcal{P}_{b,m}^{(I)}$, $\mathcal{P}_{b,m}^{(NL)}$, $\mathcal{P}_{b,m}^{(INL)}$ and $\mathcal{P}_{b,m}^{(LNL)}$.

4.2 Closed-form expressions for the involved terms in data rate

The goal of this section is to provide compact and insightful closed-form expressions for all the terms involved in the data rate expressions (4.3) and (4.5).

4.2.1 Expression for the power of the useful signal

The power of the useful signal is defined by $\mathcal{P}_{b,m}^{(L)} = \mathbb{E} \left[\left| z_{b,m,n}^{(L)} \right|^2 \right]$. According to (1.13), we obtain

$$\mathcal{P}_{b,m}^{(L)} = \gamma_1^2 G_m^{(b)} P_{b,m} \quad (4.6)$$

where $P_{b,m} = \mathbb{E}[|a_{b,m,n}|^2]$ is the transmit power of user belonging to beam b using subband m .

Result 4.1. *The term $\mathcal{P}_{b,m}^{(L)}$ is a monomial function in \mathbf{P} .*

4.2.2 Expression for the power of the linear interference

The power of the linear interference is defined by $\mathcal{P}_{b,m}^{(I)} = \mathbb{E} \left[\left| z_{b,m,n}^{(I)} \right|^2 \right]$. According to (1.14), we obtain

$$\mathcal{P}_{b,m}^{(I)} = \gamma_1^2 \sum_{\substack{b'=1 \\ b' \neq b}}^B G_m^{(b',b)} P_{b',m} \quad (4.7)$$

where $P_{b',m} = \mathbb{E}[|a_{b',m,n}|^2]$ is the transmit power of user belonging to beam b' using subband m .

Result 4.2. *The term $\mathcal{P}_{b,m}^{(I)}$ is a posynomial function in \mathbf{P} .*

4.2.3 Expression for the power of the nonlinear interference

The power of the nonlinear interference is defined by $\mathcal{P}_{b,m}^{(\text{NL})} = \mathbb{E} \left[\left| z_{b,m,n}^{(\text{NL})} \right|^2 \right]$. According to (1.15), we obtain

$$\begin{aligned} \mathcal{P}_{b,m}^{(\text{NL})} &= \gamma_3^2 \sum_{b_1, b_2, b_3=1}^B \sum_{b'_1, b'_2, b'_3=1}^B \sum_{m_1, m_2, m_3=1}^M \sum_{m'_1, m'_2, m'_3=1}^M \sum_{n_1, n_2, n_3 \in \mathbb{Z}} \sum_{n'_1, n'_2, n'_3 \in \mathbb{Z}} e^{2i\pi(m_1+m_2-m_3-m)\Delta F n T_s} \\ &\times e^{-2i\pi(m'_1+m'_2-m'_3-m)\Delta F n T_s} \\ &\times \sqrt{G_{m_1}^{(b_1,b)} G_{m_2}^{(b_2,b)} G_{m_3}^{(b_3,b)}} \sqrt{G_{m'_1}^{(b'_1,b)} G_{m'_2}^{(b'_2,b)} G_{m'_3}^{(b'_3,b)}} \\ &\times \mathbb{E} \left[a_{b_1, m_1, n-n_1} a_{b_2, m_2, n-n_2} \overline{a_{b_3, m_3, n-n_3} a_{b'_1, m'_1, n-n'_1} a_{b'_2, m'_2, n-n'_2} a_{b'_3, m'_3, n-n'_3}} \right] \\ &\times h_3(n_1 T_s, n_2 T_s, n_3 T_s, m_1 + m_2 - m_3 - m) \bar{h}_3(n'_1 T_s, n'_2 T_s, n'_3 T_s, m'_1 + m'_2 - m'_3 - m). \end{aligned} \quad (4.8)$$

This term is already involved in the derivations done in [10]. Nevertheless, the expressions provided in [10] is quite complicated and spread over the paper. Here, we propose a new way to derive $\mathcal{P}_{b,m}^{(\text{NL})}$ in order to obtain a more compact and insightful form. So, unlike [10], we start by managing the term $\mathbb{E} \left[a_{b_1, m_1, n-n_1} a_{b_2, m_2, n-n_2} \overline{a_{b_3, m_3, n-n_3} a_{b'_1, m'_1, n-n'_1} a_{b'_2, m'_2, n-n'_2} a_{b'_3, m'_3, n-n'_3}} \right]$ and then the term h_3 .

As symbols $\{a_{b,m,n}\}$ are assumed to be circularly-symmetric complex-valued Gaussian random variables, according to [42, 43] based on Isserlis' theorem for zero-mean multivariate normal random vector, we have

$$\begin{aligned} &\mathbb{E} \left[a_{b_1, m_1, n-n_1} a_{b_2, m_2, n-n_2} \overline{a_{b_3, m_3, n-n_3} a_{b'_1, m'_1, n-n'_1} a_{b'_2, m'_2, n-n'_2} a_{b'_3, m'_3, n-n'_3}} \right] = \\ &\mathbb{E} \left[a_{b_1, m_1, n-n_1} \overline{a_{b'_1, m'_1, n-n'_1}} \right] \mathbb{E} \left[a_{b_2, m_2, n-n_2} \overline{a_{b_3, m_3, n-n_3}} \right] \mathbb{E} \left[\overline{a_{b'_2, m'_2, n-n'_2} a_{b'_3, m'_3, n-n'_3}} \right] \\ &+ \mathbb{E} \left[a_{b_1, m_1, n-n_1} \overline{a_{b'_1, m'_1, n-n'_1}} \right] \mathbb{E} \left[a_{b_2, m_2, n-n_2} \overline{a_{b'_2, m'_2, n-n'_2}} \right] \mathbb{E} \left[\overline{a_{b_3, m_3, n-n_3} a_{b'_3, m'_3, n-n'_3}} \right] \\ &+ \mathbb{E} \left[a_{b_1, m_1, n-n_1} \overline{a_{b_3, m_3, n-n_3}} \right] \mathbb{E} \left[a_{b_2, m_2, n-n_2} \overline{a_{b'_2, m'_2, n-n'_2}} \right] \mathbb{E} \left[\overline{a_{b'_1, m'_1, n-n'_1} a_{b'_3, m'_3, n-n'_3}} \right] \\ &+ \mathbb{E} \left[a_{b_1, m_1, n-n_1} \overline{a_{b_3, m_3, n-n_3}} \right] \mathbb{E} \left[a_{b_2, m_2, n-n_2} \overline{a_{b'_1, m'_1, n-n'_1}} \right] \mathbb{E} \left[\overline{a_{b'_2, m'_2, n-n'_2} a_{b'_3, m'_3, n-n'_3}} \right] \\ &+ \mathbb{E} \left[a_{b_1, m_1, n-n_1} \overline{a_{b'_2, m'_2, n-n'_2}} \right] \mathbb{E} \left[a_{b_2, m_2, n-n_2} \overline{a_{b_3, m_3, n-n_3}} \right] \mathbb{E} \left[\overline{a_{b'_1, m'_1, n-n'_1} a_{b'_3, m'_3, n-n'_3}} \right] \\ &+ \mathbb{E} \left[a_{b_1, m_1, n-n_1} \overline{a_{b'_2, m'_2, n-n'_2}} \right] \mathbb{E} \left[a_{b_2, m_2, n-n_2} \overline{a_{b'_1, m'_1, n-n'_1}} \right] \mathbb{E} \left[\overline{a_{b_3, m_3, n-n_3} a_{b'_3, m'_3, n-n'_3}} \right]. \end{aligned} \quad (4.9)$$

Remark 4.5. We notice that in the case of constrained constellations currently used in communication systems, the cumulant would be added in this decomposition.

As we have six additive terms in (4.9), we can split (4.8) into six terms as follows

$$\mathcal{P}_{b,m}^{(\text{NL})} = p_{b,m}^{(\text{NL},1)} + p_{b,m}^{(\text{NL},2)} + p_{b,m}^{(\text{NL},3)} + p_{b,m}^{(\text{NL},4)} + p_{b,m}^{(\text{NL},5)} + p_{b,m}^{(\text{NL},6)} \quad (4.10)$$

with

$$\begin{aligned}
p_{b,m}^{(\text{NL},1)} &= \gamma_3^2 \sum_{b_1, b_2, b_3=1}^B \sum_{b'_1, b'_2, b'_3=1}^B \sum_{m_1, m_2, m_3=1}^M \sum_{m'_1, m'_2, m'_3=1}^M \sum_{n_1, n_2, n_3 \in \mathbb{Z}} \sum_{n'_1, n'_2, n'_3 \in \mathbb{Z}} e^{2i\pi(m_1+m_2-m_3-m)\Delta F n T_s} \\
&\times e^{-2i\pi(m'_1+m'_2-m'_3-m)\Delta F n T_s} \\
&\times \sqrt{G_{m_1}^{(b_1,b)} G_{m_2}^{(b_2,b)} G_{m_3}^{(b_3,b)}} \sqrt{G_{m'_1}^{(b'_1,b)} G_{m'_2}^{(b'_2,b)} G_{m'_3}^{(b'_3,b)}} \\
&\times \mathbb{E} \left[a_{b_1, m_1, n-n_1} \overline{a_{b'_1, m'_1, n-n'_1}} \right] \mathbb{E} \left[a_{b_2, m_2, n-n_2} \overline{a_{b'_2, m'_2, n-n'_2}} \right] \mathbb{E} \left[\overline{a_{b'_2, m'_2, n-n'_2}} a_{b'_3, m'_3, n-n'_3} \right] \\
&\times h_3(n_1 T_s, n_2 T_s, n_3 T_s, m_1 + m_2 - m_3 - m) \overline{h_3}(n'_1 T_s, n'_2 T_s, n'_3 T_s, m'_1 + m'_2 - m'_3 - m), \quad (4.11)
\end{aligned}$$

$$\begin{aligned}
p_{b,m}^{(\text{NL},2)} &= \gamma_3^2 \sum_{b_1, b_2, b_3=1}^B \sum_{b'_1, b'_2, b'_3=1}^B \sum_{m_1, m_2, m_3=1}^M \sum_{m'_1, m'_2, m'_3=1}^M \sum_{n_1, n_2, n_3 \in \mathbb{Z}} \sum_{n'_1, n'_2, n'_3 \in \mathbb{Z}} e^{2i\pi(m_1+m_2-m_3-m)\Delta F n T_s} \\
&\times e^{-2i\pi(m'_1+m'_2-m'_3-m)\Delta F n T_s} \\
&\times \sqrt{G_{m_1}^{(b_1,b)} G_{m_2}^{(b_2,b)} G_{m_3}^{(b_3,b)}} \sqrt{G_{m'_1}^{(b'_1,b)} G_{m'_2}^{(b'_2,b)} G_{m'_3}^{(b'_3,b)}} \\
&\times \mathbb{E} \left[a_{b_1, m_1, n-n_1} \overline{a_{b'_1, m'_1, n-n'_1}} \right] \mathbb{E} \left[a_{b_2, m_2, n-n_2} \overline{a_{b'_2, m'_2, n-n'_2}} \right] \mathbb{E} \left[\overline{a_{b_3, m_3, n-n_3}} a_{b'_3, m'_3, n-n'_3} \right] \\
&\times h_3(n_1 T_s, n_2 T_s, n_3 T_s, m_1 + m_2 - m_3 - m) \overline{h_3}(n'_1 T_s, n'_2 T_s, n'_3 T_s, m'_1 + m'_2 - m'_3 - m), \quad (4.12)
\end{aligned}$$

$$\begin{aligned}
p_{b,m}^{(\text{NL},3)} &= \gamma_3^2 \sum_{b_1, b_2, b_3=1}^B \sum_{b'_1, b'_2, b'_3=1}^B \sum_{m_1, m_2, m_3=1}^M \sum_{m'_1, m'_2, m'_3=1}^M \sum_{n_1, n_2, n_3 \in \mathbb{Z}} \sum_{n'_1, n'_2, n'_3 \in \mathbb{Z}} e^{2i\pi(m_1+m_2-m_3-m)\Delta F n T_s} \\
&\times e^{-2i\pi(m'_1+m'_2-m'_3-m)\Delta F n T_s} \\
&\times \sqrt{G_{m_1}^{(b_1,b)} G_{m_2}^{(b_2,b)} G_{m_3}^{(b_3,b)}} \sqrt{G_{m'_1}^{(b'_1,b)} G_{m'_2}^{(b'_2,b)} G_{m'_3}^{(b'_3,b)}} \\
&\times \mathbb{E} \left[a_{b_1, m_1, n-n_1} \overline{a_{b_3, m_3, n-n_3}} \right] \mathbb{E} \left[a_{b_2, m_2, n-n_2} \overline{a_{b'_2, m'_2, n-n'_2}} \right] \mathbb{E} \left[\overline{a_{b'_1, m'_1, n-n'_1}} a_{b'_3, m'_3, n-n'_3} \right] \\
&\times h_3(n_1 T_s, n_2 T_s, n_3 T_s, m_1 + m_2 - m_3 - m) \overline{h_3}(n'_1 T_s, n'_2 T_s, n'_3 T_s, m'_1 + m'_2 - m'_3 - m), \quad (4.13)
\end{aligned}$$

$$\begin{aligned}
p_{b,m}^{(\text{NL},4)} &= \gamma_3^2 \sum_{b_1, b_2, b_3=1}^B \sum_{b'_1, b'_2, b'_3=1}^B \sum_{m_1, m_2, m_3=1}^M \sum_{m'_1, m'_2, m'_3=1}^M \sum_{n_1, n_2, n_3 \in \mathbb{Z}} \sum_{n'_1, n'_2, n'_3 \in \mathbb{Z}} e^{2i\pi(m_1+m_2-m_3-m)\Delta F n T_s} \\
&\times e^{-2i\pi(m'_1+m'_2-m'_3-m)\Delta F n T_s} \\
&\times \sqrt{G_{m_1}^{(b_1,b)} G_{m_2}^{(b_2,b)} G_{m_3}^{(b_3,b)}} \sqrt{G_{m'_1}^{(b'_1,b)} G_{m'_2}^{(b'_2,b)} G_{m'_3}^{(b'_3,b)}} \\
&\times \mathbb{E} \left[a_{b_1, m_1, n-n_1} \overline{a_{b_3, m_3, n-n_3}} \right] \mathbb{E} \left[a_{b_2, m_2, n-n_2} \overline{a_{b'_1, m'_1, n-n'_1}} \right] \mathbb{E} \left[\overline{a_{b'_2, m'_2, n-n'_2}} a_{b'_3, m'_3, n-n'_3} \right] \\
&\times h_3(n_1 T_s, n_2 T_s, n_3 T_s, m_1 + m_2 - m_3 - m) \overline{h_3}(n'_1 T_s, n'_2 T_s, n'_3 T_s, m'_1 + m'_2 - m'_3 - m), \quad (4.14)
\end{aligned}$$

$$\begin{aligned}
p_{b,m}^{(\text{NL},5)} &= \gamma_3^2 \sum_{b_1, b_2, b_3=1}^B \sum_{b'_1, b'_2, b'_3=1}^B \sum_{m_1, m_2, m_3=1}^M \sum_{m'_1, m'_2, m'_3=1}^M \sum_{n_1, n_2, n_3 \in \mathbb{Z}} \sum_{n'_1, n'_2, n'_3 \in \mathbb{Z}} e^{2i\pi(m_1+m_2-m_3-m)\Delta F n T_s} \\
&\times e^{-2i\pi(m'_1+m'_2-m'_3-m)\Delta F n T_s} \\
&\times \sqrt{G_{m_1}^{(b_1,b)} G_{m_2}^{(b_2,b)} G_{m_3}^{(b_3,b)}} \sqrt{G_{m'_1}^{(b'_1,b)} G_{m'_2}^{(b'_2,b)} G_{m'_3}^{(b'_3,b)}} \\
&\times \mathbb{E} \left[a_{b_1, m_1, n-n_1} \overline{a_{b'_2, m'_2, n-n'_2}} \right] \mathbb{E} \left[a_{b_2, m_2, n-n_2} \overline{a_{b_3, m_3, n-n_3}} \right] \mathbb{E} \left[\overline{a_{b'_1, m'_1, n-n'_1}} a_{b'_3, m'_3, n-n'_3} \right] \\
&\times h_3(n_1 T_s, n_2 T_s, n_3 T_s, m_1+m_2-m_3-m) \overline{h_3}(n'_1 T_s, n'_2 T_s, n'_3 T_s, m'_1+m'_2-m'_3-m), \quad (4.15)
\end{aligned}$$

and

$$\begin{aligned}
p_{b,m}^{(\text{NL},6)} &= \gamma_3^2 \sum_{b_1, b_2, b_3=1}^B \sum_{b'_1, b'_2, b'_3=1}^B \sum_{m_1, m_2, m_3=1}^M \sum_{m'_1, m'_2, m'_3=1}^M \sum_{n_1, n_2, n_3 \in \mathbb{Z}} \sum_{n'_1, n'_2, n'_3 \in \mathbb{Z}} e^{2i\pi(m_1+m_2-m_3-m)\Delta F n T_s} \\
&\times e^{-2i\pi(m'_1+m'_2-m'_3-m)\Delta F n T_s} \\
&\times \sqrt{G_{m_1}^{(b_1,b)} G_{m_2}^{(b_2,b)} G_{m_3}^{(b_3,b)}} \sqrt{G_{m'_1}^{(b'_1,b)} G_{m'_2}^{(b'_2,b)} G_{m'_3}^{(b'_3,b)}} \\
&\times \mathbb{E} \left[a_{b_1, m_1, n-n_1} \overline{a_{b'_2, m'_2, n-n'_2}} \right] \mathbb{E} \left[a_{b_2, m_2, n-n_2} \overline{a_{b'_1, m'_1, n-n'_1}} \right] \mathbb{E} \left[\overline{a_{b_3, m_3, n-n_3}} a_{b'_3, m'_3, n-n'_3} \right] \\
&\times h_3(n_1 T_s, n_2 T_s, n_3 T_s, m_1+m_2-m_3-m) \overline{h_3}(n'_1 T_s, n'_2 T_s, n'_3 T_s, m'_1+m'_2-m'_3-m). \quad (4.16)
\end{aligned}$$

We can show that $p_{b,m}^{(\text{NL},1)} = p_{b,m}^{(\text{NL},5)}$, $p_{b,m}^{(\text{NL},2)} = p_{b,m}^{(\text{NL},6)}$ and $p_{b,m}^{(\text{NL},3)} = p_{b,m}^{(\text{NL},4)}$ if we switch b'_2, m'_2, n'_2 with b'_1, m'_1, n'_1 .

Finally, we have

$$\mathcal{P}_{b,m}^{(\text{NL})} = 2p_{b,m}^{(\text{NL},1)} + 2p_{b,m}^{(\text{NL},2)} + 2p_{b,m}^{(\text{NL},3)}. \quad (4.17)$$

It remains now to derive in closed-form each term. Let us focus first on $p_{b,m}^{(\text{NL},1)}$.

Derivations for $p_{b,m}^{(\text{NL},1)}$

A lot of indexes can be removed in (4.11) by remarking that the terms dealing with the symbol expectation are non-null only if both first indexes are equal to each other and if both second indexes and if both third indexes are equal to each others. Thus, we have $b_1 = b'_1$, $b_2 = b_3$, $b'_2 = b'_3$ and $m_1 = m'_1$, $m_2 = m_3$, $m'_2 = m'_3$ and $n_1 = n'_1$, $n_2 = n_3$, $n'_2 = n'_3$. Consequently, we obtain

$$\begin{aligned}
p_{b,m}^{(\text{NL},1)} &= \gamma_3^2 \sum_{m_1, m_2, m'_2=1}^M \sum_{b_1, b_2, b'_2=1}^B \sum_{n_1, n_2, n'_2 \in \mathbb{Z}} e^{2i\pi(m_1+m_2-m_2-m)\Delta F n T_s} e^{-2i\pi(m_1+m'_2-m'_2-m)\Delta F n T_s} \\
&\times G_{m_1}^{(b_1,b)} G_{m_2}^{(b_2,b)} G_{m'_2}^{(b'_2,b)} \\
&\times \mathbb{E} \left[a_{b_1, m_1, n-n_1} \overline{a_{b_1, m_1, n-n_1}} \right] \mathbb{E} \left[a_{b_2, m_2, n-n_2} \overline{a_{b_2, m_2, n-n_2}} \right] \mathbb{E} \left[\overline{a_{b'_2, m'_2, n-n'_2}} a_{b'_2, m'_2, n-n'_2} \right] \\
&\times h_3(n_1 T_s, n_2 T_s, n_2 T_s, m_1+m_2-m_2-m) \overline{h_3}(n_1 T_s, n'_2 T_s, n'_2 T_s, m_1+m'_2-m'_2-m), \quad (4.18)
\end{aligned}$$

which simplifies as follows

$$\begin{aligned}
p_{b,m}^{(\text{NL},1)} &= \gamma_3^2 \sum_{b_1, b_2, b'_2=1}^B \sum_{m_1, m_2, m'_2=1}^M \sum_{n_1, n_2, n'_2 \in \mathbb{Z}} G_{m_1}^{(b_1,b)} G_{m_2}^{(b_2,b)} G_{m'_2}^{(b'_2,b)} P_{b_1, m_1} P_{b_2, m_2} P_{b'_2, m'_2} \\
&\times h_3(n_1 T_s, n_2 T_s, n_2 T_s, m_1-m) \overline{h_3}(n_1 T_s, n'_2 T_s, n'_2 T_s, m_1-m). \quad (4.19)
\end{aligned}$$

According to [10], the interference coming from the subband is non-negligible only for the current subband and its adjacent subbands. In Figs 4.2 and 4.3, we plot the term third order Volterra kernel h_3 (in semilog-scale) as a function of frequency and time respectively. We effectively observe in Fig. 4.2 that the current subband and its adjacent subbands plays a major role. We can notice in Fig. 4.3 that h_3 is not zero and finally we have to keep all time indexes for the transmission model.

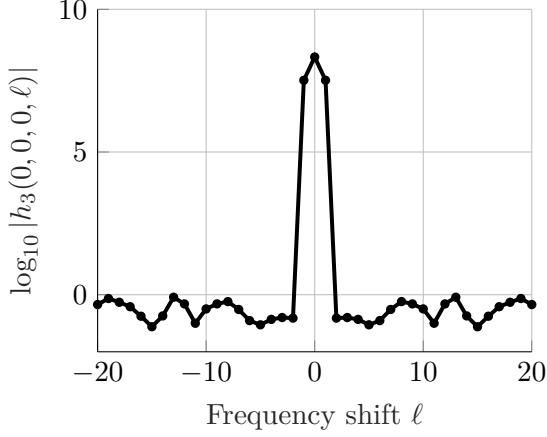


Figure 4.2: Volterra coefficient h_3 versus the frequency shift ℓ , for $t_1 = t_2 = t_3 = 0$.

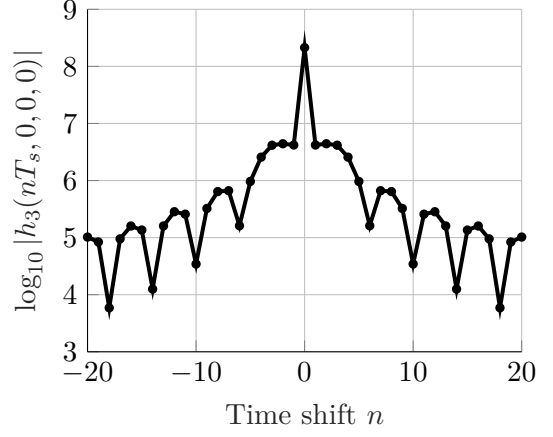


Figure 4.3: Volterra coefficient h_3 versus the time shift n , for $t_1 = nT_s$, $t_2 = t_3 = 0$, and $\ell = 0$.

Consequently, only $(m_1 - m) \in \{-1, 0, 1\}$ are considered (majority of the interference comes from the subband itself and its adjacent neighbors). Therefore, (4.19) can be decomposed into three terms,

$$p_{b,m}^{(\text{NL},1)} = p_{b,m}^{(\text{NL},1),0} + p_{b,m}^{(\text{NL},1),1} + p_{b,m}^{(\text{NL},1),-1}, \quad (4.20)$$

where

$$p_{b,m}^{(\text{NL},1),0} = \gamma_3^2 \sum_{b_1, b_2, b'_2=1}^B \sum_{m_1, m_2, m'_2=1}^M \sum_{n_1, n_2, n'_2 \in \mathbb{Z}} G_{m_1}^{(b_1,b)} G_{m_2}^{(b_2,b)} G_{m'_2}^{(b'_2,b)} P_{b_1, m_1} P_{b_2, m_2} P_{b'_2, m'_2} \times h_3(n_1 T_s, n_2 T_s, n_2 T_s, m_1 - m = 0) \overline{h_3}(n_1 T_s, n'_2 T_s, n'_2 T_s, m_1 - m = 0), \quad (4.21)$$

is the interference created by the subband itself,

$$p_{b,m}^{(\text{NL},1),1} = \gamma_3^2 \sum_{b_1, b_2, b'_2=1}^B \sum_{m_1, m_2, m'_2=1}^M \sum_{n_1, n_2, n'_2 \in \mathbb{Z}} G_{m_1}^{(b_1,b)} G_{m_2}^{(b_2,b)} G_{m'_2}^{(b'_2,b)} P_{b_1, m_1} P_{b_2, m_2} P_{b'_2, m'_2} \times h_3(n_1 T_s, n_2 T_s, n_2 T_s, m_1 - m = 1) \overline{h_3}(n_1 T_s, n'_2 T_s, n'_2 T_s, m_1 - m = 1), \quad (4.22)$$

is the interference created by the left adjacent subband, and

$$p_{b,m}^{(\text{NL},1),-1} = \gamma_3^2 \sum_{b_1, b_2, b'_2=1}^B \sum_{m_1, m_2, m'_2=1}^M \sum_{n_1, n_2, n'_2 \in \mathbb{Z}} G_{m_1}^{(b_1,b)} G_{m_2}^{(b_2,b)} G_{m'_2}^{(b'_2,b)} P_{b_1, m_1} P_{b_2, m_2} P_{b'_2, m'_2} \times h_3(n_1 T_s, n_2 T_s, n_2 T_s, m_1 - m = -1) \overline{h_3}(n_1 T_s, n'_2 T_s, n'_2 T_s, m_1 - m = -1), \quad (4.23)$$

is the interference created by the right adjacent subband.

It remains now to focus on the third order Volterra kernel in order to derive in closed-form these three terms:

- Case $m_1 - m = 0$ (intra-subband interference). As a consequence, we have

$$p_{b,m}^{(\text{NL},1),0} = \gamma_3^2 \sum_{b_1, b_2, b'_2=1}^B \sum_{m_2, m'_2=1}^M G_m^{(b_1,b)} G_{m_2}^{(b_2,b)} G_{m'_2}^{(b'_2,b)} P_{b_1,m} P_{b_2,m_2} P_{b'_2,m'_2} \sum_{n_1 \in \mathbb{Z}} \sum_{n_2 \in \mathbb{Z}} \sum_{n'_2 \in \mathbb{Z}} \times h_3(n_1 T_s, n_2 T_s, n_2 T_s, 0) \overline{h_3}(n_1 T_s, n'_2 T_s, n'_2 T_s, 0). \quad (4.24)$$

By changing some indexes notations, we finally obtain for user belonging to beam b using subband m

$$p_{b,m}^{(\text{NL},1),0} = \gamma_3^2 \alpha_0^{(1)} \sum_{b_1, b_2, b_3}^B \sum_{m', m''=1}^M G_m^{(b_1,b)} G_{m'}^{(b_2,b)} G_{m''}^{(b_3,b)} P_{b_1,m} P_{b_2,m'} P_{b_3,m''} \quad (4.25)$$

with

$$\alpha_\ell^{(1)} = \sum_{n' \in \mathbb{Z}} \left| \sum_{n'' \in \mathbb{Z}} h_3(n' T_s, n'' T_s, n'' T_s, \ell) \right|^2. \quad (4.26)$$

Result 4.3. We conclude that $\alpha_\ell^{(1)}$ is positive $\forall \ell$.

- Case $m_1 - m = 1$ (right adjacent subband interference). As a consequence, we have for $m \neq M$

$$p_{b,m}^{(\text{NL},1),1} = \gamma_3^2 \alpha_1^{(1)} \sum_{b_1, b_2, b_3=1}^B \sum_{m', m''=1}^M G_{m+1}^{(b_1,b)} G_{m'}^{(b_2,b)} G_{m''}^{(b_3,b)} P_{b_1,m+1} P_{b_2,m'} P_{b_3,m''}. \quad (4.27)$$

- Case $m_1 - m = -1$ (left adjacent subband interference). As a consequence, we have for $m \neq 1$

$$p_{b,m}^{(\text{NL},1),-1} = \gamma_3^2 \alpha_1^{(1)} \sum_{b_1, b_2, b_3=1}^B \sum_{m', m''=1}^M G_{m-1}^{(b_1,b)} G_{m'}^{(b_2,b)} G_{m''}^{(b_3,b)} P_{b_1,m-1} P_{b_2,m'} P_{b_3,m''}. \quad (4.28)$$

Remark 4.6. We notice that $\alpha_{-1}^{(1)} = \alpha_1^{(1)}$.

Derivations for $p_{b,m}^{(\text{NL},2)}$

A lot of indexes can be removed in (4.12) by remarking that the terms dealing with the symbol expectation are non-null only if both first indexes are equal to each other and if both second indexes are equal to each others and if both third indexes are equal to each others. Consequently, we have $b_1 = b'_1$, $b_2 = b'_2$, $b_3 = b'_3$ and $m_1 = m'_1$, $m_2 = m'_2$, $m_3 = m'_3$ and $n_1 = n'_1$, $n_2 = n'_2$,

$n_3 = n'_3$. So

$$\begin{aligned}
p_{b,m}^{(\text{NL},2)} &= \gamma_3^2 \sum_{b_1, b_2, b_3=1}^B \sum_{m_1, m_2, m_3=1}^M \sum_{n_1, n_2, n_3 \in \mathbb{Z}} e^{2i\pi(m_1+m_2-m_3-m)\Delta F n T_s} e^{-2i\pi(m_1+m_2-m_3-m)\Delta F n T_s} \\
&\times G_{m_1}^{(b_1, b)} G_{m_2}^{(b_2, b)} G_{m_3}^{(b_3, b)} \\
&\times \mathbb{E}[a_{b_1, m_1, n-n_1} \overline{a_{b_1, m_1, n-n_1}}] \mathbb{E}[a_{b_2, m_2, n-n_2} \overline{a_{b_2, m_2, n-n_2}}] \mathbb{E}[\overline{a_{b_3, m_3, n-n_3}} a_{b_3, m_3, n-n_3}] \\
&\times h_3(n_1 T_s, n_2 T_s, n_3 T_s, m_1 + m_2 - m_3 - m) \overline{h_3}(n_1 T_s, n_2 T_s, n_3 T_s, m_1 + m_2 - m_3 - m), \quad (4.29)
\end{aligned}$$

which simplifies as follows

$$\begin{aligned}
p_{b,m}^{(\text{NL},2)} &= \gamma_3^2 \sum_{b_1, b_2, b_3=1}^B \sum_{m_1, m_2, m_3=1}^M \sum_{n_1, n_2, n_3 \in \mathbb{Z}} G_{m_1}^{(b_1, b)} G_{m_2}^{(b_2, b)} G_{m_3}^{(b_3, b)} P_{b_1, m_1} P_{b_2, m_2} P_{b_3, m_3} \\
&\times h_3(n_1 T_s, n_2 T_s, n_3 T_s, m_1 + m_2 - m_3 - m) \overline{h_3}(n_1 T_s, n_2 T_s, n_3 T_s, m_1 + m_2 - m_3 - m). \quad (4.30)
\end{aligned}$$

According to [10], the interference coming from the subband is non-negligible only for the current subband and its adjacent subbands. Consequently, only $(m_1 + m_2 - m_3 - m) \in \{-1, 0, 1\}$ are considered (majority of the interference comes from the subband itself and its adjacent neighbors).

It means that (4.30) can be decomposed into three terms,

$$p_{b,m}^{(\text{NL},2)} = p_{b,m}^{(\text{NL},2),0} + p_{b,m}^{(\text{NL},2),1} + p_{b,m}^{(\text{NL},2),-1}, \quad (4.31)$$

where

$$\begin{aligned}
p_{b,m}^{(\text{NL},2),0} &= \gamma_3^2 \sum_{b_1, b_2, b_3=1}^B \sum_{m_1, m_2, m_3=1}^M \sum_{n_1, n_2, n_3 \in \mathbb{Z}} G_{m_1}^{(b_1, b)} G_{m_2}^{(b_2, b)} G_{m_3}^{(b_3, b)} P_{b_1, m_1} P_{b_2, m_2} P_{b_3, m_3} \\
&\times h_3(n_1 T_s, n_2 T_s, n_3 T_s, m_1 + m_2 - m_3 - m = 0) \\
&\times \overline{h_3}(n_1 T_s, n_2 T_s, n_3 T_s, m_1 + m_2 - m_3 - m = 0), \quad (4.32)
\end{aligned}$$

is the interference created by the subband itself,

$$\begin{aligned}
p_{b,m}^{(\text{NL},2),1} &= \gamma_3^2 \sum_{b_1, b_2, b_3=1}^B \sum_{m_1, m_2, m_3=1}^M \sum_{n_1, n_2, n_3 \in \mathbb{Z}} G_{m_1}^{(b_1, b)} G_{m_2}^{(b_2, b)} G_{m_3}^{(b_3, b)} P_{b_1, m_1} P_{b_2, m_2} P_{b_3, m_3} \\
&\times h_3(n_1 T_s, n_2 T_s, n_3 T_s, m_1 + m_2 - m_3 - m = 1) \\
&\times \overline{h_3}(n_1 T_s, n_2 T_s, n_3 T_s, m_1 + m_2 - m_3 - m = 1), \quad (4.33)
\end{aligned}$$

is the interference created by the left adjacent subband, and

$$\begin{aligned}
p_{b,m}^{(\text{NL},2),-1} &= \gamma_3^2 \sum_{b_1, b_2, b_3=1}^B \sum_{m_1, m_2, m_3=1}^M \sum_{n_1, n_2, n_3 \in \mathbb{Z}} G_{m_1}^{(b_1, b)} G_{m_2}^{(b_2, b)} G_{m_3}^{(b_3, b)} P_{b_1, m_1} P_{b_2, m_2} P_{b_3, m_3} \\
&\times h_3(n_1 T_s, n_2 T_s, n_3 T_s, m_1 + m_2 - m_3 - m = -1) \\
&\times \overline{h_3}(n_1 T_s, n_2 T_s, n_3 T_s, m_1 + m_2 - m_3 - m = -1), \quad (4.34)
\end{aligned}$$

is the interference created by the right adjacent subband.

It remains now to focus on the third order Volterra kernel in order to derive in closed-form these three terms:

- Case $m_1 + m_2 - m_3 - m = 0$ (intra-subband interference) : As a consequence, we have

$$p_{b,m}^{(\text{NL},2),0} = \gamma_3^2 \sum_{b_1, b_2, b_3=1}^B \sum_{\substack{m_1, m_2, m_3=1 \\ m=m_1+m_2-m_3}}^M G_{m_1}^{(b_1,b)} G_{m_2}^{(b_2,b)} G_{m_3}^{(b_3,b)} P_{b_1, m_1} P_{b_2, m_2} P_{b_3, m_3} \sum_{n_1, n_2, n'_2 \in \mathbb{Z}} \times h_3(n_1 T_s, n_2 T_s, n_2 T_s, 0) \bar{h}_3(n_1 T_s, n'_2 T_s, n'_2 T_s, 0). \quad (4.35)$$

By changing some indexes notations, we finally obtain for user belonging to beam b using subband m

$$p_{b,m}^{(\text{NL},2),0} = \gamma_3^2 \alpha_0^{(2)} \sum_{b_1, b_2, b_3}^B \sum_{\substack{m_1, m_2, m_3=1 \\ m=m_1+m_2-m_3}}^M G_{m_1}^{(b_1,b)} G_{m_2}^{(b_2,b)} G_{m_3}^{(b_3,b)} P_{b_1, m_1} P_{b_2, m_2} P_{b_3, m_3} \quad (4.36)$$

with

$$\alpha_\ell^{(2)} = \sum_{n_1, n_2, n_3 \in \mathbb{Z}} |h_3(n_1 T_s, n_2 T_s, n_3 T_s, \ell)|^2. \quad (4.37)$$

Result 4.4. We conclude that $\alpha_\ell^{(2)}$ is positive $\forall \ell$.

- Case $m_1 + m_2 - m_3 - m = 1$ (right adjacent subband interference). As a consequence, we have

$$p_{b,m}^{(\text{NL},2),1} = \gamma_3^2 \alpha_1^{(2)} \sum_{b_1, b_2, b_3=1}^B \sum_{\substack{m_1, m_2, m_3=1 \\ m=m_1+m_2-m_3-1}}^M G_{m_1}^{(b_1,b)} G_{m_2}^{(b_2,b)} G_{m_3}^{(b_3,b)} P_{b_1, m_1} P_{b_2, m_2} P_{b_3, m_3}. \quad (4.38)$$

- Case $m_1 + m_2 - m_3 - m = -1$ (left adjacent subband interference). As a consequence, we have

$$p_{b,m}^{(\text{NL},2),-1} = \gamma_3^2 \alpha_1^{(2)} \sum_{b_1, b_2, b_3=1}^B \sum_{\substack{m_1, m_2, m_3=1 \\ m=m_1+m_2-m_3+1}}^M G_{m_1}^{(b_1,b)} G_{m_2}^{(b_2,b)} G_{m_3}^{(b_3,b)} P_{b_1, m_1} P_{b_2, m_2} P_{b_3, m_3}. \quad (4.39)$$

Remark 4.7. We notice that $\alpha_{-1}^{(2)} = \alpha_1^{(2)}$.

Derivations for $p_{b,m}^{(\text{NL},3)}$

A lot of indexes can be removed in (4.13) by remarking that the terms dealing with the symbol expectation are non-null only if both first indexes are equal to each other and if both second indexes are equal to each others and if both third indexes are equal to each others. Consequently, we have $b_1 = b_3$, $b_2 = b'_2$, $b'_1 = b'_3$ and $m_1 = m_3$, $m_2 = m'_2$, $m'_1 = m'_3$ and $n_1 = n_3$, $n_2 = n'_2$, $n'_1 = n'_3$. So

$$\begin{aligned} p_{b,m}^{(\text{NL},3)} &= \gamma_3^2 \sum_{b_1, b_2, b'_1=1}^B \sum_{m_1, m_2, m'_1=1}^M \sum_{n_1, n_2, n'_1 \in \mathbb{Z}} e^{2i\pi(m_1+m_2-m_1-m)\Delta F n T_s} e^{-2i\pi(m'_1+m_2-m'_1-m)\Delta F n T_s} \\ &\times G_{m_1}^{(b_1,b)} G_{m_2}^{(b_2,b)} G_{m'_1}^{(b'_1,b)} \\ &\times \mathbb{E}[a_{b_1, m_1, n-n_1} \overline{a_{b_1, m_1, n-n_1}}] \mathbb{E}[a_{b_2, m_2, n-n_2} \overline{a_{b_2, m_2, n-n_2}}] \mathbb{E}[\overline{a_{b'_1, m'_1, n-n'_1}} a_{b'_1, m'_1, n-n'_1}] \\ &\times h_3(n_1 T_s, n_2 T_s, n_1 T_s, m_1+m_2-m_1-m) \bar{h}_3(n'_1 T_s, n_2 T_s, n'_1 T_s, m'_1+m_2-m'_1-m), \end{aligned} \quad (4.40)$$

which simplifies as follows

$$p_{b,m}^{(\text{NL},3)} = \gamma_3^2 \sum_{b_1, b_2, b'_1=1}^B \sum_{m_1, m_2, m'_1=1}^M \sum_{n_1, n_2, n'_1 \in \mathbb{Z}} G_{m_1}^{(b_1, b)} G_{m_2}^{(b_2, b)} G_{m'_1}^{(b'_1, b)} P_{b_1, m_1} P_{b_2, m_2} P_{b'_1, m'_1} \times h_3(n_1 T_s, n_2 T_s, n_1 T_s, m_2 - m) \overline{h_3}(n'_1 T_s, n_2 T_s, n'_1 T_s, m_2 - m). \quad (4.41)$$

By changing some index notations, and notice that in h_3 , we can do any permutation of t_1, t_2, t_3 , we show that $p_{b,m}^{(\text{NL},3)} = p_{b,m}^{(\text{NL},1)}$.

Final expression for the power of the nonlinear interference

Finally, we have $\mathcal{P}_{b,m}^{(\text{NL})} = 4p_{b,m}^{(\text{NL},1)} + 2p_{b,m}^{(\text{NL},2)}$ and the final expression of the nonlinear interference power is

$$\begin{aligned} \mathcal{P}_{b,m}^{(\text{NL})} &= 4\gamma_3^2 \alpha_0^{(1)} \sum_{b_1, b_2, b_3=1}^B \sum_{m', m''=1}^M G_{m'}^{(b_1, b)} G_{m''}^{(b_2, b)} G_{m''}^{(b_3, b)} P_{b_1, m} P_{b_2, m'} P_{b_3, m''} \\ &+ 4\tilde{\delta}_{m,M} \gamma_3^2 \alpha_1^{(1)} \sum_{b_1, b_2, b_3=1}^B \sum_{m', m''=1}^M G_{m+1}^{(b_1, b)} G_{m'}^{(b_2, b)} G_{m''}^{(b_3, b)} P_{b_1, m+1} P_{b_2, m'} P_{b_3, m''} \\ &+ 4\tilde{\delta}_{m,1} \gamma_3^2 \alpha_1^{(1)} \sum_{b_1, b_2, b_3=1}^B \sum_{m', m''=1}^M G_{m-1}^{(b_1, b)} G_{m'}^{(b_2, b)} G_{m''}^{(b_3, b)} P_{b_1, m-1} P_{b_2, m'} P_{b_3, m''} \\ &+ 2\gamma_3^2 \alpha_0^{(2)} \sum_{b_1, b_2, b_3=1}^B \sum_{\substack{m_1, m_2, m_3=1 \\ m=m_1+m_2-m_3}}^M G_{m_1}^{(b_1, b)} G_{m_2}^{(b_2, b)} G_{m_3}^{(b_3, b)} P_{b_1, m_1} P_{b_2, m_2} P_{b_3, m_3} \\ &+ 2\gamma_3^2 \alpha_1^{(2)} \sum_{b_1, b_2, b_3=1}^B \sum_{\substack{m_1, m_2, m_3=1 \\ m=m_1+m_2-m_3 \pm 1}}^M G_{m_1}^{(b_1, b)} G_{m_2}^{(b_2, b)} G_{m_3}^{(b_3, b)} P_{b_1, m_1} P_{b_2, m_2} P_{b_3, m_3}, \end{aligned} \quad (4.42)$$

where $\tilde{\delta}_{m,m'} = 1 - \delta_{m,m'}$ with $\delta_{m,m'}$ the Kronecker index.

Result 4.5. The term $\mathcal{P}_{b,m}^{(\text{NL})}$ is a posynomial function in \mathbf{P} .

4.2.4 Expression for the cross-correlation between the useful signal and the nonlinear part

The cross-correlation between the linear useful part and the nonlinear part is defined by $\mathcal{P}_{b,m}^{(\text{LNL})} = \mathbb{E} [z_{b,m,n}^{(\text{L})} \bar{z}_{b,m,n}^{(\text{NL})}]$. According to (1.13) and (1.15), we obtain

$$\begin{aligned} \mathcal{P}_{b,m}^{(\text{LNL})} &= \gamma_1 \gamma_3 \sum_{b_1, b_2, b_3=1}^B \sum_{m_1, m_2, m_3=1}^M \sum_{n_1, n_2, n_3 \in \mathbb{Z}} e^{-2i\pi(m_1+m_2-m_3-m)\Delta F n T_s} \\ &\times \sqrt{G_m^{(b)} G_{m_1}^{(b_1, b)} G_{m_2}^{(b_2, b)} G_{m_3}^{(b_3, b)}} \mathbb{E} [a_{b,m,n} \overline{a_{b_1, m_1, n-n_1} a_{b_2, m_2, n-n_2} a_{b_3, m_3, n-n_3}}] \\ &\times \overline{h_3}(n_1 T_s, n_2 T_s, n_3 T_s, m_1 + m_2 - m_3 - m). \end{aligned} \quad (4.43)$$

As symbols $\{a_{b,m,n}\}$ are assumed to be circularly-symmetric complex-valued Gaussian random variables and according to [43] based on Isserlis' theorem for zero-mean multivariate normal

random vector, we know that

$$\begin{aligned}\mathbb{E}[a_{b,m,n}\overline{a_{b_1,m_1,n-n_1}}a_{b_2,m_2,n-n_2}a_{b_3,m_3,n-n_3}] &= \mathbb{E}[a_{b,m,n}\overline{a_{b_1,m_1,n-n_1}}] \mathbb{E}[\overline{a_{b_2,m_2,n-n_2}}a_{b_3,m_3,n-n_3}] \\ &+ \mathbb{E}[a_{b,m,n}\overline{a_{b_2,m_2,n-n_2}}] \mathbb{E}[\overline{a_{b_1,m_1,n-n_1}}a_{b_3,m_3,n-n_3}].\end{aligned}\quad (4.44)$$

Remark 4.8. We notice that in case of constrained constellations currently used in communication systems, the cumulant term has to be added.

Consequently, we can split (4.44) into two terms as follows

$$\mathcal{P}_{b,m}^{(\text{LNL})} = p_{b,m}^{(\text{LNL},1)} + p_{b,m}^{(\text{LNL},2)} \quad (4.45)$$

with

$$\begin{aligned}p_{b,m}^{(\text{LNL},1)} &= \gamma_1\gamma_3 \sum_{b_1,b_2,b_3=1}^B \sum_{m_1,m_2,m_3=1}^M \sum_{n_1,n_2,n_3 \in \mathbb{Z}} e^{-2i\pi(m_1+m_2-m_3-m)nT_s} \sqrt{G_m^{(b)} G_{m_1}^{(b_1,b)} G_{m_2}^{(b_2,b)} G_{m_3}^{(b_3,b)}} \\ &\times \mathbb{E}[a_{b,m,n}\overline{a_{b_1,m_1,n-n_1}}] \mathbb{E}[\overline{a_{b_2,m_2,n-n_2}}a_{b_3,m_3,n-n_3}] \\ &\times \overline{h_3}(n_1T_s, n_2T_s, n_3T_s, m_1 + m_2 - m_3 - m),\end{aligned}\quad (4.46)$$

$$\begin{aligned}p_{b,m}^{(\text{LNL},2)} &= \gamma_1\gamma_3 \sum_{b_1,b_2,b_3=1}^B \sum_{m_1,m_2,m_3=1}^M \sum_{n_1,n_2,n_3 \in \mathbb{Z}} e^{-2i\pi(m_1+m_2-m_3-m)nT_s} \sqrt{G_m^{(b)} G_{m_1}^{(b_1,b)} G_{m_2}^{(b_2,b)} G_{m_3}^{(b_3,b)}} \\ &\times \mathbb{E}[a_{b,m,n}\overline{a_{b_2,m_2,n-n_2}}] \mathbb{E}[\overline{a_{b_1,m_1,n-n_1}}a_{b_3,m_3,n-n_3}] \\ &\times \overline{h_3}(n_1T_s, n_2T_s, n_3T_s, m_1 + m_2 - m_3 - m).\end{aligned}\quad (4.47)$$

We can show that $p_{b,m}^{(\text{LNL},1)} = p_{b,m}^{(\text{LNL},2)}$ if we switch b_1, m_1, n_1 with b_2, m_2, n_2 .

Finally, we have

$$\mathcal{P}_{b,m}^{(\text{LNL})} = 2p_{b,m}^{(\text{LNL},1)}. \quad (4.48)$$

Let us focus on $p_{b,m}^{(\text{LNL},1)}$.

Derivations for $p_{b,m}^{(\text{LNL},1)}$

In each symbols expectation, the term is non-null only if both first indexes are equal to each other and if both second indexes are equal to each others and if both third indexes are equal to each other. Consequently, we have $b = b_1$, $b_2 = b_3$ and $m = m_1$, $m_2 = m_3$ and $n_1 = 0$, $n_2 = n_3$. So

$$\begin{aligned}p_{b,m}^{(\text{LNL},1)} &= \gamma_1\gamma_3 \sum_{b_2=1}^B \sum_{m_2=1}^M \sum_{n_2 \in \mathbb{Z}} e^{-2i\pi(m+m_2-m_2-m)\Delta F nT_s} G_m^{(b)} G_{m_2}^{(b_2,b)} \\ &\times \mathbb{E}[a_{b,m,n}\overline{a_{b,m,n}}] \mathbb{E}[\overline{a_{b_2,m_2,n-n_2}}a_{b_2,m_2,n-n_2}] \overline{h_3}(0, n_2T_s, n_2T_s, m+m_2-m_2-m),\end{aligned}\quad (4.49)$$

which simplifies as follows

$$p_{b,m}^{(\text{LNL},1)} = \gamma_1\gamma_3\beta G_m^{(b)} P_{b,m} \sum_{b'=1}^B \sum_{m'=1}^M G_{m'}^{(b',b)} P_{b',m'}, \quad (4.50)$$

where

$$\begin{aligned}
\beta &= \sum_{n' \in \mathbb{Z}} \overline{h_3}(0, n'T_s, n'T_s, 0) \\
&= \sum_{n' \in \mathbb{Z}} \int_{\mathbb{R}} p_T(-\tau) p_T(n'T_s - \tau) p_T(n'T_s - \tau) p_R(\tau) d\tau \\
&= \sum_{n' \in \mathbb{Z}} \int_{\mathbb{R}} (p_T(n'T_s - \tau) p_R(\tau))^2 d\tau.
\end{aligned} \tag{4.51}$$

Result 4.6. *We conclude that β is positive.*

Final expression for the cross-correlation between the useful signal and the nonlinear part

Finally, the expression of $\mathcal{P}_{b,m}^{(\text{LNL})}$ is

$$\mathcal{P}_{b,m}^{(\text{LNL})} = 2\gamma_1\gamma_3\beta G_m^{(b)} P_{b,m} \sum_{b'=1}^B \sum_{m'=1}^M G_{m'}^{(b',b)} P_{b',m'}. \tag{4.52}$$

Result 4.7. *The term $\mathcal{P}_{b,m}^{(\text{LNL})}$ is a posynomial function in \mathbf{P} .*

4.2.5 Expression for the cross-correlation between the linear interference and the nonlinear part

The cross-correlation between the linear interference part and the nonlinear part is defined by $\mathcal{P}_{b,m}^{(\text{INL})} = \mathbb{E} \left[z_{b,m,n}^{(\text{I})} \overline{z_{b,m,n}^{(\text{NL})}} \right]$. According to (1.14) and (1.15), we have

$$\begin{aligned}
\mathcal{P}_{b,m}^{(\text{INL})} &= \gamma_1\gamma_3 \sum_{\substack{b'=1 \\ b' \neq b}}^B \sum_{b_1, b_2, b_3=1}^B \sum_{m_1, m_2, m_3=1}^M \sum_{n_1, n_2, n_3 \in \mathbb{Z}} e^{-2i\pi(m_1+m_2-m_3-m)\Delta F n T_s} \\
&\quad \times \sqrt{G_m^{(b',b)} G_{m_1}^{(b_1,b)} G_{m_2}^{(b_2,b)} G_{m_3}^{(b_3,b)}} \mathbb{E} \left[a_{b',m,n} \overline{a_{b_1,m_1,n-n_1} a_{b_2,m_2,n-n_2} a_{b_3,m_3,n-n_3}} \right] \\
&\quad \times \overline{h_3}(n_1 T_s, n_2 T_s, n_3 T_s, m_1 + m_2 - m_3 - m).
\end{aligned} \tag{4.53}$$

As symbols $\{a_{b,m,n}\}$ are assumed to be circularly-symmetric complex-valued Gaussian random variables and according to [43] based on Isserlis' theorem for zero-mean multivariate normal random vector, we know that

$$\begin{aligned}
\mathbb{E} \left[a_{b',m,n} \overline{a_{b_1,m_1,n-n_1} a_{b_2,m_2,n-n_2} a_{b_3,m_3,n-n_3}} \right] &= \mathbb{E} \left[a_{b',m,n} \overline{a_{b_1,m_1,n-n_1}} \right] \mathbb{E} \left[\overline{a_{b_2,m_2,n-n_2} a_{b_3,m_3,n-n_3}} \right] \\
&\quad + \mathbb{E} \left[a_{b',m,n} \overline{a_{b_2,m_2,n-n_2}} \right] \mathbb{E} \left[\overline{a_{b_1,m_1,n-n_1} a_{b_3,m_3,n-n_3}} \right] \\
&\quad + \mathbb{E} \left[a_{b',m,n} \overline{a_{b_3,m_3,n-n_3}} \right] \mathbb{E} \left[\overline{a_{b_1,m_1,n-n_1} a_{b_2,m_2,n-n_2}} \right].
\end{aligned} \tag{4.54}$$

Remark 4.8 is also relevant for this decomposition of the fourth-order moment.

Consequently, we can split (4.54) into two terms as follows

$$\mathcal{P}_{b,m}^{(\text{INL})} = p_{b,m}^{(\text{INL},1)} + p_{b,m}^{(\text{INL},2)}$$

with

$$\begin{aligned}
p_{b,m}^{(\text{INL},1)} &= \gamma_1 \gamma_3 \sum_{\substack{b'=1 \\ b' \neq b}}^B \sum_{b_1, b_2, b_3=1}^B \sum_{m_1, m_2, m_3=1}^M \sum_{n_1, n_2, n_3 \in \mathbb{Z}} e^{-2i\pi(m_1+m_2-m_3-m)nT_s} \\
&\times \sqrt{G_m^{(b',b)} G_{m_1}^{(b_1,b)} G_{m_2}^{(b_2,b)} G_{m_3}^{(b_3,b)}} \mathbb{E} [a_{b',m,n} \overline{a_{b_1,m_1,n-n_1}}] \mathbb{E} [\overline{a_{b_2,m_2,n-n_2}} a_{b_3,m_3,n-n_3}] \\
&\times \overline{h_3}(n_1 T_s, n_2 T_s, n_3 T_s, m_1 + m_2 - m_3 - m),
\end{aligned} \tag{4.55}$$

and

$$\begin{aligned}
p_{b,m}^{(\text{INL},2)} &= \gamma_1 \gamma_3 \sum_{\substack{b'=1 \\ b' \neq b}}^B \sum_{b_1, b_2, b_3=1}^B \sum_{m_1, m_2, m_3=1}^M \sum_{n_1, n_2, n_3 \in \mathbb{Z}} e^{-2i\pi(m_1+m_2-m_3-m)nT_s} \\
&\times \sqrt{G_m^{(b',b)} G_{m_1}^{(b_1,b)} G_{m_2}^{(b_2,b)} G_{m_3}^{(b_3,b)}} \mathbb{E} [a_{b',m,n} \overline{a_{b_2,m_2,n-n_2}}] \mathbb{E} [\overline{a_{b_1,m_1,n-n_1}} a_{b_3,m_3,n-n_3}] \\
&\times \overline{h_3}(n_1 T_s, n_2 T_s, n_3 T_s, m_1 + m_2 - m_3 - m).
\end{aligned} \tag{4.56}$$

We can show that $p_{b,m}^{(\text{INL},1)} = p_{b,m}^{(\text{INL},2)}$ if we switch b_1, m_1, n_1 with b_2, m_2, n_2 .

Finally, we have

$$\mathcal{P}_{b,m}^{(\text{INL})} = 2p_{b,m}^{(\text{INL},1)}. \tag{4.57}$$

Let us focus on $p_{b,m}^{(\text{INL},1)}$.

Derivations for $p_{b,m}^{(\text{INL},1)}$

In each symbol expectation, the term is non-null only if both first indexes are equal to each other and if both second indexes are equal to each others and if both third indexes are equal to each other. Consequently, we have $b' = b_1$, $b_2 = b_3$ and $m = m_1$, $m_2 = m_3$ and $n_1 = 0$, $n_2 = n_3$. So

$$\begin{aligned}
p_{b,m}^{(\text{INL},1)} &= \gamma_1 \gamma_3 \sum_{\substack{b'=1 \\ b' \neq b}}^B \sum_{b_2=1}^B \sum_{m_2=1}^M \sum_{n_2 \in \mathbb{Z}} e^{-2i\pi(m+m_2-m_2-m)\Delta F n T_s} G_m^{(b',b)} G_{m_2}^{(b_2,b)} \\
&\times \mathbb{E} [a_{b',m,n} \overline{a_{b',m,n}}] \mathbb{E} [\overline{a_{b_2,m_2,n-n_2}} a_{b_2,m_2,n-n_2}] \overline{h_3}(0, n_2 T_s, n_2 T_s, m+m_2-m_2-m)
\end{aligned} \tag{4.58}$$

which simplifies as follows

$$p_{b,m}^{(\text{INL},1)} = \gamma_1 \gamma_3 \beta \sum_{\substack{b'=1 \\ b' \neq b}}^B \sum_{b''=1}^B \sum_{m'=1}^M G_m^{(b',b)} G_{m'}^{(b'',b)} P_{b',m} P_{b'',m'}. \tag{4.59}$$

Final expression for the cross-correlation between the linear interference signal and the nonlinear part

Finally, the expression of $\mathcal{P}_{b,m}^{(\text{INL})}$ is

$$\mathcal{P}_{b,m}^{(\text{INL})} = 2\gamma_1 \gamma_3 \beta \sum_{\substack{b'=1 \\ b' \neq b}}^B \sum_{b''=1}^B \sum_{m'=1}^M G_m^{(b',b)} G_{m'}^{(b'',b)} P_{b',m} P_{b'',m'}. \tag{4.60}$$

Result 4.8. The term $\mathcal{P}_{b,m}^{(\text{INL})}$ is a posynomial function in \mathbf{P} .

Thanks to these closed-form expressions, two remarks can be done: the cross-correlation between the useful linear part and the nonlinear part, $\mathcal{P}_{b,m}^{(\text{LNL})}$, is a positive term which implies that it enables us to increase the data rate given by (4.3), as seen in Remark 4.2. In addition, each subband of each beam has significant impact on $\mathcal{P}_{b,m}^{(\text{NL})}$, $\mathcal{P}_{b,m}^{(\text{LNL})}$ and $\mathcal{P}_{b,m}^{(\text{INL})}$ since the terms related to subband m' of beam b' are not multiplied by negligible weights.

4.3 Numerical results

A multiband multibeam satellite is considered with $B = 2$ beams. The system operates in the Ka-band for the uplink (27.5-29.5 GHz) and $M = 6$ terrestrial users are in each beam. The number of subbands is equal to M , and the subband assignment has been already performed [3]. The channel gains $\{G_m^{(b',b)}\}_{b,b',m}$ are computed according to [3, 14, 15]. The roll-off of *Square-Root-Raised-Cosine* (SRRC) filters is 0.25. The values γ_1 and γ_3 are 1 and 0.05 respectively.

In Table. 4.1, we give the values of the Volterra coefficient for our system. Notice that these coefficients depend on the shaping filter and symbol rate.

Volterra coefficient	Value
$\alpha_0^{(1)}$	7.2960×10^{16}
$\alpha_0^{(2)}$	5.1625×10^{16}
$\alpha_1^{(1)}$	3.3775×10^{14}
$\alpha_1^{(2)}$	5.3155×10^{15}
β	2.7003×10^8

Table 4.1: Values of the Volterra coefficients.

In Fig. 4.4, we plot the sum-rate versus the transmit power of users, where all users use the same transmit power P , with $P_{\max} = 50\text{W}$ (47dBm). We consider three configurations: each of them corresponds to a satellite pre-amplifier gain value. Actually, this device is located before HPA which operates into linear or nonlinear mode depending on the tuning of the pre-amplifier. This device modify uniformly the values of channel gains $\{G_m^{(b',b)}\}_{b,b',m}$ and finally the input power of the HPA. Here A, B, and C deal with linear, transient and nonlinear modes respectively. We denote by R^{li} the sum-rate evaluated without nonlinear effects (but with linear inter-beam interference) given by (3.1), R^{nli} the sum-rate evaluated for the nonlinearity-agnostic receiver, given by (4.5), and R^{lnl} the sum-rate evaluated for the nonlinearity-aware receiver, given by (4.3). The respective asymptotic limit when the transmit power P goes to infinity is drawn in dotted line. In nonlinear mode, we observe that taking into account the nonlinear effects at the receiver increases the system sum-rate for the same transmission power. Moreover, a well-chosen resource allocation allows to reach the maximum of the system sum-rate.

In Fig. 4.5, we plot the sum-rate versus the transmit power of users in semi-log scale, where all users use the same transmit power P , with $P_{\max} = 10\text{kW}$ (70dBm). Notice that this figure is a zoom out of Fig. 4.4. We observe that R^{li} and R^{lnl} have a nonzero limit when the power is constantly increased, whereas R^{nli} downs to zero.

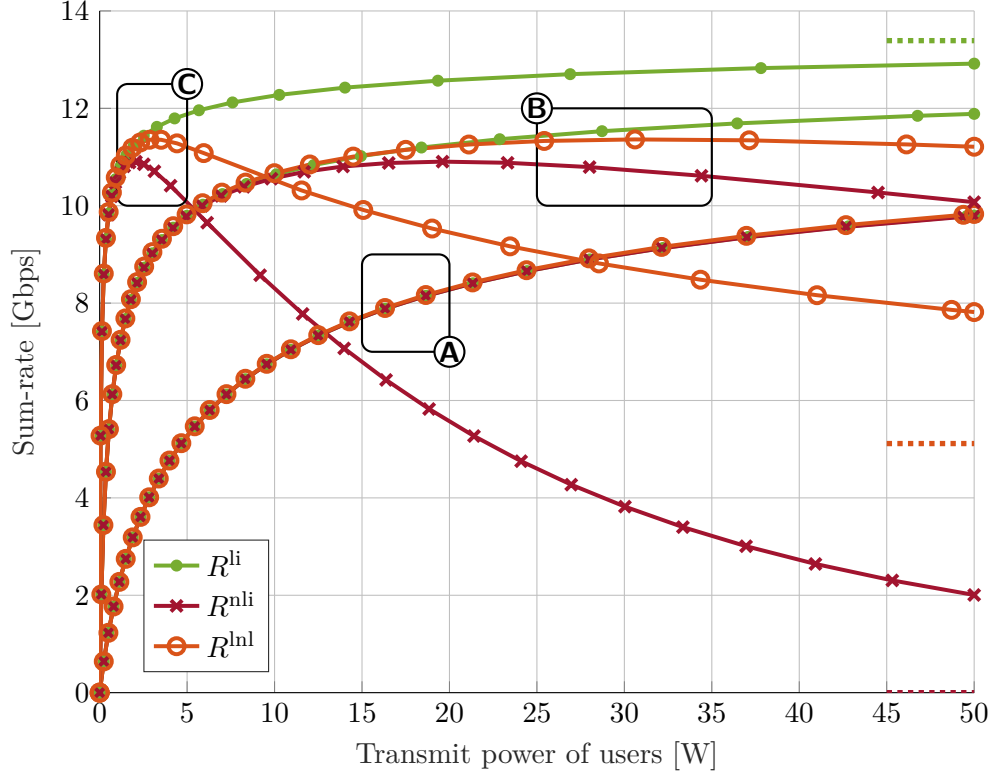


Figure 4.4: Sum-rate vs. transmit power of users $P_{b,m} = P$, for $G_{\text{amp}} \in \{-10, 0, 10\}$ dB, respectively A, B and C.

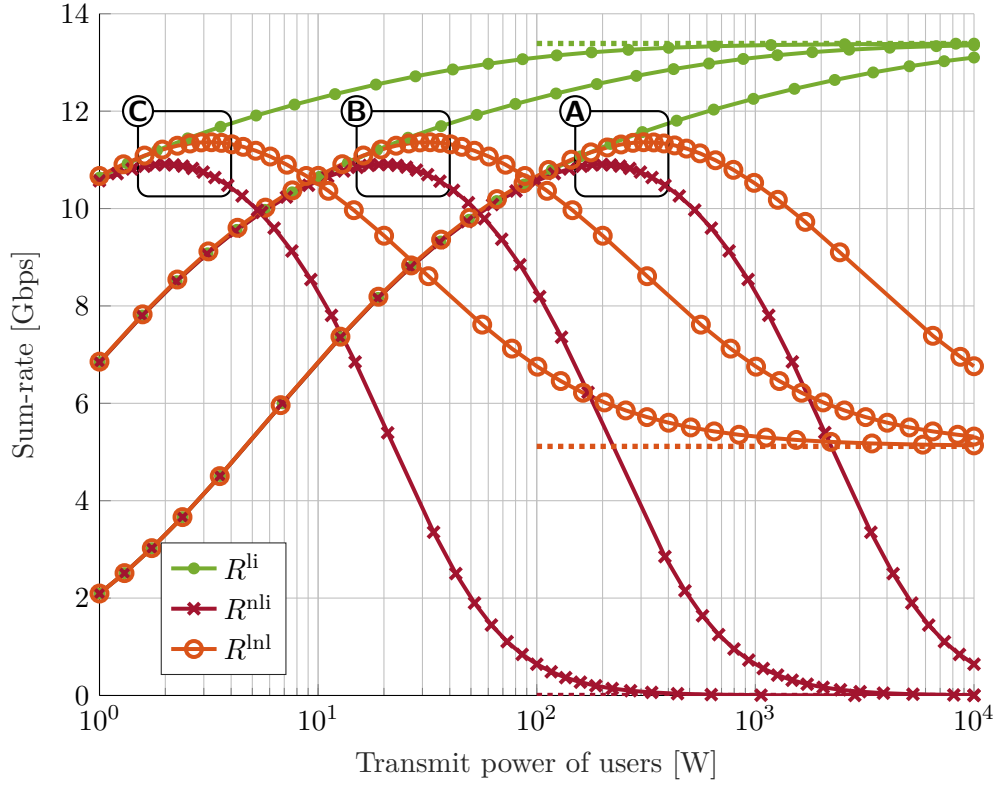


Figure 4.5: Sum-rate vs. transmit power of users $P_{b,m} = P$, for $G_{\text{amp}} \in \{-10, 0, 10\}$ dB, respectively A, B and C.

4.4 Conclusion

In this chapter, we have established two expressions for the data rate in the presence of nonlinearity in the channel, depending on the receiver considered. The nonlinearity-aware receiver exploits the additional information contained in the nonlinear effects. The nonlinearity-agnostic receiver sees the nonlinear effects as additional noise. Using an alternative and elegant method of calculation, we then expressed the terms involved in the data rate expression in a closed-form manner. We then concluded that these terms turn out to be posynomials. The numerical results show us a significant gain in terms of data rate when the nonlinear effects are exploited at the receiver level. It was also observed that finding an intelligent power allocation scheme would allow to reach the maximum of the data rate, which is done in Chapters 5 and 6.

Finally, part of the material presented in this chapter has been published in [C2] and [J2].

Resource allocation for nonlinearity-agnostic receiver

With the exponential increase in data traffic, satellite communication systems coupled with the next generation of cellular networks are becoming a key element. We actually focus on uplink/return link satellite communications around Ka-band where the terrestrial antennas may correspond to relay points from terrestrial systems, the satellite acts as a relay to the final terrestrial gateway [9, 3]. In this context, Chapter 3 dealing with resource allocation and references therein, assumed that the satellite's *High-Power Amplifier* (HPA) operates in a linear regime. In Chapter 4, a closed-form expression for the sum-rate has been derived when nonlinearity at the HPA is considered. Nevertheless, a smart resource allocation is not performed. The main originality and contribution of this chapter is to take into account the nonlinear behavior of the satellite HPA for deriving generic and practical resource allocation algorithms. We consider that the data rate relies on the achievable data rate where the nonlinear interference is seen as an additional noise, called *nonlinearity-agnostic receiver*.

When the HPA operates as a nonlinear device, the data rate (obtained through the achievable data rate) depends on the nonlinear interference. The case of linear interference has been widely studied in the literature dealing with wireless communications, e.g., [16, 44]. The case of nonlinear interference has been only pointed out in few papers [20, 44].

Actually, it is mentioned in [20] that the third-order intermodulation interference may be managed through *Geometric Programming* (GP) for power optimization, but no simulations are performed. In [44], only a class of nonlinear interference is considered and does not fit with our case. This chapter is technically related to [16] since their tools remain valid in our case although this reference deals with linear interference.

The rest of the chapter is organized as follows. In Section 5.1, the main problem of sum-rate maximization, for nonlinearity-agnostic receiver, is stated and is solved in Section 5.2. In Section 5.3, the fairness issue is addressed for nonlinearity-agnostic receiver, where the maximization of minimum per-user data rate problem is formulated and solved. In Section 5.5, we take the liberty of dealing with the problem of sum-power minimization subject to a target data rate, for nonlinearity-agnostic receiver. In Section 5.6, concluding remarks are drawn.

5.1 Problem formulation

The first problem to be solved, which is the main issue of the thesis, is that of maximizing the system sum-rate formulated in Problem 1.1. We gave in Chapter 4 the data rate expression $\underline{R}_{b,m}$ for user belonging to beam b using subband m in the presence of nonlinear effects, according to a nonlinearity-agnostic receiver. By putting (4.5) in the main Problem 1.1, the resulting power optimization problem is

Problem 5.1.

$$\begin{aligned} \mathbf{P}^* &= \arg \max_{\mathbf{P}} \sum_{b=1}^B \sum_{m=1}^M \log_2 (1 + Q_{b,m}) \\ \text{with } Q_{b,m} &= \frac{\mathcal{P}_{b,m}^{(L)}}{\mathcal{P}_{b,m}^{(I)} + \mathcal{P}_{b,m}^{(NL)} + \mathcal{P}_W} \\ \text{s.t. } & \text{(1.16) and (1.17).} \end{aligned} \quad (5.1)$$

Consequently, the powers of the users are all coupled through the expression of the data rate (4.5) and the interference-temperature constraint (1.16). The optimization of the problem is challenging. Indeed, the problem is non-convex due to the objective function which involves a ratio of the variable to be optimized.

5.2 Solution for the maximization of the sum-rate

In this section, the Problem 5.1 of maximization of the sum-rate is solved. We have seen that the problem is non-convex. Nevertheless, we proved in Chapter 4 that the terms $\mathcal{P}_{b,m}^{(I)}$ and $\mathcal{P}_{b,m}^{(NL)}$ involved in the data rate expression are posynomials. The term $Q_{b,m}$ given by (5.1) is therefore a ratio of a monomial function over a posynomial function (since posynomials are closed under the addition). In Chapter 2, a method has been proposed to manage such a ratio.

First, thanks to the monotonic growth of the logarithm function, Problem 5.1 is equivalent to the following one.

Problem 5.2.

$$\begin{aligned} \mathbf{P}^* &= \arg \max_{\mathbf{P}} \prod_{b=1}^B \prod_{m=1}^M 1 + \frac{\mathcal{P}_{b,m}^{(L)}}{\mathcal{P}_{b,m}^{(I)} + \mathcal{P}_{b,m}^{(NL)} + \mathcal{P}_W} \\ \text{s.t. } & \text{(1.16) and (1.17).} \end{aligned} \quad (5.2)$$

Remark 5.1. *Note that in high SINR regime, we can use the approximation of the logarithm $\log(1+x) \approx \log(x)$. In that case, the resulting problem maximizes a ratio of monomial function over posynomial function (alternatively, minimizes a ratio of posynomial over monomial), leading to a valid posynomial and finally a problem in GP form.*

Then, Problem 5.2 is rewritten using the inverse of the objective function, as follows,

Problem 5.3.

$$\mathbf{P}^* = \arg \min_{\mathbf{P}} \prod_{b=1}^B \prod_{m=1}^M \frac{\mathcal{P}_{b,m}^{(I)} + \mathcal{P}_{b,m}^{(NL)} + \mathcal{P}_W}{\mathcal{P}_{b,m}^{(L)} + \mathcal{P}_{b,m}^{(I)} + \mathcal{P}_{b,m}^{(NL)} + \mathcal{P}_W} \quad (5.3)$$

s.t. (1.16) and (1.17).

The difficulty is still located in the objective function, where we have a ratio of posynomial functions, so the problem is non-convex and boils down to *Complementary Geometric Programming (CGP)*. In Chapter 2, we presented a standard way for reaching a stationary point of CGP problem. First, we use the so-called *Successive Convex Approximation (SCA)* method for non-convex problem, presented in Chapter 2. In order to apply SCA procedure, our objective is now to find a tight upper-bound for (5.3) which is either directly convex or GP. Secondly, we propose to replace the denominator with a monomial satisfying the SCA conditions at a given point. A straightforward and easy way was shown in Section 2.4.2 to build this monomial which satisfies SCA conditions. Finally, this leads to a GP problem since a ratio of posynomial and monomial is a posynomial. Since the monomial approximation satisfies the SCA conditions, the SCA procedure converges toward a stationary point. In [16], the authors use the same approach where, in their case, the interference is linear.

We denote the posynomial of the denominator by

$$D_{b,m}(\mathbf{P}) = \mathcal{P}_{b,m}^{(L)} + \mathcal{P}_{b,m}^{(I)} + \mathcal{P}_{b,m}^{(NL)} + \mathcal{P}_W. \quad (5.4)$$

The monomial approximation at the point \mathbf{P}_i is denoted by $\tilde{D}_{b,m}^{(i)}$. This approximation is built in such a way that it satisfies the SCA conditions, thanks to the method explained in Section 2.4.2,

$$\begin{aligned} \tilde{D}_{b,m}^{(i)}(\mathbf{P}) &= \left(\frac{\gamma_1^2 G_m^{(b)} P_{b,m}}{\lambda_{b,m}^{(1)}} \right)^{\lambda_{b,m}^{(1)}} \\ &\times \prod_{\substack{b'=1 \\ b' \neq b}}^B \left(\frac{\gamma_1^2 G_m^{(b',b)} P_{b',m}}{\lambda_{b,m}^{(2)}(b')} \right)^{\lambda_{b,m}^{(2)}(b')} \\ &\times \prod_{b_1, b_2, b_3}^B \prod_{m', m''=1}^M \left(\frac{4\gamma_3^2 \alpha_0^{(1)} G_m^{(b_1,b)} G_{m'}^{(b_2,b)} G_{m''}^{(b_3,b)} P_{b_1,m} P_{b_2,m'} P_{b_3,m''}}{\lambda_{b,m}^{(3)}(b_1, b_2, b_3, m', m'')} \right)^{\lambda_{b,m}^{(3)}(b_1, b_2, b_3, m', m'')} \\ &\times \prod_{b_1, b_2, b_3=1}^B \prod_{m', m''=1}^M \left(\frac{4\tilde{\delta}_{m,M} \gamma_3^2 \alpha_1^{(1)} G_{m+1}^{(b_1,b)} G_{m'}^{(b_2,b)} G_{m''}^{(b_3,b)} P_{b_1, m+1} P_{b_2, m'} P_{b_3, m''}}{\lambda_{b,m}^{(4)}(b_1, b_2, b_3, m', m'')} \right)^{\lambda_{b,m}^{(4)}(b_1, b_2, b_3, m', m'')} \\ &\times \prod_{b_1, b_2, b_3=1}^B \prod_{m', m''=1}^M \left(\frac{4\tilde{\delta}_{m,1} \gamma_3^2 \alpha_1^{(1)} G_{m-1}^{(b_1,b)} G_{m'}^{(b_2,b)} G_{m''}^{(b_3,b)} P_{b_1, m-1} P_{b_2, m'} P_{b_3, m''}}{\lambda_{b,m}^{(5)}(b_1, b_2, b_3, m', m'')} \right)^{\lambda_{b,m}^{(5)}(b_1, b_2, b_3, m', m'')} \\ &\times \prod_{b_1, b_2, b_3}^B \prod_{\substack{m_1, m_2, m_3=1 \\ m=m_1+m_2-m_3}}^M \left(\frac{2\gamma_3^2 \alpha_0^{(2)} G_{m_1}^{(b_1,b)} G_{m_2}^{(b_2,b)} G_{m_3}^{(b_3,b)} P_{b_1, m_1} P_{b_2, m_2} P_{b_3, m_3}}{\lambda_{b,m}^{(6)}(b_1, b_2, b_3, m_1, m_2, m_3)} \right)^{\lambda_{b,m}^{(6)}(b_1, b_2, b_3, m_1, m_2, m_3)} \end{aligned}$$

$$\begin{aligned}
& \times \prod_{b_1, b_2, b_3=1}^B \prod_{\substack{m_1, m_2, m_3=1 \\ m=m_1+m_2-m_3 \pm 1}}^M \left(\frac{2\gamma_3^2 \alpha_1^{(2)} G_{m_1}^{(b_1, b)} G_{m_2}^{(b_2, b)} G_{m_3}^{(b_3, b)} P_{b_1, m_1} P_{b_2, m_2} P_{b_3, m_3}}{\lambda_{b, m}^{(7)}(b_1, b_2, b_3, m_1, m_2, m_3)} \right)^{\lambda_{b, m}^{(7)}(b_1, b_2, b_3, m_1, m_2, m_3)} \\
& \times \left(\frac{\mathcal{P}_W}{\lambda_{b, m}^{(7)}} \right)^{\lambda_{b, m}^{(7)}}, \tag{5.5}
\end{aligned}$$

where

$$\lambda_{b, m}^{(1)} = \frac{\gamma_1^2 G_m^{(b)} P_{b, m}^{(i)}}{D_{b, m}(\mathbf{P}_i)}, \tag{5.6}$$

$$\lambda_{b, m}^{(2)}(b') = \frac{\gamma_1^2 G_m^{(b', b)} P_{b', m}^{(i)}}{D_{b, m}(\mathbf{P}_i)}, \tag{5.7}$$

$$\lambda_{b, m}^{(3)}(b_1, b_2, b_3, m', m'') = \frac{4\gamma_3^2 \alpha_0^{(1)} G_m^{(b_1, b)} G_{m'}^{(b_2, b)} G_{m''}^{(b_3, b)} P_{b_1, m}^{(i)} P_{b_2, m'}^{(i)} P_{b_3, m''}^{(i)}}{D_{b, m}(\mathbf{P}_i)}, \tag{5.8}$$

$$\lambda_{b, m}^{(4)}(b_1, b_2, b_3, m', m'') = \frac{4\tilde{\delta}_{m, M} \gamma_3^2 \alpha_1^{(1)} G_{m+1}^{(b_1, b)} G_{m'}^{(b_2, b)} G_{m''}^{(b_3, b)} P_{b_1, m+1}^{(i)} P_{b_2, m'}^{(i)} P_{b_3, m''}^{(i)}}{D_{b, m}(\mathbf{P}_i)}, \tag{5.9}$$

$$\lambda_{b, m}^{(5)}(b_1, b_2, b_3, m', m'') = \frac{4\tilde{\delta}_{m, 1} \gamma_3^2 \alpha_1^{(1)} G_{m-1}^{(b_1, b)} G_{m'}^{(b_2, b)} G_{m''}^{(b_3, b)} P_{b_1, m-1}^{(i)} P_{b_2, m'}^{(i)} P_{b_3, m''}^{(i)}}{D_{b, m}(\mathbf{P}_i)}, \tag{5.10}$$

$$\lambda_{b, m}^{(6)}(b_1, b_2, b_3, m_1, m_2, m_3) = \frac{2\gamma_3^2 \alpha_0^{(2)} G_{m_1}^{(b_1, b)} G_{m_2}^{(b_2, b)} G_{m_3}^{(b_3, b)} P_{b_1, m_1}^{(i)} P_{b_2, m_2}^{(i)} P_{b_3, m_3}^{(i)}}{D_{b, m}(\mathbf{P}_i)}, \tag{5.11}$$

$$\lambda_{b, m}^{(7)}(b_1, b_2, b_3, m_1, m_2, m_3) = \frac{2\gamma_3^2 \alpha_1^{(2)} G_{m_1}^{(b_1, b)} G_{m_2}^{(b_2, b)} G_{m_3}^{(b_3, b)} P_{b_1, m_1}^{(i)} P_{b_2, m_2}^{(i)} P_{b_3, m_3}^{(i)}}{D_{b, m}(\mathbf{P}_i)}, \tag{5.12}$$

$$\lambda_{b, m}^{(8)} = \frac{\mathcal{P}_W}{D_{b, m}(\mathbf{P}_i)}. \tag{5.13}$$

Lemma 5.1. *The term $\tilde{D}_{b, m}^{(i)}$ is a monomial approximation of $D_{b, m}$ at the point \mathbf{P}_i which satisfies the [SCA](#) conditions, shown in [Section 2.4.2](#).*

By replacing $D_{b, m}$ with $\tilde{D}_{b, m}^{(i)}$ in [Problem 5.3](#), the resulting optimization problem is

Problem 5.4.

$$\begin{aligned}
\mathbf{P}_i^* &= \arg \min_{\mathbf{P}} \prod_{b=1}^B \prod_{m=1}^M \left(\tilde{D}_{b, m}^{(i-1)}(\mathbf{P}) \right)^{-1} \left(\mathcal{P}_{b, m}^{(I)} + \mathcal{P}_{b, m}^{(NL)} + \mathcal{P}_W \right) \\
&\text{s.t. (1.16) and (1.17).}
\end{aligned}$$

Result 5.1. *Problem 5.4 is [GP](#) since it minimizes a posynomial function over a set in [GP](#) form and can be efficiently solved by numerical algorithms.*

Proof. The objective function is a posynomial function since the inverse of a monomial is still a monomial, and the posynomials are closed under the addition and multiplication. \square

Since the monomial approximation satisfies the [SCA](#) conditions, the [SCA](#) procedure depicted in [Algorithm 5.1](#) converges towards a stationary point. The obtained solution is sub-optimal. As starting feasible point, we can use the solution obtained by [Algorithm 3.3](#).

Algorithm 5.1 SCA based procedure for solving Problem 5.1

```
1: Set  $\epsilon > 0$ ,  $E = \epsilon + 1$ ,  $i = 0$ 
2: Find  $\mathbf{P}_0$  a feasible solution of Problem 5.1
3: Compute the sum-rate  $R_0$  using (4.5)
4: while  $E > \epsilon$  do
5:    $i = i + 1$ 
6:   Compute the monomial approximation  $\tilde{D}_{b,m}^{(i-1)}(\mathbf{P})$  around the point  $\mathbf{P}_{i-1}$ , using (5.5)
7:   Find  $\mathbf{P}_i^*$  the optimal solution of Problem 5.4
8:   Compute the sum-rate  $R_i$  and  $E = |R_i - R_{i-1}|$ 
9: end while
10: return  $\mathbf{P}^* = \mathbf{P}_i$ 
```

In this section, we have proposed an optimization algorithm for the problem of system sum-rate maximization, in presence of nonlinear effects and when a nonlinearity-agnostic receiver is considered. However, the notion of fairness is not present in this problem. Indeed, the best users will be assigned the best data rates, while the worst users will have very low data rates.

5.3 Maximization of the minimum per-user rate

In this section, we address the fairness issue between users in presence of nonlinear effects and for the nonlinearity-agnostic receiver. Here we consider only the *max-min fairness*. The problem of maximization of the minimum per-user rate is formulated as following

Problem 5.5.

$$\begin{aligned} \mathbf{P}^* &= \arg \max_{\mathbf{P}} \min_{b,m} \log_2 (1 + Q_{b,m}) \\ \text{with } Q_{b,m} &= \frac{\mathcal{P}_{b,m}^{(L)}}{\mathcal{P}_{b,m}^{(I)} + \mathcal{P}_{b,m}^{(NL)} + \mathcal{P}_W} \\ \text{s.t. } & (1.16) \text{ and } (1.17). \end{aligned}$$

Thanks to the monotonic growth of the logarithm function, Problem 5.5 is equivalent to the following one.

Problem 5.6.

$$\begin{aligned} \mathbf{P}^* &= \arg \max_{\mathbf{P}} \min_{b,m} Q_{b,m} \\ \text{s.t. } & (1.16) \text{ and } (1.17). \end{aligned}$$

The difficulty is located in the objective function, which is not concave nor a posynomial function because of the minimum operator and the ratio of a monomial function over a posynomial function $Q_{b,m}$. First, we introduce a new variable $t \in \mathbb{R}^{+*}$ in order to remove the minimum operator. Problem 5.6 becomes

Problem 5.7.

$$\begin{aligned}
(\mathbf{P}^*, t^*) &= \arg \max_{\mathbf{P}, t} t \\
\text{s.t. } & (1.16), (1.17), \\
& Q_{b,m} \geq t, \quad \forall b, m.
\end{aligned} \tag{5.14}$$

Remark 5.2. We notice that $\max t$ is equivalent to $\min t^{-1}$

The objective function of Problem 5.7 is now a valid monomial function. Moreover, the constraint (5.14) can be rewritten as

$$\mathcal{P}_{b,m}^{(L)-1} t \left(\mathcal{P}_{b,m}^{(I)} + \mathcal{P}_{b,m}^{(NL)} + \mathcal{P}_W \right) \leq 1, \quad \forall b, m \tag{5.15}$$

Lemma 5.2. The constraint (5.15) has the form of a posynomial less than or equal to one, leading to a valid constraint for GP.

Proof. The term $\mathcal{P}_{b,m}^{(L)-1}$ is a monomial function. By reminding that posynomials are close to addition and multiplication, the *Left-Hand Side (LHS)* is a posynomial function. \square

The resulting optimization problem writes as

Problem 5.8.

$$\begin{aligned}
(\mathbf{P}^*, t^*) &= \arg \min_{\mathbf{P}, t} t^{-1} \\
\text{s.t. } & (1.16), (1.17) \text{ and } (5.15).
\end{aligned}$$

Result 5.2. Problem 5.8 is GP since it minimizes of monomial (which is a posynomial term) over a set in GP form.

Finally, we obtained a GP problem after a clever rewriting of the problem when the user data rate is evaluated by (4.5) for a nonlinearity-agnostic receiver. We recall that GP problems are easily solved by numerical solvers.

5.4 Minimization of the sum-power

In this section, we also cover the sum-power minimization problem, subject to a target data rate constraint. Indeed, this problem can be easily solved when the SINR is written as a posynomial ratio, which is our case for a nonlinearity-agnostic receiver. The problem of minimization of the sum-power is formulated as follows

Problem 5.9.

$$\begin{aligned}
\mathbf{P}^* &= \arg \min_{\mathbf{P}} \sum_{b=1}^B \sum_{m=1}^M P_{b,m} \\
\text{s.t. } & (1.16) \text{ and } (1.17), \\
& \log_2 (1 + Q_{b,m}) \geq R_{b,m}^t, \quad \forall b, m, \\
& \text{with } Q_{b,m} = \frac{\mathcal{P}_{b,m}^{(L)}}{\mathcal{P}_{b,m}^{(I)} + \mathcal{P}_{b,m}^{(NL)} + \mathcal{P}_W}.
\end{aligned} \tag{5.16}$$

where $R_{b,m}^t$ is the target data rate for user belonging to beam b using subband m . Note that the problem may be infeasible if $R_{b,m}^t$ is too large. In the case of a linear interference, the feasibility conditions are given in [45].

The formulation of Problem 5.9 is neither concave nor of the GP form. It is therefore impossible to use tools to solve it analytically or numerically with acceptable complexity, i.e., in polynomial time. The main contribution of this section is to rewrite this problem in a standard form, i.e., concave or GP, in order to be able to apply the standard tools of convex or GP optimization.

The difficulty is located in the constraint (5.16), where we have ratios of posynomial functions. However, this constraint can be rewritten as

$$\left(2^{R_{b,m}^t} - 1\right) \mathcal{P}_{b,m}^{(L)^{-1}} \left(\mathcal{P}_{b,m}^{(I)} + \mathcal{P}_{b,m}^{(NL)} + \mathcal{P}_W\right) \leq 1, \quad \forall b, m. \quad (5.17)$$

Lemma 5.3. *The constraint (5.17) has the form of a posynomial less than or equal to one, leading to a valid constraint for GP.*

Proof. The term $2^{R_{b,m}^t} - 1$ is a positive scalar, $\mathcal{P}_{b,m}^{(L)^{-1}}$ is a monomial function. Thanks to the addition rule of posynomial, the rest of the LHS is a posynomial function. Finally, thanks to multiplication rule between a monomial and a posynomial function, the LHS is a posynomial function. \square

The resulting optimization problem writes as

Problem 5.10.

$$\begin{aligned} \mathbf{P}^* &= \arg \min_{\mathbf{P}} \sum_{b=1}^B \sum_{m=1}^M P_{b,m} \\ \text{s.t. } & (1.16), (1.17) \text{ and } (5.17). \end{aligned} \quad (5.18)$$

Result 5.3. *Problem 5.10 is GP since it minimizes of posynomial over a set in GP form.*

Finally, we obtain a GP problem after an intelligent rewriting of the problem when the user data rate is evaluated by (4.5) for a nonlinearity-agnostic receiver. We recall that GP problems are easily solved by numerical solvers.

5.5 Numerical results

We consider a multibeam satellite system operating in the Ka-band for the uplink (27.5-29.5 GHz). The satellite is composed of $B = 2$ beams and there are $M = 6$ users per beam. The subband assignment has been already performed. The HPA distortion coefficients γ_1 and γ_3 are 1 and 0.05 respectively. In addition, we add a variable gain pre-amplifier just before the HPA. This device allows to set the HPA regime by changing the channel gains (and so input powers) uniformly for incoming signal of the same antenna. For simplicity, we assume that the gains of the pre-amplifiers are identical for all HPAs. The shaping filter is a *Square-Root-Raised-Cosine*

(SRRC) filter with roll-off 0.25 for all users. The maximum power is $P_{\max} = 50\text{W}$ (47dBm). The primary *Fixed Service* (FS) subband contains $S = 2$ *Fixed-Satellite Service* (FSS) subbands. The channel gains $\{G_m^{(b',b)}\}_{b,m,b'}$ and $\{F_{b,m}^{(\ell)}\}_{b,m,\ell}$ are computed according to [3, 15, 2, 14]. Notice that the channel gain values within a same beam $\{G_m^{(b)}\}_m$ are close to each others. The maximum interference-temperature level is fixed to $I_{th}^{(\ell)}(m') = 1\text{pW}$ (−90dBm) for any ℓ, m' . Unless otherwise stated, we consider 1 FS per square kilometer. We use the CVX toolbox to solve GP problems [33].

5.5.1 Sum-rate analysis

We denote the power allocations related to the maximization of the sum-rate by

- P^{naive1} , the power allocation where the users use the same transmit power P , which is then optimized for maximizing the system sum-rate where the nonlinear interference is taken into account,
- P^{naive2} , the power allocation where the received power at the satellite level is the same, so $G_m^{(b)} P_{b,m} = G_{m'}^{(b')} P_{b',m'}$, which is then optimized for maximizing the system sum-rate where the nonlinear interference is taken into account,
- P^{sota1} , the power allocation given by [3] and detailed in Section 3.2 where the (linear and nonlinear) interference is not taking into account,
- P' , the power allocation given by Algorithm 3.1 related to Problem 3.2, where there is no interference,
- P^{li} , the power allocation given by Algorithm 3.3 related to Problem 3.12, where only linear interference occurs, i.e. $\mathcal{P}_{b,m}^{(\text{NL})} = 0$,
- P^* , the power allocation given by Algorithm 5.1 which is the SCA procedure for Problem 5.1.

In solid line, the sum-rate is evaluated with (4.5) for nonlinearity-agnostic receiver. In addition, we display in dotted line the sum-rate for the linear inter-beam interference case, i.e., when we enforce no nonlinear interference in the expression of the data rate (4.5) and finally obtain the data rate (3.1).

In Fig. 5.1, we plot the sum-rate versus the pre-amplifier gain for the six above mentioned power allocations. The proposed Algorithm 5.1 is the best one and offers a gain, whatever the operating regime of the HPA. We remark that the solutions obtained when the optimization problems assume a linear HPA are very bad and not suitable when the HPA is in nonlinear regime. Even worse, the lack of knowledge of the data rate expression in the nonlinear regime degrades the sum-rate, because we can wrongly think that increasing the gain of the pre-amplifier is beneficial for the sum-rate.

In Fig. 5.2, we plot the sum-rate versus the FS density, for a pre-amplifier gain value set to 6dB. For high primary user density, we observe that the interference-temperature constraints prevails in the problem. Indeed, the sum-rates obtained with solutions P^{li} and P^* are close. We can therefore say that taking into account the nonlinear interference is not necessary when the

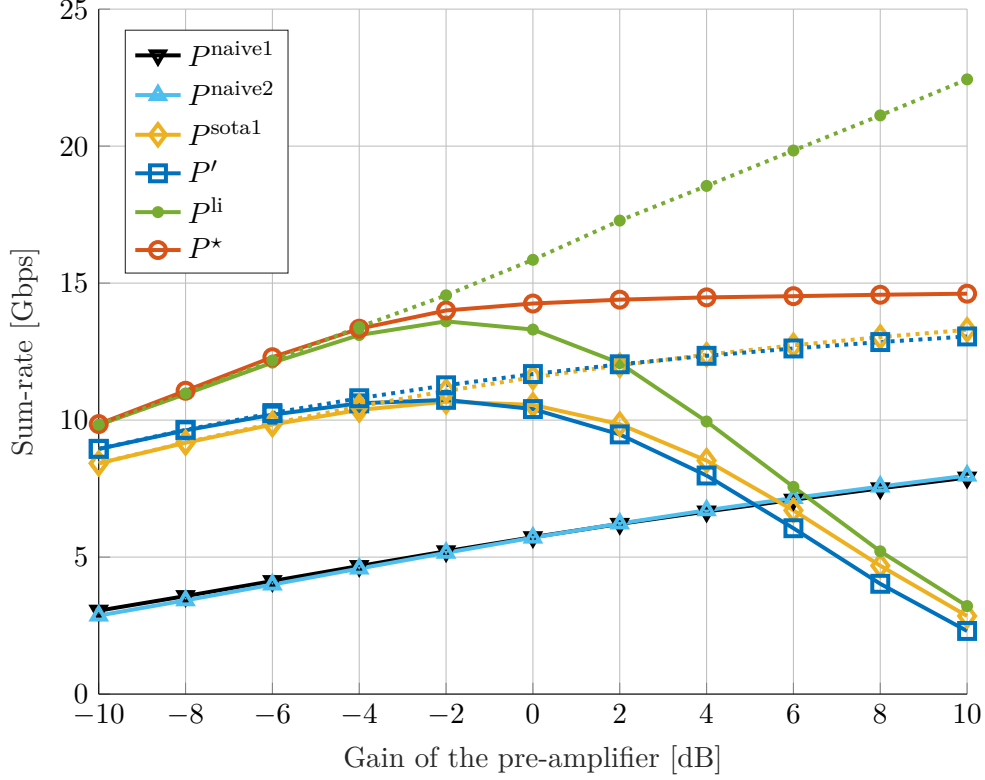


Figure 5.1: Sum-rate vs. pre-amplifier gain for 1 FS per 100 km².

density of the FS is high. When the density of the FS is low, the proposed P^* solution is then the best. Indeed, the nonlinear effects are more important because the users transmit on average at a higher power.

5.5.2 Minimum per-user data rate analysis

We denote the power allocations related to the maximization of minimum per-user data rate by

- P^{naive1} , the power allocation where the users use the same transmit power P which is then optimized for maximizing the minimum per-user data rate where the nonlinear interference is taken into account,
- P^{naive2} , the power allocation where the received power at the satellite level is the same, so $G_m^{(b)} P_{b,m} = G_{m'}^{(b')} P_{b',m'}$, which is then optimized for maximizing the minimum per-user data rate where the nonlinear interference is taken into account,
- P^{sota2} , the power allocation given by [8] and detailed in Section 3.5 where the (linear and nonlinear) interference is not taking into account,
- P^{li} , the power allocation which is the optimal solution of Problem 3.14 obtained by numerical solver [33], where only linear interference occurs, i.e. $\mathcal{P}_{b,m}^{(\text{NL})} = 0$,
- P^* , the power allocation which is the optimal solution of Problem 5.5 obtained by numerical solver [33].

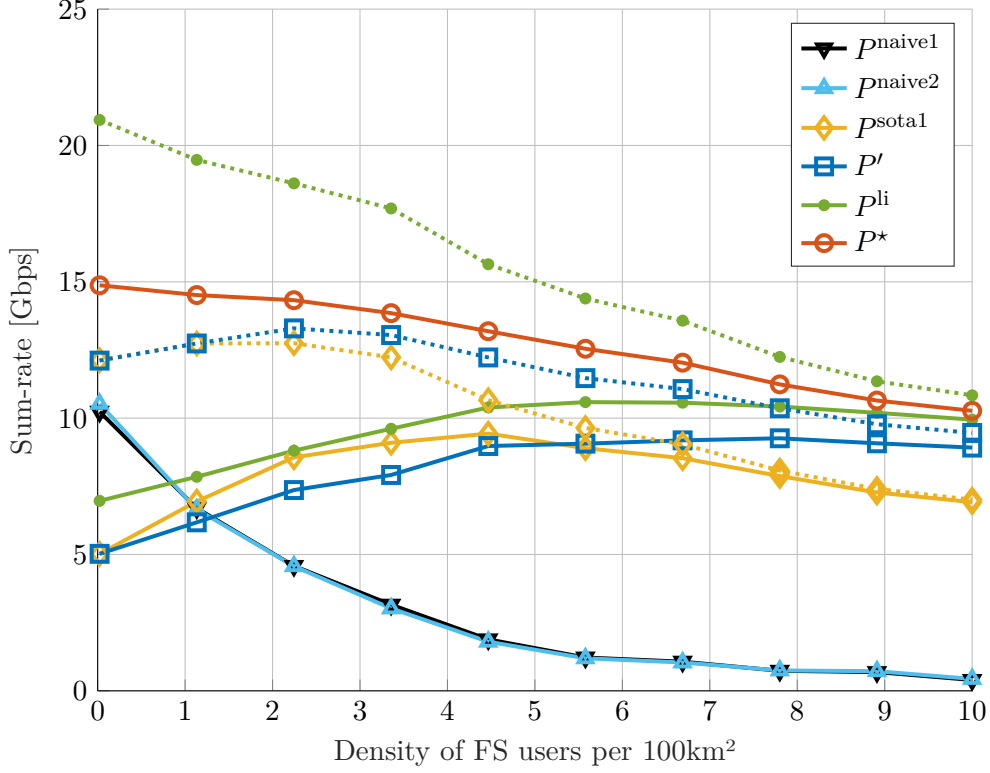


Figure 5.2: Sum-rate vs. FS density for $G_{\text{amp}} = 6\text{dB}$.

In solid line, the minimum per-user data rate is evaluated with (4.5) for nonlinearity-agnostic receiver. In addition, we display in dotted line the minimum per-user data rate for the linear inter-beam interference case, i.e., when we enforce no nonlinear interference in the expression of the data rate (4.5) and finally obtain the data rate (3.1).

In Fig. 5.3, we plot the minimum per-user data rate versus the pre-amplifier gain for the five above mentioned power allocations. We observe that taking into account the nonlinear interference in the optimization problem allows to obtain higher minimum data rates.

5.5.3 Sum-power analysis

We denote the power allocations related to the minimization of the sum-power by

- P^{naive1} , the power allocation where the users use the same transmit power P which is then optimized for minimizing the sum-power where the nonlinear interference is taken into account,
- P^{naive2} , the power allocation where the received power at the satellite level is the same, so $G_m^{(b)} P_{b,m} = G_{m'}^{(b')} P_{b',m'}$, which is then optimized for minimizing the sum-power where the nonlinear interference is taken into account,
- P^{li} , the power allocation which is the optimal solution of Problem 5.9 when we force $\mathcal{P}_{b,m}^{(\text{NL})} = 0$,

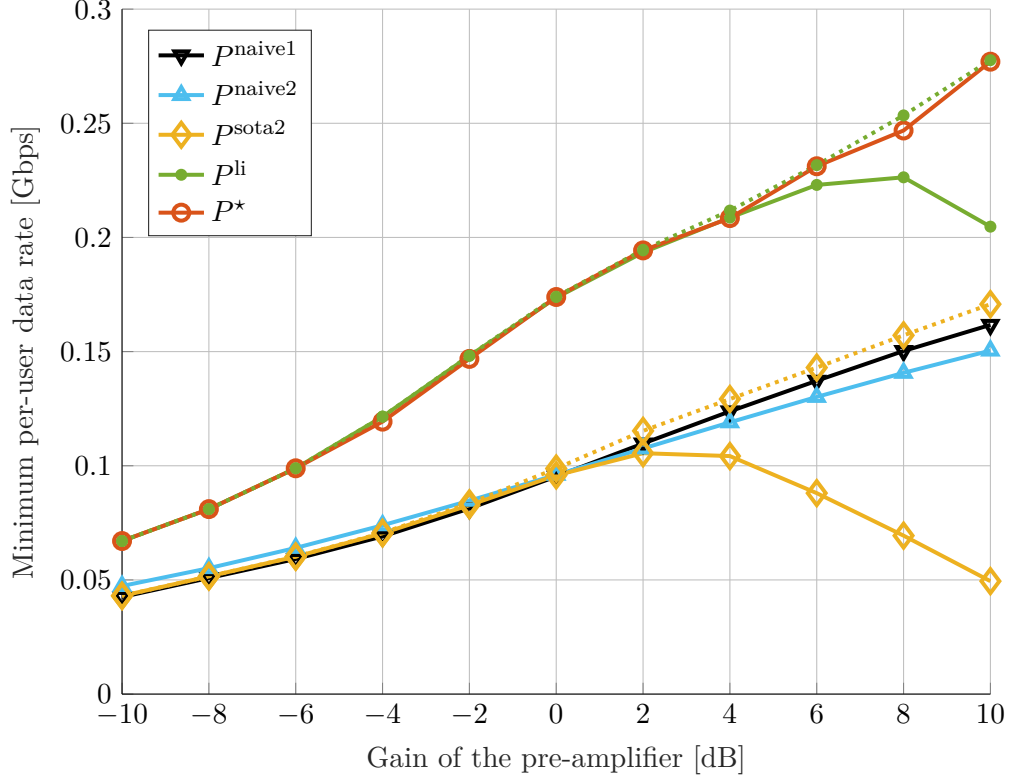


Figure 5.3: Minimum per-user data rate vs. pre-amplifier gain G_{amp} for 1 FS per 100 km².

- P^* , the power allocation which is the optimal solution of Problem 5.9 obtained by numerical solver [33].

In solid line, the data rate is evaluated with (4.5) for nonlinearity-agnostic receiver. In addition, we display in dotted line the data rate for the linear inter-beam interference case, i.e., when we enforce no nonlinear interference in the expression of the data rate (4.5) and finally obtain the data rate (3.1).

In Fig. 5.4, we plot the sum-power versus the target data rate obtained for the four above mentioned power allocations. We fix the same target data rate for all users, and we inspect two values for the pre-amplifier gain, denoted by G_{amp} . We set the FS density to 0.1 per km². We observe nonlinear effects only for a high target data rate, which is coherent because the minimization of the powers allows to stay in the linear zone of the HPA. We can conclude that the consideration of nonlinear interference for the minimization of the sum-power is not necessary.

5.6 Conclusion

In this chapter, we have addressed optimization problems in the context of a multibeam satellite with a nonlinear HPA for nonlinearity-agnostic receiver. More precisely, we formalized three optimization problems. The first one maximizes the system sum-rate by taking into account the nonlinear interference. The obtained problem boiled down to CGP and we have proposed a SCA procedure with monomial approximation. The second problem maximizes the minimum per-user

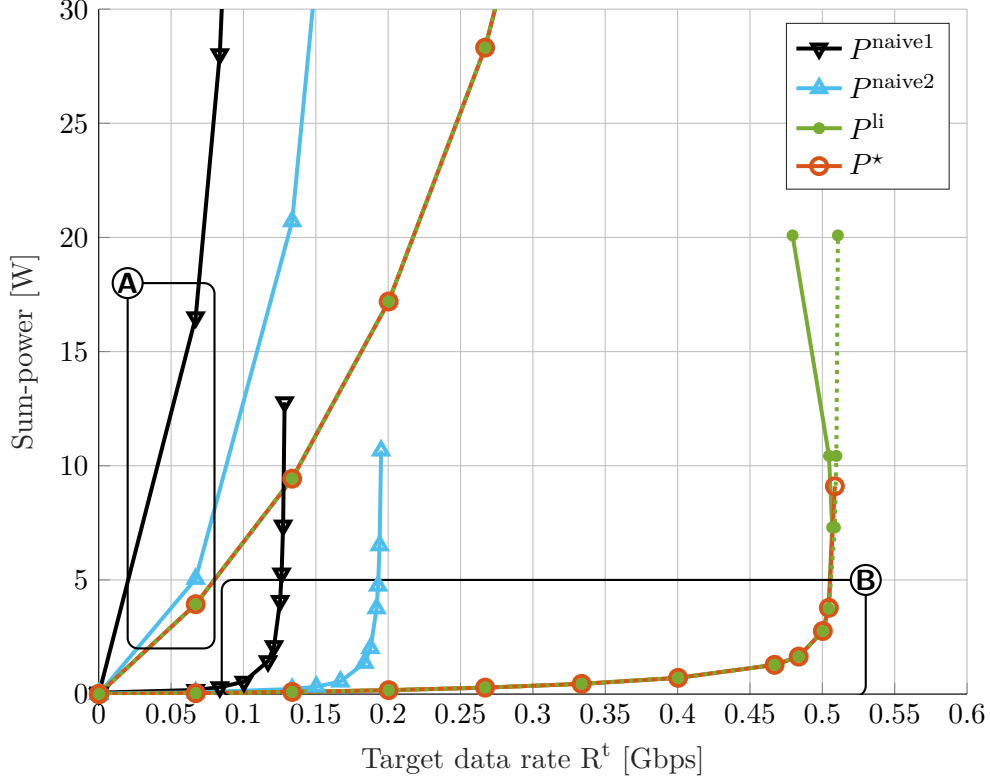


Figure 5.4: Sum-power vs. target data rate $R_{b,m}^t = R^t$ with $G_{amp} \in \{-10, 10\}$ dB (respectively A and B), and 0.1 FS per 100 km².

data rate. After a rewriting, the resulting problem became naturally convex and the optimal solution was obtained thanks to numerical solver. The last problem minimizes the sum-power of the system, subject to a target data-rate. The rewriting of the constraints allowed to obtain a convex problem, which is solved in an optimal way by a numerical solver. A summary of the addressed problems along with the proposed solutions is presented in Table 5.1.

Issue	Problem	Solution
Sum-rate	Problem 5.1	SCA – Algorithm 5.1
Fairness	Problem 5.5	CVX
Sum-power	Problem 5.9	CVX

Table 5.1: Addressed problems and proposed solutions.

Resource allocation for nonlinearity-aware receiver

Communication networks need to carry more and more data with new user cases. The hybridization of cellular and satellite networks allows to answer the exponential increase of data traffic. Indeed, the satellite system serves as relay between two points of a terrestrial system. The satellite uplink/return link is studied in this chapter, where terrestrial users transmit data to the satellite, which then sends it to a terrestrial gateway.

In order to respond to the increase in data rates, a new frequency range around the Ka-band is considered. In this context, some studies have proposed resource allocation algorithms to maximize the system sum-rate [9, 3]. However, these studies assume that the satellite *High-Power Amplifier* (HPA) operates in the linear regime.

When nonlinear regime of the HPA is taken into account, data rate expressions have been provided in Chapter 4. Actually we exhibited two different expressions according to the way the nonlinear interference has been treated by the receiver. The first way is called *nonlinearity-agnostic* since the nonlinear interference is seen as an extra noise. The second way is called *nonlinearity-aware* since the nonlinear interference is seen as an extra signal carrying useful information. Practical and scalable power allocations have been proposed in Chapter 5 for the case of nonlinearity-agnostic receivers. In the case of nonlinearity-aware receivers, significant gains have been observed in comparison with in nonlinearity-agnostic receivers in Chapter 4. However, a smart resource allocation has to be performed in order to reach this gain. In this chapter, we aim to propose power allocation algorithms for the nonlinearity-aware receivers. We will show that the data rate expression involves a posynomial over signomial ratio, leading to *Signomial Programming* (SP) optimization problem. This type of problem has been rarely studied in the context of wireless communications [46, 47].

In [16] and Chapter 5, the presence of the linear and nonlinear interference respectively involves a ratio of posynomials in the data rate expression and is thus solved using the same methodology, i.e., *Successive Convex Approximation* (SCA) followed by *Geometric Programming* (GP). Here, this approach is not suitable because the cost function is not a ratio of posynomials. As initially seen by [18], we suggest moving the ratio of signomials into the constraint set and rewriting it into a ratio of posynomials. Then similarly to [16] and Chapter 5, SCA procedure

followed by GP can be used to solve the considered optimization problems. We show that this approach leads to practical and scalable power allocation algorithms.

The rest of the chapter is organized as follows. In Section 6.1, the main problem of sum-rate maximization, for nonlinearity-aware receiver, is stated and is solved in Section 6.2. In Section 6.3, the fairness issue is addressed for nonlinearity-aware receiver, where the maximization of minimum per-user data rate problem is formulated and solved. In Section 6.5, we take the liberty of dealing with the problem of sum-power minimization subject to a target data rate, for nonlinearity-aware receiver. In Section 6.6, concluding remarks are drawn.

6.1 Problem formulation

The first problem to be solved, which is one of the main goal of the thesis, is that of maximizing the system sum-rate formulated in Problem 1.1. We gave in Chapter 4 the data rate expression $R_{b,m}$ for user belonging to beam b using subband m in the presence of nonlinear effects, according to a nonlinearity-aware receiver. By putting (4.3) in the main Problem 1.1, the resulting power optimization problem is

Problem 6.1.

$$\begin{aligned} \mathbf{P}^* &= \arg \max_{\mathbf{P}} \sum_{b=1}^B \sum_{m=1}^M \log_2 (1 + Q_{b,m}) \\ \text{with } Q_{b,m}(\mathbf{P}) &= \frac{\mathcal{P}_{b,m}^{(L)^2} + 2\mathcal{P}_{b,m}^{(L)}\mathcal{P}_{b,m}^{(LNL)} + \mathcal{P}_{b,m}^{(LNL)^2}}{\mathcal{P}_{b,m}^{(L)}\mathcal{P}_{b,m}^{(NL)} + 2\mathcal{P}_{b,m}^{(L)}\mathcal{P}_{b,m}^{(INL)} + \mathcal{P}_{b,m}^{(L)}\mathcal{P}_{b,m}^{(I)} + \mathcal{P}_{b,m}^{(L)}\mathcal{P}_W - \mathcal{P}_{b,m}^{(LNL)^2}} \quad (6.1) \\ \text{s.t. } & (1.16) \text{ and } (1.17). \end{aligned}$$

Remark 6.1. Notice that the real parts and the modulus involved in (4.3) have been removed since all the corresponding terms are real-valued.

Consequently, the powers of the users are all coupled through the expression of the data rate (4.3) and the interference-temperature constraint (1.16). The optimization of the problem is challenging. Indeed, the problem is non-convex due to the objective function which involves a ratio of the variable to be optimized.

6.2 Solution for the maximization of the sum-rate

The contribution of this section is to solve the Problem 6.1. We have seen that the problem is non-convex. Nevertheless, we proved in Chapter 4 that the terms $\mathcal{P}_{b,m}^{(I)}$, $\mathcal{P}_{b,m}^{(NL)}$, $\mathcal{P}_{b,m}^{(INL)}$ and $\mathcal{P}_{b,m}^{(LNL)}$ involved in the data rate expression are posynomials. The term $Q_{b,m}$ given by (6.1) is therefore a ratio of a posynomial function over a signomial function. In Chapter 2, a method has been proposed to manage such a ratio.

Thanks to the monotonic growth of the logarithm function, Problem 6.1 is equivalent to the following one.

Problem 6.2.

$$\begin{aligned} \mathbf{P}^* &= \arg \max_{\mathbf{P}} \prod_{b=1}^B \prod_{m=1}^M (1 + Q_{b,m}) \\ \text{s.t. } & (1.16) \text{ and } (1.17). \end{aligned}$$

Lemma 6.1. *Problem 6.2 is SP.*

Remark 6.2. *The approximation of logarithmic function in high SINR regime cannot simplify the problem, since we have a ratio of posynomial function over signomial function.*

Proof. All the constraints are linear in \mathbf{P} . In addition, all the terms involved in (6.1), $\mathcal{P}_{b,m}^{(L)}$, $\mathcal{P}_{b,m}^{(I)}$, $\mathcal{P}_{b,m}^{(LNL)}$, $\mathcal{P}_{b,m}^{(INL)}$, and $\mathcal{P}_{b,m}^{(NL)}$ are posynomials. Due to the minus sign in the denominator of $Q_{b,m}$, the utility function is a product of ratios of posynomial function over signomial function. Finally, Problem 6.2 boils down to the so-called SP. \square

The difficulty is located in the objective function, where we have a product of ratios of posynomial function over signomial function. By mimicking the approach introduced in [18], the idea is to move the ratio inside the constraint set. We put the signomial cost function into the constraints by adding auxiliary variables $\mathbf{t} = (t_{b,m}) \in \mathbb{R}_{+*}^{B \times M}$. Then we have the equivalent Problem 6.3.

Problem 6.3.

$$\begin{aligned} (\mathbf{P}^*, \mathbf{t}^*) &= \arg \max_{\mathbf{P}, \mathbf{t}} \prod_{b=1}^B \prod_{m=1}^M t_{b,m} \\ \text{s.t. } & (1.16), (1.17), \\ & t_{b,m} \leq 1 + Q_{b,m}(\mathbf{P}), \quad \forall b, m. \end{aligned} \tag{6.2}$$

The second idea is to transform the constraints, which correspond to ratios of signomial functions, as ratios of posynomial functions. A ratio of signomial functions can always be rewritten as a ratio of posynomial functions, when the denominator has a constant sign inside the region of interest [18, 17]. First, we put in the same denominator the *Right-Hand Side (RHS)* of (6.2), as follows,

$$t_{b,m} \leq \frac{\mathcal{P}_{b,m}^{(NL)} + 2\mathcal{P}_{b,m}^{(INL)} + \mathcal{P}_{b,m}^{(I)} + \mathcal{P}_W + \mathcal{P}_{b,m}^{(L)} + 2\mathcal{P}_{b,m}^{(LNL)}}{\mathcal{P}_{b,m}^{(NL)} + 2\mathcal{P}_{b,m}^{(INL)} + \mathcal{P}_{b,m}^{(I)} + \mathcal{P}_W - \left(\mathcal{P}_{b,m}^{(L)}\right)^{-1} \mathcal{P}_{b,m}^{(LNL)^2}}, \quad \forall b, m. \tag{6.3}$$

As the denominator of $Q_{b,m}(\mathbf{P})$ is always positive (see Remark 4.1), we replace (6.3) with

$$t_{b,m} \left(\mathcal{P}_{b,m}^{(NL)} + 2\mathcal{P}_{b,m}^{(INL)} + \mathcal{P}_{b,m}^{(I)} + \mathcal{P}_W \right) \leq D_{b,m}(\mathbf{P}, \mathbf{t}), \quad \forall b, m, \tag{6.4}$$

where

$$D_{b,m}(\mathbf{P}, \mathbf{t}) = \mathcal{P}_{b,m}^{(L)} + \mathcal{P}_{b,m}^{(I)} + \mathcal{P}_{b,m}^{(NL)} + 2\mathcal{P}_{b,m}^{(INL)} + 2\mathcal{P}_{b,m}^{(LNL)} + t_{b,m} \mathcal{P}_{b,m}^{(L)-1} \mathcal{P}_{b,m}^{(LNL)^2} + \mathcal{P}_W. \tag{6.5}$$

Thus, $D_{b,m}(\mathbf{P}, \mathbf{t})$ is posynomial and we can rewrite the constraint (6.4) as

$$\frac{t_{b,m} \left(\mathcal{P}_{b,m}^{(NL)} + 2\mathcal{P}_{b,m}^{(INL)} + \mathcal{P}_{b,m}^{(I)} + \mathcal{P}_W \right)}{D_{b,m}(\mathbf{P}, \mathbf{t})} \leq 1, \quad \forall b, m. \tag{6.6}$$

Lemma 6.2. *The constraint (6.6) is a ratio of posynomials less or equal to one.*

Moreover we replace the maximization by a minimization by taking the inverse (see Remark 3.3). The resulting equivalent optimization problem is

Problem 6.4.

$$\begin{aligned}
 (\mathbf{P}^*, \mathbf{t}^*) &= \arg \min_{\mathbf{P}, \mathbf{t}} \prod_{b=1}^B \prod_{m=1}^M t_{b,m}^{-1} \\
 \text{s.t. } & (1.16), (1.17) \text{ and } (6.6).
 \end{aligned} \tag{6.7}$$

Lemma 6.3. *Problem 6.4 is a Complementary Geometric Programming (CGP) since the constraints (6.6) are ratios of posynomial functions*

The difficulty is now located in the constraint set, where there are ratios of posynomial functions. We have seen in Section 2.4.2 how to manage CGP problems.

First, we use the so-called SCA method for non-convex problem, presented in Section 2.3.2. In order to apply SCA procedure, our objective is now to find a tight upper-bound for the constraint (6.6) which is either directly convex or GP. Secondly, we propose to replace the denominator with a monomial satisfying the SCA conditions at a given point. A straightforward and easy way was shown in Section 2.4.2 to build this monomial which satisfies SCA conditions. Finally, this leads to a GP problem, since a ratio of posynomial and monomial is a posynomial, which can be solved efficiently by numerical solvers. Since the monomial approximation satisfies the SCA conditions, the SCA procedure converges toward a stationary point. In [16], the authors use the same approach for the objective function of their problem, where in their case the interference is linear. In Chapter 5, we also used the same method to manage CGP when the ratio of posynomials is in the objective function.

The monomial approximation at the point $(\mathbf{P}_i, \mathbf{t}_i)$ is denoted by $\tilde{D}_{b,m}^{(i)}$. This approximation is built in such a way that it satisfies the SCA conditions, thanks to the method explained in Chapter 2,

$$\begin{aligned}
 \tilde{D}_{b,m}^{(i)}(\mathbf{P}, \mathbf{t}) &= \left(\frac{\gamma_1^2 G_m^{(b)} P_{b,m}}{\lambda_{b,m}^{(1)}} \right)^{\lambda_{b,m}^{(1)}} \\
 &\times \prod_{\substack{b'=1 \\ b' \neq b}}^B \left(\frac{\gamma_1^2 G_m^{(b',b)} P_{b',m}}{\lambda_{b,m}^{(2)}(b')} \right)^{\lambda_{b,m}^{(2)}(b')} \\
 &\times \prod_{b_1, b_2, b_3}^B \prod_{m', m''=1}^M \left(\frac{4\gamma_3^2 \alpha_0^{(1)} G_m^{(b_1,b)} G_{m'}^{(b_2,b)} G_{m''}^{(b_3,b)} P_{b_1,m} P_{b_2,m'} P_{b_3,m''}}{\lambda_{b,m}^{(3)}(b_1, b_2, b_3, m', m'')} \right)^{\lambda_{b,m}^{(3)}(b_1, b_2, b_3, m', m'')} \\
 &\times \prod_{b_1, b_2, b_3=1}^B \prod_{m', m''=1}^M \left(\frac{4\tilde{\delta}_{m,M} \gamma_3^2 \alpha_1^{(1)} G_{m+1}^{(b_1,b)} G_{m'}^{(b_2,b)} G_{m''}^{(b_3,b)} P_{b_1, m+1} P_{b_2, m'} P_{b_3, m''}}{\lambda_{b,m}^{(4)}(b_1, b_2, b_3, m', m'')} \right)^{\lambda_{b,m}^{(4)}(b_1, b_2, b_3, m', m'')}
 \end{aligned}$$

$$\begin{aligned}
& \times \prod_{b_1, b_2, b_3=1}^B \prod_{m', m''=1}^M \left(\frac{4\tilde{\delta}_{m,1} \gamma_3^2 \alpha_1^{(1)} G_{m-1}^{(b_1,b)} G_{m'}^{(b_2,b)} G_{m''}^{(b_3,b)} P_{b_1, m-1} P_{b_2, m'} P_{b_3, m''}}{\lambda_{b,m}^{(5)}(b_1, b_2, b_3, m', m'')} \right)^{\lambda_{b,m}^{(5)}(b_1, b_2, b_3, m', m'')} \\
& \times \prod_{b_1, b_2, b_3}^B \prod_{\substack{m_1, m_2, m_3=1 \\ m=m_1+m_2-m_3}}^M \left(\frac{2\gamma_3^2 \alpha_0^{(2)} G_{m_1}^{(b_1,b)} G_{m_2}^{(b_2,b)} G_{m_3}^{(b_3,b)} P_{b_1, m_1} P_{b_2, m_2} P_{b_3, m_3}}{\lambda_{b,m}^{(6)}(b_1, b_2, b_3, m_1, m_2, m_3)} \right)^{\lambda_{b,m}^{(6)}(b_1, b_2, b_3, m_1, m_2, m_3)} \\
& \times \prod_{b_1, b_2, b_3=1}^B \prod_{\substack{m_1, m_2, m_3=1 \\ m=m_1+m_2-m_3 \pm 1}}^M \left(\frac{2\gamma_3^2 \alpha_1^{(2)} G_{m_1}^{(b_1,b)} G_{m_2}^{(b_2,b)} G_{m_3}^{(b_3,b)} P_{b_1, m_1} P_{b_2, m_2} P_{b_3, m_3}}{\lambda_{b,m}^{(7)}(b_1, b_2, b_3, m_1, m_2, m_3)} \right)^{\lambda_{b,m}^{(7)}(b_1, b_2, b_3, m_1, m_2, m_3)} \\
& \times \prod_{\substack{b'=1 \\ b' \neq b}}^B \prod_{b''=1}^B \prod_{m'=1}^M \left(\frac{4\gamma_1 \gamma_3 \beta G_m^{(b',b)} G_{m'}^{(b'',b)} P_{b', m} P_{b'', m'}}{\lambda_{b,m}^{(8)}(b', b'', m')} \right)^{\lambda_{b,m}^{(8)}(b', b'', m')} \\
& \times \prod_{b'=1}^B \prod_{m'=1}^M \left(\frac{4\gamma_1 \gamma_3 \beta G_m^{(b)} G_{m'}^{(b',b)} P_{b, m} P_{b', m'}}{\lambda_{b,m}^{(9)}(b', m')} \right)^{\lambda_{b,m}^{(9)}(b', m')} \\
& \times \prod_{b', b''=1}^B \prod_{m', m''=1}^M \left(\frac{4\gamma_3^2 \beta^2 t_{b,m} G_m^{(b)} G_{m'}^{(b',b)} G_{m''}^{(b'',b)} P_{b, m} P_{b', m'} P_{b'', m''}}{\lambda_{b,m}^{(10)}(b', b'', m', m'')} \right)^{\lambda_{b,m}^{(10)}(b', b'', m', m'')} \\
& \times \left(\frac{P_W}{\lambda_{b,m}^{(11)}} \right)^{\lambda_{b,m}^{(11)}}, \tag{6.8}
\end{aligned}$$

where

$$\lambda_{b,m}^{(1)} = \frac{\gamma_1^2 G_m^{(b)} P_{b,m}^{(i)}}{D_{b,m}(\mathbf{P}_i)}, \tag{6.9}$$

$$\lambda_{b,m}^{(2)}(b') = \frac{\gamma_1^2 G_m^{(b',b)} P_{b',m}^{(i)}}{D_{b,m}(\mathbf{P}_i)}, \tag{6.10}$$

$$\lambda_{b,m}^{(3)}(b_1, b_2, b_3, m', m'') = \frac{4\gamma_3^2 \alpha_0^{(1)} G_m^{(b_1,b)} G_{m'}^{(b_2,b)} G_{m''}^{(b_3,b)} P_{b_1, m}^{(i)} P_{b_2, m'}^{(i)} P_{b_3, m''}^{(i)}}{D_{b,m}(\mathbf{P}_i)}, \tag{6.11}$$

$$\lambda_{b,m}^{(4)}(b_1, b_2, b_3, m', m'') = \frac{4\tilde{\delta}_{m,M} \gamma_3^2 \alpha_1^{(1)} G_{m+1}^{(b_1,b)} G_{m'}^{(b_2,b)} G_{m''}^{(b_3,b)} P_{b_1, m+1}^{(i)} P_{b_2, m'}^{(i)} P_{b_3, m''}^{(i)}}{D_{b,m}(\mathbf{P}_i)}, \tag{6.12}$$

$$\lambda_{b,m}^{(5)}(b_1, b_2, b_3, m', m'') = \frac{4\tilde{\delta}_{m,1} \gamma_3^2 \alpha_1^{(1)} G_{m-1}^{(b_1,b)} G_{m'}^{(b_2,b)} G_{m''}^{(b_3,b)} P_{b_1, m-1}^{(i)} P_{b_2, m'}^{(i)} P_{b_3, m''}^{(i)}}{D_{b,m}(\mathbf{P}_i)}, \tag{6.13}$$

$$\lambda_{b,m}^{(6)}(b_1, b_2, b_3, m_1, m_2, m_3) = \frac{2\gamma_3^2 \alpha_0^{(2)} G_{m_1}^{(b_1,b)} G_{m_2}^{(b_2,b)} G_{m_3}^{(b_3,b)} P_{b_1, m_1}^{(i)} P_{b_2, m_2}^{(i)} P_{b_3, m_3}^{(i)}}{D_{b,m}(\mathbf{P}_i)}, \tag{6.14}$$

$$\lambda_{b,m}^{(7)}(b_1, b_2, b_3, m_1, m_2, m_3) = \frac{2\gamma_3^2 \alpha_1^{(2)} G_{m_1}^{(b_1,b)} G_{m_2}^{(b_2,b)} G_{m_3}^{(b_3,b)} P_{b_1, m_1}^{(i)} P_{b_2, m_2}^{(i)} P_{b_3, m_3}^{(i)}}{D_{b,m}(\mathbf{P}_i)}, \tag{6.15}$$

$$\lambda_{b,m}^{(8)}(b', b'', m') = \frac{4\gamma_1 \gamma_3 \beta G_m^{(b',b)} G_{m'}^{(b'',b)} P_{b', m}^{(i)} P_{b'', m'}^{(i)}}{D_{b,m}(\mathbf{P}_i)}, \tag{6.16}$$

$$\lambda_{b,m}^{(9)}(b', m') = \frac{4\gamma_1 \gamma_3 \beta G_m^{(b)} G_{m'}^{(b',b)} P_{b, m}^{(i)} P_{b', m'}^{(i)}}{D_{b,m}(\mathbf{P}_i)}, \tag{6.17}$$

$$\lambda_{b,m}^{(10)}(b', b'', m', m'') = \frac{4\gamma_3^2 \beta^2 t_{b,m}^{(i)} G_m^{(b)} G_{m'}^{(b',b)} G_{m''}^{(b'',b)} P_{b,m}^{(i)} P_{b',m'}^{(i)} P_{b'',m''}^{(i)}}{D_{b,m}(\mathbf{P}_i)}, \quad (6.18)$$

$$\lambda_{b,m}^{(11)} = \frac{\mathcal{P}_W}{D_{b,m}(\mathbf{P}_i)}. \quad (6.19)$$

Lemma 6.4. *The term $\tilde{D}_{b,m}^{(i)}$ is a monomial approximation of $D_{b,m}$ at the point \mathbf{P}_i which satisfies the [SCA](#) conditions.*

By replacing $D_{b,m}$ with $\tilde{D}_{b,m}^{(i)}$ in Problem [6.2](#), the resulting approximated optimization problem is

Problem 6.5.

$$\begin{aligned} \mathbf{P}_i^*, \mathbf{t}_i^* &= \arg \min_{\mathbf{P}, \mathbf{t}} \prod_{b=1}^B \prod_{m=1}^M t_{b,m}^{-1} \\ \text{s.t. } & (1.16), (1.17), \\ & \left(\tilde{D}_{b,m}^{(i-1)}(\mathbf{P}, \mathbf{t}) \right)^{-1} t_{b,m} \left(\mathcal{P}_{b,m}^{(\text{NL})} + 2\mathcal{P}_{b,m}^{(\text{INL})} + \mathcal{P}_{b,m}^{(\text{I})} + \mathcal{P}_W \right) \leq 1, \quad \forall b, m. \end{aligned} \quad (6.20)$$

Result 6.1. *Problem [6.5](#) is [GP](#) since it minimizes a posynomial function over a set in [GP](#) form and can be efficiently solved by numerical algorithms.*

Proof. The objective function is a monomial function since the inverse of a monomial is still a monomial. The constraint set is composed of posynomial functions less or equal to one, since posynomials are close under the addition and multiplication. \square

Since the monomial approximation satisfies the [SCA](#) conditions, the [SCA](#) procedure depicted in Algorithm [6.1](#) converges towards a stationary point. The obtained solution is sub-optimal.

Algorithm 6.1 [SCA](#) based procedure for solving Problem [6.1](#)

- 1: Set $\epsilon > 0$, $E = \epsilon + 1$, $i = 0$
 - 2: Find $\mathbf{P}_0, \mathbf{t}_0$ a feasible solution of Problem [6.1](#)
 - 3: Compute the sum-rate R_0 using [\(4.3\)](#)
 - 4: **while** $E > \epsilon$ **do**
 - 5: $i = i + 1$
 - 6: Compute the monomial approximation $\tilde{D}_{b,m}^{(i-1)}(\mathbf{P}, \mathbf{t})$ around the point $(\mathbf{P}_{i-1}, \mathbf{t}_{i-1})$, using [\(6.8\)](#)
 - 7: Find $(\mathbf{P}_i^*, \mathbf{t}_i^*)$ the optimal solution of Problem [6.5](#)
 - 8: Compute the sum-rate R_i and $E = |R_i - R_{i-1}|$
 - 9: **end while**
 - 10: **return** $\mathbf{P}^* = \mathbf{P}_i$
-

In this section, we have proposed an optimization algorithm for the problem of system sum-rate maximization, in presence of nonlinear effects and when a nonlinearity-aware receiver is considered. Starting from a non-convex optimization problem, we rewrote it in the [SP](#) form, then introduced additional variables in order to obtain a [CGP](#) form, finally the combination of the [SCA](#) procedure and the monomial approximation allows to obtain a [GP](#) problem at each iteration. However, the notion of fairness is not present in this problem. The maximization of sum-rate will benefit the best users while neglecting the users with unfavorable conditions.

6.3 Maximization of the minimum per-user rate

In this section, we address the fairness issue between users in presence of nonlinear effects and for the nonlinearity-aware receiver. Here we consider only the *max-min fairness*. The problem of maximization of the minimum per-user rate is formulated as follows

Problem 6.6.

$$\begin{aligned} \mathbf{P}^* &= \arg \max_{\mathbf{P}} \min_{b,m} \log_2 (1 + Q_{b,m}) \\ \text{with } Q_{b,m}(\mathbf{P}) &= \frac{\mathcal{P}_{b,m}^{(L)^2} + 2\mathcal{P}_{b,m}^{(L)}\mathcal{P}_{b,m}^{(LNL)} + \mathcal{P}_{b,m}^{(LNL)^2}}{\mathcal{P}_{b,m}^{(L)}\mathcal{P}_{b,m}^{(NL)} + 2\mathcal{P}_{b,m}^{(L)}\mathcal{P}_{b,m}^{(INL)} + \mathcal{P}_{b,m}^{(L)}\mathcal{P}_{b,m}^{(I)} + \mathcal{P}_{b,m}^{(L)}\mathcal{P}_W - \mathcal{P}_{b,m}^{(LNL)^2}} \\ \text{s.t. } & (1.16) \text{ and } (1.17). \end{aligned}$$

Thanks to the monotonic growth of the logarithm function, Problem 6.6 is equivalent to the following one.

Problem 6.7.

$$\begin{aligned} \mathbf{P}^* &= \arg \max_{\mathbf{P}} \min_{b,m} Q_{b,m} \\ \text{s.t. } & (1.16) \text{ and } (1.17). \end{aligned}$$

The difficulty is located in the objective function, which is not concave nor a posynomial function because of the minimum operator and the ratio of a posynomial function over a signomial function $Q_{b,m}$. As in Chapter 5, we introduce a new variable $t \in \mathbb{R}^{+*}$ in order to remove the minimum operator. By doing so, the ratio of posynomials over signomials also moves into the constraints set. Then we obtain the equivalent Problem 6.8

Problem 6.8.

$$\begin{aligned} (\mathbf{P}^*, t^*) &= \arg \max_{\mathbf{P}, t} t \\ \text{s.t. } & (1.16), (1.17), \\ & \frac{\mathcal{P}_{b,m}^{(L)^2} + 2\mathcal{P}_{b,m}^{(L)}\mathcal{P}_{b,m}^{(LNL)} + \mathcal{P}_{b,m}^{(LNL)^2}}{\mathcal{P}_{b,m}^{(L)}\mathcal{P}_{b,m}^{(NL)} + 2\mathcal{P}_{b,m}^{(L)}\mathcal{P}_{b,m}^{(INL)} + \mathcal{P}_{b,m}^{(L)}\mathcal{P}_{b,m}^{(I)} + \mathcal{P}_{b,m}^{(L)}\mathcal{P}_W - \mathcal{P}_{b,m}^{(LNL)^2}} \geq t, \quad \forall b, m. \end{aligned} \quad (6.21)$$

Lemma 6.5. *Problem 6.8 is SP since it involves ratios of signomial function over posynomial function.*

The second idea is to transform the constraints, which correspond to ratios of signomial functions, as ratios of posynomial functions. A ratio of signomial functions can always be rewritten as a ratio of posynomial functions, when the denominator has a constant sign inside the region of interest [18, 17]. As the denominator is always positive, we replace (6.21) with

$$\frac{t \left(\mathcal{P}_{b,m}^{(NL)} + 2\mathcal{P}_{b,m}^{(INL)} + \mathcal{P}_{b,m}^{(I)} + \mathcal{P}_W \right)}{D_{b,m}(\mathbf{P}, t)} \leq 1, \quad \forall b, m, \quad (6.22)$$

where

$$D_{b,m}(\mathbf{P}, t) = \mathcal{P}_{b,m}^{(L)} + 2\mathcal{P}_{b,m}^{(LNL)} + (t+1)\mathcal{P}_{b,m}^{(L)-1}\mathcal{P}_{b,m}^{(LNL)^2}. \quad (6.23)$$

Lemma 6.6. *The constraint (6.22) is a ratio of posynomials less or equal to one.*

Moreover we replace the maximization by a minimization by taking the inverse (see Remark 3.3). The resulting equivalent optimization problem is

Problem 6.9.

$$\begin{aligned} \mathbf{P}^*, t^* &= \arg \min_{\mathbf{P}, t} t^{-1} \\ \text{s.t. } & (1.16), (1.17) \text{ and } (6.22). \end{aligned}$$

Lemma 6.7. *Problem 6.9 is a CGP since the constraints (6.22) are ratios of posynomial functions*

The difficulty is now located in the constraint set, where there are ratios of posynomial functions. We have seen in Section 2.4.2 how to manage CGP problems.

First, we use the so-called SCA method for non-convex problem, presented in Chapter 2. In order to apply SCA procedure, our objective is now to find a tight upper-bound for the constraint (6.22) which is either directly convex or GP. Secondly, we propose to replace the denominator with a monomial satisfying the SCA conditions at a given point. A straightforward and easy way was shown in Section 2.4.2 to build this monomial which satisfies SCA conditions. Finally, this leads to a GP problem, since a ratio of posynomial and monomial is a posynomial, which can be solved efficiently by numerical solvers. Since the monomial approximation satisfies the SCA conditions, the SCA procedure converges toward a stationary point. In Section 6.2, we use the same method for the sum-rate maximization.

The monomial approximation at the point (\mathbf{P}_i, t_i) is denoted by $\tilde{D}_{b,m}^{(i)}$. This approximation is built in such a way that it satisfies the SCA conditions, thanks to the method explained in Chapter 2,

$$\begin{aligned} \tilde{D}_{b,m}^{(i)}(\mathbf{P}, t) &= \left(\frac{\gamma_1^2 G_m^{(b)} P_{b,m}}{\lambda_{b,m}^{(1)}} \right)^{\lambda_{b,m}^{(1)}} \\ &\times \prod_{b'=1}^B \prod_{m'=1}^M \left(\frac{4\gamma_1\gamma_3\beta G_m^{(b)} G_{m'}^{(b',b)} P_{b,m} P_{b',m'}}{\lambda_{b,m}^{(2)}(b', m')} \right)^{\lambda_{b,m}^{(2)}(b', m')} \\ &\times \prod_{b', b''=1}^B \prod_{m', m''=1}^M \left(\frac{4\gamma_3^2\beta^2 G_m^{(b)} G_{m'}^{(b',b)} G_{m''}^{(b'',b)} P_{b,m} P_{b',m'} P_{b'',m''}}{\lambda_{b,m}^{(3)}(b', b'', m', m'')} \right)^{\lambda_{b,m}^{(3)}(b', b'', m', m'')} \\ &\times \prod_{b', b''=1}^B \prod_{m', m''=1}^M \left(\frac{4\gamma_3^2\beta^2 t G_m^{(b)} G_{m'}^{(b',b)} G_{m''}^{(b'',b)} P_{b,m} P_{b',m'} P_{b'',m''}}{\lambda_{b,m}^{(4)}(b', b'', m', m'')} \right)^{\lambda_{b,m}^{(4)}(b', b'', m', m'')} \quad , \quad (6.24) \end{aligned}$$

where

$$\lambda_{b,m}^{(1)} = \frac{\gamma_1^2 G_m^{(b)} P_{b,m}}{D_{b,m}(\mathbf{P}_i, t_i)}, \quad (6.25)$$

$$\lambda_{b,m}^{(2)}(b', m') = \frac{4\gamma_1\gamma_3\beta G_m^{(b)} G_{m'}^{(b',b)} P_{b,m} P_{b',m'}}{D_{b,m}(\mathbf{P}_i, t_i)}, \quad (6.26)$$

$$\lambda_{b,m}^{(3)}(b', b'', m', m'') = \frac{4\gamma_3^2 \beta^2 G_m^{(b)} G_{m'}^{(b',b)} G_{m''}^{(b'',b)} P_{b,m}^{(i)} P_{b',m'}^{(i)} P_{b'',m''}^{(i)}}{D_{b,m}(\mathbf{P}_i, t_i)}, \quad (6.27)$$

$$\lambda_{b,m}^{(4)}(b', b'', m', m'') = \frac{4\gamma_3^2 \beta^2 t_i G_m^{(b)} G_{m'}^{(b',b)} G_{m''}^{(b'',b)} P_{b,m}^{(i)} P_{b',m'}^{(i)} P_{b'',m''}^{(i)}}{D_{b,m}(\mathbf{P}_i, t_i)}. \quad (6.28)$$

Lemma 6.8. *The term $\tilde{D}_{b,m}^{(i)}$ is a monomial approximation of $D_{b,m}$ at the point \mathbf{P}_i which satisfies the [SCA](#) conditions.*

By replacing $D_{b,m}$ with $\tilde{D}_{b,m}^{(i)}$ in Problem [6.9](#), the resulting approximated optimization problem is

Problem 6.10.

$$\begin{aligned} (\mathbf{P}_i^*, t_i^*) &= \arg \min_{\mathbf{P}, t} \prod_{b=1}^B \prod_{m=1}^M t^{-1} \\ \text{s.t. } & (1.16), (1.17), \\ & \left(\tilde{D}_{b,m}^{(i-1)}(\mathbf{P}, t) \right)^{-1} t \left(\mathcal{P}_{b,m}^{(\text{NL})} + 2\mathcal{P}_{b,m}^{(\text{INL})} + \mathcal{P}_{b,m}^{(\text{I})} + \mathcal{P}_W \right) \leq 1, \quad \forall b, m. \end{aligned} \quad (6.29)$$

Result 6.2. *Problem [6.10](#) is [GP](#) since it minimizes a posynomial function over a set in [GP](#) form and can be efficiently solved by numerical algorithms.*

Since the monomial approximation satisfies the [SCA](#) conditions, the [SCA](#) procedure depicted in Algorithm [6.2](#) converges towards a stationary point. The obtained solution is sub-optimal.

Algorithm 6.2 [SCA](#) based procedure for solving Problem [6.6](#)

- 1: Set $\epsilon > 0$, $E = \epsilon + 1$, $i = 0$
 - 2: Find \mathbf{P}_0, t_0 a feasible solution of Problem [6.6](#)
 - 3: Compute the minimum per-user data rate R_0 using [\(4.3\)](#)
 - 4: **while** $E > \epsilon$ **do**
 - 5: $i = i + 1$
 - 6: Compute the monomial approximation $\tilde{D}_{b,m}^{(i-1)}(\mathbf{P}, t)$ around the point $\mathbf{P}_{i-1}, t_{i-1}$, using [\(6.24\)](#)
 - 7: Find \mathbf{P}_i^*, t_i^* the optimal solution of Problem [6.10](#)
 - 8: Compute the minimum per-user data rate R_i and $E = |R_i - R_{i-1}|$
 - 9: **end while**
 - 10: **return** $\mathbf{P}^* = \mathbf{P}_i$
-

In this section, we have proposed an optimization algorithm for the problem of maximization of the minimum per-user data rate, in presence of nonlinear effects and when a nonlinearity-aware receiver is considered. Starting from a non-convex optimization problem, we introduced an additional variable in order to get a [SP](#) form, then we rewrote the constraint set to obtain a [CGP](#) form, finally the combination of the [SCA](#) procedure and the monomial approximation allows to obtain a [GP](#) problem at each iteration.

6.4 Minimization of the sum-power

In this section, we cover the sum-power minimization problem, subject to a target data rate constraint. The problem of minimization of the sum-power is formulated as follows

Problem 6.11.

$$\begin{aligned}
\mathbf{P}^* &= \arg \min_{\mathbf{P}} \sum_{b=1}^B \sum_{m=1}^M P_{b,m} \\
\text{s.t. } & (1.16), (1.17), \\
& \log_2(1 + Q_{b,m}) \geq R_{b,m}^t, \quad \forall b, m, \\
& \text{with } Q_{b,m}(\mathbf{P}) = \frac{\mathcal{P}_{b,m}^{(L)^2} + 2\mathcal{P}_{b,m}^{(L)}\mathcal{P}_{b,m}^{(LNL)} + \mathcal{P}_{b,m}^{(LNL)^2}}{\mathcal{P}_{b,m}^{(L)}\mathcal{P}_{b,m}^{(NL)} + 2\mathcal{P}_{b,m}^{(L)}\mathcal{P}_{b,m}^{(INL)} + \mathcal{P}_{b,m}^{(L)}\mathcal{P}_{b,m}^{(I)} + \mathcal{P}_{b,m}^{(L)}\mathcal{P}_W - \mathcal{P}_{b,m}^{(LNL)^2}}.
\end{aligned} \tag{6.30}$$

The Problem 6.11 is non-convex and not SP because of constraints (6.30). However we easily rewrite these constraints by applying the increasing function 2^x . The resulting problem is

Problem 6.12.

$$\begin{aligned}
\mathbf{P}^* &= \arg \min_{\mathbf{P}} \sum_{b=1}^B \sum_{m=1}^M P_{b,m} \\
\text{s.t. } & (1.16), (1.17), \\
& Q_{b,m}(\mathbf{P}) \geq 2^{R_{b,m}^t} - 1, \quad \forall b, m.
\end{aligned} \tag{6.31}$$

Lemma 6.9. *Problem 6.12 is SP.*

Now, the idea is to transform the constraints (6.31), which correspond to ratios of signomial functions, as ratios of posynomial functions. As the denominator is always positive, we replace (6.31) with

$$\frac{(2^{R_{b,m}^t} - 1) (\mathcal{P}_{b,m}^{(NL)} + 2\mathcal{P}_{b,m}^{(INL)} + \mathcal{P}_{b,m}^{(I)} + \mathcal{P}_W)}{D_{b,m}(\mathbf{P})} \leq 1, \quad \forall b, m, \tag{6.32}$$

where

$$D_{b,m}(\mathbf{P}) = \mathcal{P}_{b,m}^{(L)} + 2\mathcal{P}_{b,m}^{(LNL)} + 2^{R_{b,m}^t} \mathcal{P}_{b,m}^{(L)-1} \mathcal{P}_{b,m}^{(LNL)^2}. \tag{6.33}$$

Lemma 6.10. *The constraint (6.32) is a ratio of posynomials less or equal to one.*

The resulting equivalent optimization problem is

Problem 6.13.

$$\begin{aligned}
\mathbf{P}^* &= \arg \min_{\mathbf{P}} \sum_{b=1}^B \sum_{m=1}^M P_{b,m} \\
\text{s.t. } & (1.16), (1.17) \text{ and } (6.32).
\end{aligned}$$

Lemma 6.11. *Problem 6.13 is a CGP since the constraints (6.32) are ratios of posynomial functions*

The difficulty is now located in the constraint set, where there are ratios of posynomial functions. We have seen in Section 2.4.2 how to manage CGP problems. First, we use the so-called SCA method for non-convex problem, presented in Chapter 2. In order to apply SCA procedure, our objective is now to find a tight upper-bound for the constraint (6.22) which is

either directly convex or **GP**. Secondly, we propose to replace the denominator with a monomial satisfying the **SCA** conditions at a given point. A straightforward and easy way was shown in Section 2.4.2 to build this monomial which satisfies **SCA** conditions. Finally, this leads to a **GP** problem, since a ratio of posynomial and monomial is a posynomial, which can be solved efficiently by numerical solvers. Since the monomial approximation satisfies the **SCA** conditions, the **SCA** procedure converges toward a stationary point. In Section 6.3, we use the same method for the sum-rate maximization.

The monomial approximation at the point (\mathbf{P}_i, t_i) is denoted by $\tilde{D}_{b,m}^{(i)}$. This approximation is built in such a way that it satisfies the **SCA** conditions, thanks to the method explained in Chapter 2,

$$\begin{aligned} \tilde{D}_{b,m}^{(i)}(\mathbf{P}) &= \left(\frac{\gamma_1^2 G_m^{(b)} P_{b,m}}{\lambda_{b,m}^{(1)}} \right)^{\lambda_{b,m}^{(1)}} \\ &\times \prod_{b'=1}^B \prod_{m'=1}^M \left(\frac{4\gamma_1 \gamma_3 \beta G_m^{(b)} G_{m'}^{(b',b)} P_{b,m} P_{b',m'}}{\lambda_{b,m}^{(2)}(b', m')} \right)^{\lambda_{b,m}^{(2)}(b', m')} \\ &\times \prod_{b', b''=1}^B \prod_{m', m''=1}^M \left(\frac{4\gamma_3^2 \beta^2 2^{R_{b,m}^t} G_m^{(b)} G_{m'}^{(b',b)} G_{m''}^{(b'',b)} P_{b,m} P_{b',m'} P_{b'',m''}}{\lambda_{b,m}^{(3)}(b', b'', m', m'')} \right)^{\lambda_{b,m}^{(3)}(b', b'', m', m'')}, \end{aligned} \quad (6.34)$$

where

$$\lambda_{b,m}^{(1)} = \frac{\gamma_1^2 G_m^{(b)} P_{b,m}^{(i)}}{D_{b,m}(\mathbf{P}_i)}, \quad (6.35)$$

$$\lambda_{b,m}^{(2)}(b', m') = \frac{4\gamma_1 \gamma_3 \beta G_m^{(b)} G_{m'}^{(b',b)} P_{b,m}^{(i)} P_{b',m'}^{(i)}}{D_{b,m}(\mathbf{P}_i)}, \quad (6.36)$$

$$\lambda_{b,m}^{(3)}(b', b'', m', m'') = \frac{4\gamma_3^2 \beta^2 2^{R_{b,m}^t} G_m^{(b)} G_{m'}^{(b',b)} G_{m''}^{(b'',b)} P_{b,m}^{(i)} P_{b',m'}^{(i)} P_{b'',m''}^{(i)}}{D_{b,m}(\mathbf{P}_i)}. \quad (6.37)$$

Lemma 6.12. *The term $\tilde{D}_{b,m}^{(i)}$ is a monomial approximation of $D_{b,m}$ at the point \mathbf{P}_i which satisfies the **SCA** conditions.*

By replacing $D_{b,m}$ with $\tilde{D}_{b,m}^{(i)}$ in Problem 6.13, the resulting approximated optimization problem is

Problem 6.14.

$$\begin{aligned} \mathbf{P}_i^* &= \arg \min_{\mathbf{P}} \sum_{b=1}^B \sum_{m=1}^M P_{b,m} \\ \text{s.t. } & (1.16), (1.17), \\ & \left(\tilde{D}_{b,m}^{(i-1)}(\mathbf{P}) \right)^{-1} \left(2^{R_{b,m}^t} - 1 \right) \left(\mathcal{P}_{b,m}^{(\text{NL})} + 2\mathcal{P}_{b,m}^{(\text{INL})} + \mathcal{P}_{b,m}^{(\text{I})} + \mathcal{P}_W \right) \leq 1, \quad \forall b, m. \end{aligned} \quad (6.38)$$

Result 6.3. *Problem 6.14 is **GP** since it minimizes a posynomial function over a set in **GP** form and can be efficiently solved by numerical algorithms.*

Algorithm 6.3 SCA based procedure for solving Problem 6.11

```
1: Set  $\epsilon > 0$ ,  $E = \epsilon + 1$ ,  $i = 0$ 
2: Find  $\mathbf{P}_0$  a feasible solution of Problem 6.11
3: Compute the sum-power  $R_0$  using (4.3)
4: while  $E > \epsilon$  do
5:    $i = i + 1$ 
6:   Compute the monomial approximation  $\tilde{D}_{b,m}^{(i-1)}(\mathbf{P})$  around the point  $\mathbf{P}_{i-1}$ , using (6.34)
7:   Find  $\mathbf{P}_i^*$  the optimal solution of Problem 6.14
8:   Compute the sum-power  $R_i$  and  $E = |R_i - R_{i-1}|$ 
9: end while
10: return  $\mathbf{P}^* = \mathbf{P}_i$ 
```

Since the monomial approximation satisfies the SCA conditions, the SCA procedure depicted in Algorithm 6.3 converges towards a stationary point. The obtained solution is sub-optimal.

In this section, we have proposed an optimization algorithm for the problem of sum-power minimization subject to target data rate, in presence of nonlinear effects and when a nonlinearity-aware receiver is considered. Starting from a non-convex optimization problem, we rewrote the constraint set to obtain a CGP form, finally the combination of the SCA procedure and the monomial approximation allows to obtain a GP problem at each iteration.

6.5 Numerical results

A multibeam multiband satellite with an uplink in the Ka-band (27.5-29.5GHz) is considered. The satellite is composed of $B = 2$ beams and there are $M = 6$ users per beam. The subband assignment has already been completed. The shaping filter is a *Square-Root-Raised-Cosine* (SRRC) filter with a roll-off of 0.25. The HPA distortion coefficients γ_1 and γ_3 are 1 and 0.05 respectively. In addition, we add a variable gain pre-amplifier just before the HPA. This device allows to set the HPA regime by changing the channel gains (and so input powers) uniformly for incoming signal of the same antenna. For simplicity, we assume that the gains of the pre-amplifiers are identical for all HPAs. $P_{\max} = 50\text{W}$ (47dBm) is the maximum transmit power. As in [3, 15, 2, 14], the channel gains $\{G_m^{(b',b)}\}_{b,m,b'}$ and $\{F_{b,m}^{(\ell)}\}_{b,m,\ell}$ are computed using location. Notice that the channel gain values within a same beam $\{G_m^{(b)}\}_m$ are close to each others. The maximum interference-temperature level is fixed to $I_{th}^{(\ell)}(m') = 1\text{pW}$ (−90dBm) for any ℓ, m' . Unless otherwise stated, we consider 1 *Fixed Service* (FS) per square kilometer. We use the CVX toolbox to solve GP problems [33].

6.5.1 Sum-rate analysis

We denote the power allocations related to the maximization of the sum-rate by

- P^{naive1} , the power allocation where the users use the same transmit power P which is then optimized for this objective function,
- P^{naive2} , the power allocation where the received power at the satellite level is the same, so $G_m^{(b)} P_{b,m} = G_{m'}^{(b')} P_{b',m'}$, which is then optimized for this objective function,

- P^{sota1} , the power allocation given by [3] and detailed in Section 3.2 where the interference is not taking into account,
- P' , the power allocation given by Algorithm 3.1 related to Problem 3.2, where there is no interference,
- P^{li} , the power allocation given by Algorithm 3.3 related to Problem 3.12, where only linear interference occurs, i.e. $\mathcal{P}_{b,m}^{(\text{NL})} = 0$,
- P^{nli} , the power allocation given by Algorithm 5.1 related to Problem 5.1 for nonlinearity-agnostic receiver, i.e. $\mathcal{P}_{b,m}^{(\text{LNL})} = 0$ and $\mathcal{P}_{b,m}^{(\text{INL})} = 0$,
- P^* , the power allocation given by Algorithm 6.1 which is the SCA procedure for Problem 6.1 where nonlinearity-aware receiver is considered.

In solid line, the sum-rate is evaluated with (4.3) for nonlinearity-aware receiver. In addition, we display in dotted line the sum-rate for the linear inter-beam interference case, i.e., when we enforce no nonlinear interference in the expression of the data rate (4.3) and finally obtain the data rate (3.1). We also display in dashed line the sum-rate for nonlinearity-agnostic receiver, i.e., the data rate is evaluated with (4.5) when the receiver is not able to exploit the correlation between the linear and the nonlinear part.

In Fig. 6.1, we plot the sum-rate versus the pre-amplifier gain, for the seven above mentioned power allocations. We set the FS density to 1 per square kilometer. The proposed Algorithm 6.1 is the best one, whatever the operating regime of the HPA. In nonlinear regime, our proposed Algorithm 6.1 allows to increase the sum-rate and have a gain by exploiting in an intelligent way the nonlinear effects. The solution obtained for nonlinearity-agnostic receiver allows to be robust against the nonlinear effects, but does not increase the sum-rate. We remark that the solutions obtained when the optimization problems assume a linear HPA are very bad and not suitable when the HPA is in nonlinear regime. Even worse, the lack of knowledge of the data rate expression in the nonlinear regime degrades the sum-rate, because we can wrongly think that increasing the gain of the pre-amplifier is beneficial for the sum-rate.

In Fig. 6.2, we plot the sum-rate versus the FS density, for a pre-amplifier gain value set to 6dB. For high primary user density, we observe that the interference-temperature constraints prevails in the problem. Indeed, the sum-rates obtained with solutions P^{li} , P^{nli} and P^* are close. We can therefore say that taking into account the nonlinear effects is not necessary when the density of the FS is high. When the density of the FS is low, the proposed P^* solution is then the best. Indeed, the nonlinear effects are more important because the users transmit on average at a higher power.

6.5.2 Minimum per-user data rate analysis

We denote the power allocations related to the maximization of minimum per-user data rate by

- P^{naive1} , the power allocation where the users use the same transmit power P which is then optimized for this objective function,

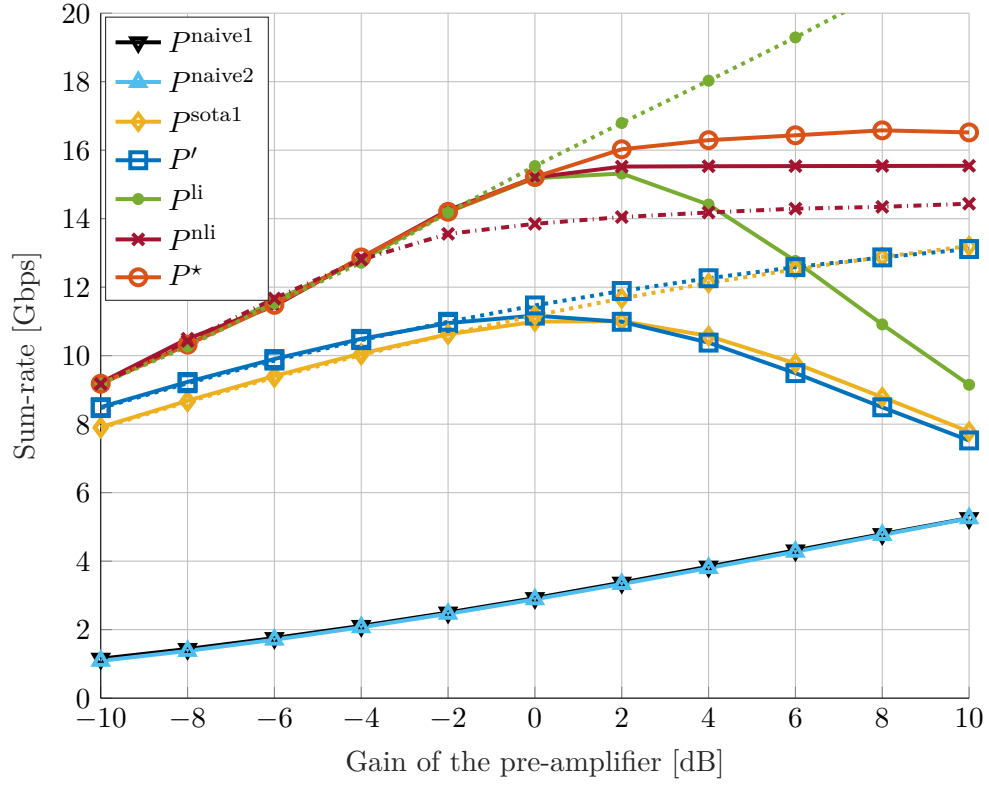


Figure 6.1: Sum-rate vs. pre-amplifier gain for 1 FS per 100 km².

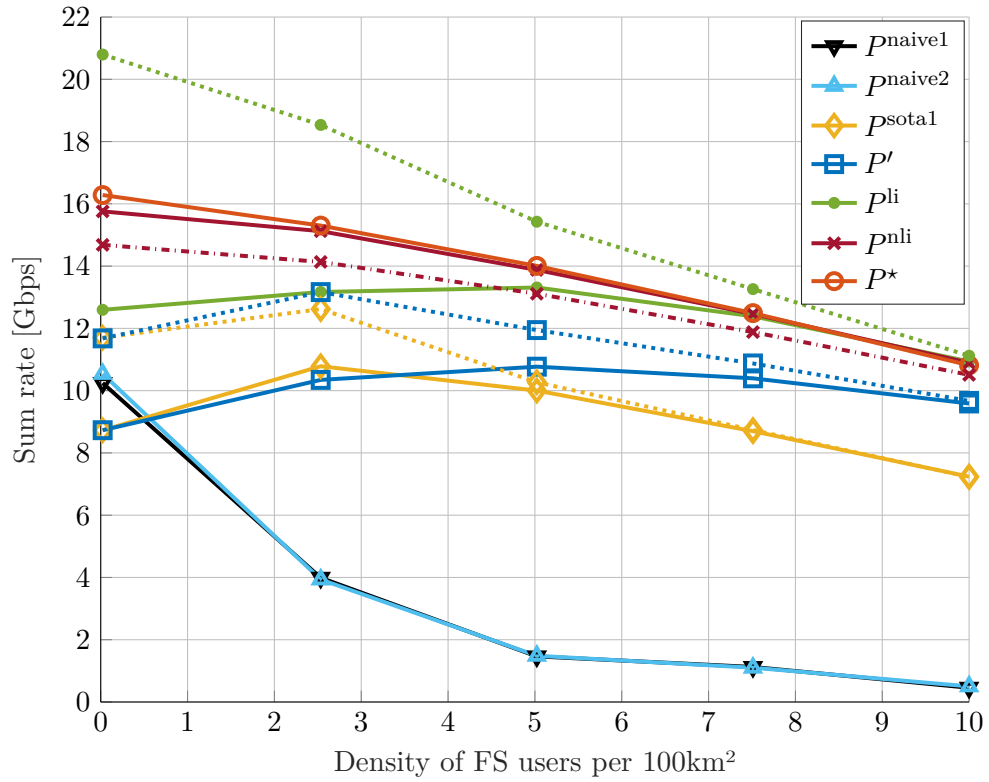


Figure 6.2: Sum-rate vs. FS density for $G_{amp} = 6\text{dB}$.

- P^{naive2} , the power allocation where the received power at the satellite level is the same, so $G_m^{(b)} P_{b,m} = G_{m'}^{(b')} P_{b',m'}$, which is then optimized for this objective function,
- P^{sota2} , the power allocation given by [8] and detailed in Section 3.5 where the interference is not taking into account,
- P^{li} , the power allocation which is the optimal solution of Problem 3.14 obtained by numerical solver [33], where only linear interference occurs, i.e. $\mathcal{P}_{b,m}^{(\text{NL})} = 0$,
- P^{nli} , the power allocation which is the optimal solution of Problem 5.5 obtained by numerical solver [33], for nonlinearity-agnostic receiver, i.e. $\mathcal{P}_{b,m}^{(\text{LNL})} = 0$ and $\mathcal{P}_{b,m}^{(\text{INL})} = 0$,
- P^* , the power allocation given by Algorithm 6.2 which is the SCA procedure for Problem 6.6 where nonlinearity-aware receiver is considered.

In solid line, the minimum per-user data rate is evaluated with (4.3) for nonlinearity-aware receiver. In addition, we display in dotted line the minimum per-user data rate for the linear inter-beam interference case, i.e., when we enforce no nonlinear interference in the expression of the data rate (4.3) and finally obtain the data rate (3.1). We also display in dashed line the minimum per-user data rate for nonlinearity-agnostic receiver, i.e., the data rate is evaluated with (4.5) when the receiver is not able to exploit the correlation between the linear and the nonlinear part.

In Fig. 6.3, we plot the minimum per-user data rate versus the pre-amplifier gain for the six above mentioned power allocations. We observe that taking into account the nonlinear interference in the optimization problem allows to obtain higher minimum data rates. However, the solutions P^* and P^{nli} provide almost the same results. Thus, the complexity added in the optimization problem by the expression of the data rate for nonlinearity-aware receiver is not necessary.

6.5.3 Sum-power analysis

We denote the power allocations related to the minimization of the sum-power by

- P^{naive1} , the power allocation where the users use the same transmit power P which is then optimized for this objective function,
- P^{naive2} , the power allocation where the received power at the satellite level is the same, so $G_m^{(b)} P_{b,m} = G_{m'}^{(b')} P_{b',m'}$, which is then optimized for this objective function,
- P^{li} , the power allocation which is the optimal solution of Problem 5.9 when we force $\mathcal{P}_{b,m}^{(\text{NL})} = 0$,
- P^{nli} , the power allocation which is the optimal solution of Problem 5.9 for the nonlinearity-agnostic receiver,
- P^* , the power allocation given by Algorithm 6.3 which is the SCA procedure for Problem 6.11 where nonlinearity-aware receiver is considered.

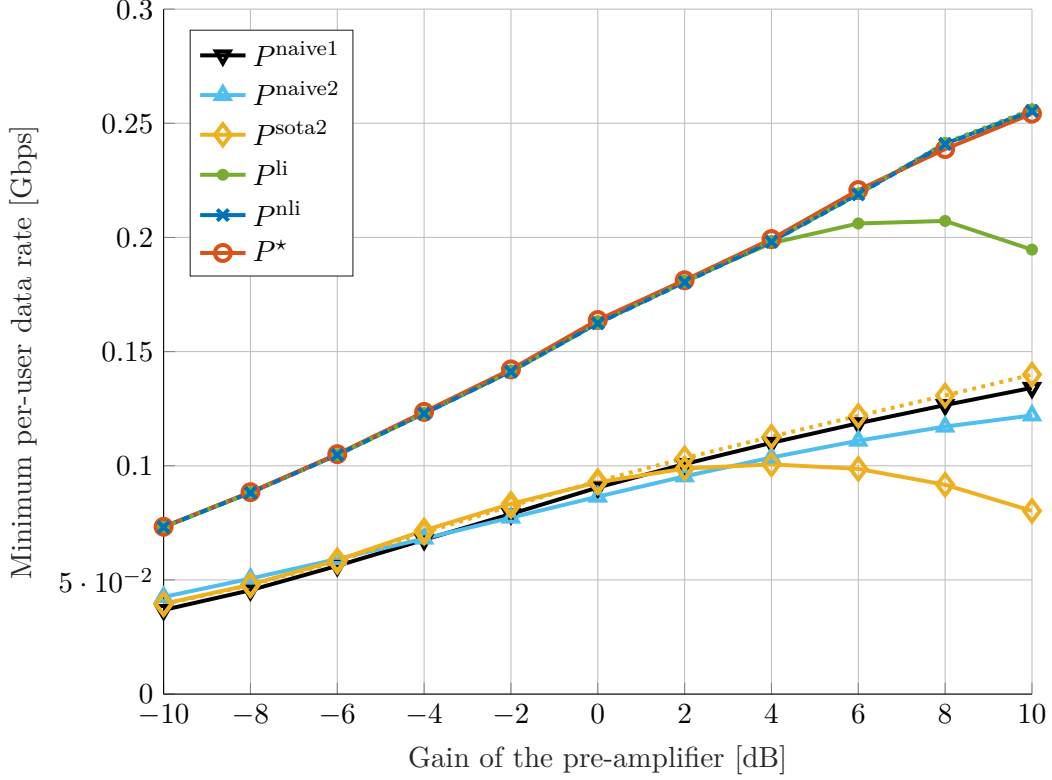


Figure 6.3: Minimum per-user data rate vs. pre-amplifier gain G_{amp} for 1 FS per 100 km².

In solid line, the data rate is evaluated with (4.3) for nonlinearity-aware receiver. In addition, we display in dotted line the data rate for the linear inter-beam interference case, i.e., when we enforce no nonlinear interference in the expression of the data rate (4.3) and finally obtain the data rate (3.1). We also display in dashed line the data rate for nonlinearity-agnostic receiver, i.e., the data rate is evaluated with (4.5) when the receiver is not able to exploit the correlation between the linear and the nonlinear part.

In Fig. 6.4, we plot the sum-power versus the target data rate obtained for the five above mentioned power allocations. We fix the same target data rate for all users, and we inspect two values for the pre-amplifier gain, denoted by G_{amp} . We set the FS density to 0.1 per km². We observe nonlinear effects only for a high target data rate, which is coherent because the minimization of the powers allows to stay in the linear zone of the HPA. We can conclude that the consideration of nonlinear effect for the minimization of the power sum is not necessary.

6.6 Conclusion

In this chapter, we have addressed optimization problems in the context of a multibeam satellite with a nonlinear HPA for nonlinearity-aware receiver. More precisely, we formalized three optimization problems. The first one maximizes the system sum-rate by taking into account the nonlinear effects. The obtained problem boiled down to SP and we have rewritten it in CGP form, then we have proposed a SCA procedure with monomial approximation. The second problem maximizes the minimum per-user data rate. After introducing an additional variable,

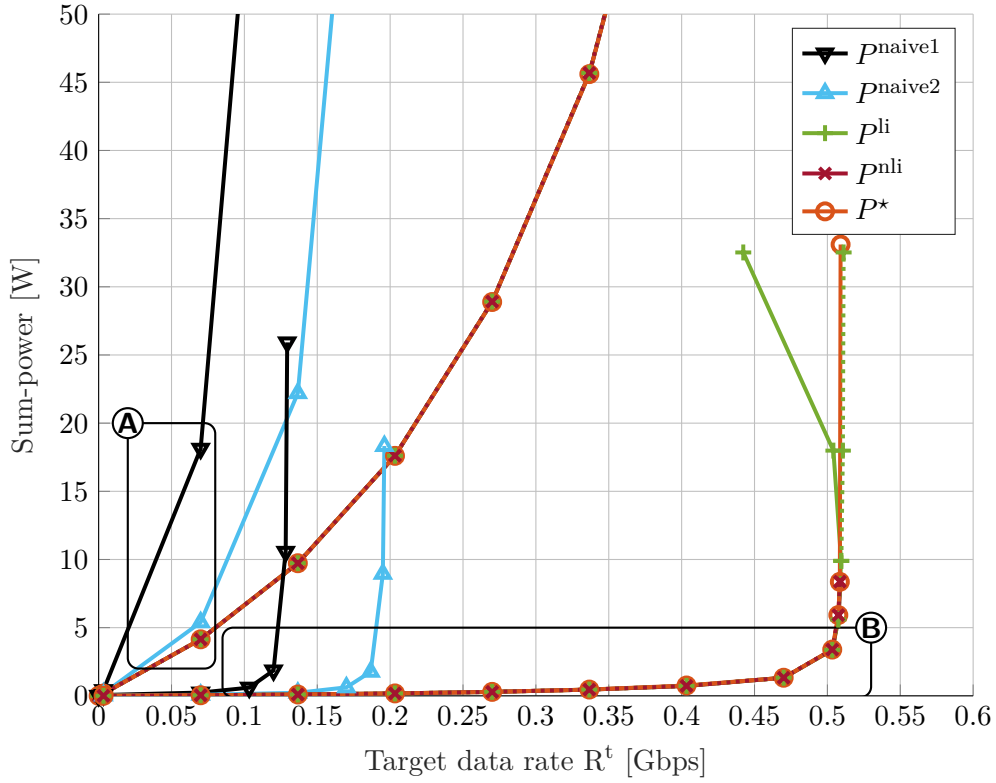


Figure 6.4: Sum-power vs. target data rate $R_{b,m}^t = R^t$ with $G_{amp} \in \{-10, 10\}$ dB (respectively A and B), and 0.1 FS per 100 km².

we obtain a [SP](#) that we have rewritten as a [CGP](#), then we have proposed a [SCA](#) procedure with monomial approximation. The last problem minimizes the sum-power of the system, subject to a target data-rate. The rewriting of the constraints allowed to obtain a [CGP](#), which is solved using [SCA](#) procedure with monomial approximation. A summary of the addressed problems along with the proposed solutions is presented in Table 6.1.

Issue	Problem	Solution
Sum-rate	Problem 6.1	SCA – Algorithm 6.1
Fairness	Problem 6.6	SCA – Algorithm 6.2
Sum-power	Problem 6.11	SCA – Algorithm 6.3

Table 6.1: Addressed problems and proposed solutions.

Conclusions and perspectives

The main objective of the thesis was to perform resource allocation to maximize the system sum-rate, while satisfying the interference temperature limits regarding the primary systems, by taking into account nonlinear impairments due to satellite components modeled by Volterra series.

In Chapter 1, we presented the satellite communication system. We derived the signal model in presence of nonlinear effects resulting from *High-Power Amplifier* (HPA) modeled as a memoryless polynomial, leading to Volterra series. The paradigm of underlay cognitive radio, with the presence of primary network, was taken into account by relevant interference-temperature constraints that the cognitive satellite network has to not exceed. Then the general optimization problem of sum-rate maximization has been stated.

In Chapter 2, we introduced the concept of convex optimization and provided conventional procedure to solve non-convex problems. We then presented non-convex problems with a particular form, namely *Difference of Concave* (DC), *Logarithm of Difference of Concave* (LDC), *Geometric Programming* (GP), *Complementary Geometric Programming* (CGP) and *Signomial Programming* (SP), allowing to easily apply the *Successive Convex Approximation* (SCA) procedure. We encountered these types of problems in the following chapters dealing with resource allocation.

In Chapter 3, we stated the sum-rate optimization problem in the case of a linear HPA and proposed relevant resource allocations. Even under this assumption, we encountered non-convex problems, for which we proposed algorithms for finding solutions. Noting that sum-rate maximization was not fair among users, we then formulated and solved problems dealing with fairness between users.

In Chapter 4, we given two closed-form expressions of the data rate in the presence of nonlinear effects, related to two different receivers. The first one, called *nonlinearity-aware receiver*, exploiting the nonlinear effects as additional information. The other one, called *nonlinearity-agnostic receiver*, considering the nonlinearities as additional noise. We finally emphasized the mathematical properties of data rate expressions and involved terms.

In Chapter 5, we stated the sum-rate optimization problem in the presence of nonlinear effects and using the nonlinearity-agnostic receiver. Based on the corresponding data rate expression, the resulting problem boiled down to CGP and we proposed an algorithm to find the relevant power allocation. In addition, we also stated and solved related problems, namely the maximization of

the minimum per-user data rate and the minimization of the sum-power subject to a target data rate. These two problems boiled down to [GP](#). Finally, we illustrated that the power allocations obtained under the assumption of a linear [HPA](#) do not perform well in the presence of nonlinear interference. The consideration of this interference in the optimization problem is fundamental.

In Chapter 6, we stated the sum-rate the optimization problem in the presence of nonlinear effects and using the nonlinearity-aware receiver. From the expression of the data rate evaluated with this receiver, the resulting problem boiled down to [SP](#) and we proposed an algorithm to find the relevant power allocation. In addition, we also stated and solved related problems, namely the maximization of the minimum per-user data rate and the minimization of the sum-power subject to a target data rate. These two problems also boiled down to [SP](#). Finally, we illustrated that the power allocations obtained under the assumption of a linear [HPA](#) do not perform well for the nonlinearity-aware receiver. The consideration of the signomial expression of the data rate in the optimization problem is essential.

Perspectives

The following concerns should be addressed in future works.

High-power amplifier model

- In Chapter 1, the Volterra series is truncated to the third order. It would be interesting to consider larger orders to see the impact on the terms involved in data rate expression.
- We used a memoryless polynomial model to characterize the input-output of the [HPA](#), leading to Volterra series. However, [HPAs](#) have a memory effect. The use of [HPA](#) model with memory [48] would be interesting to investigate.

Data rate expression in presence of nonlinearities

- In Chapter 4, we assume that the transmitted symbol sequence is complex-valued circularly-symmetric Gaussian random process. This assumption simplifies the decomposition of the fourth- and sixth-order moment. However, in the case of constellation currently used for satellite communications (e.g. APSK), the cumulant must be added in the moment decomposition. It would be interesting to observe the impact of this cumulant on the terms involved in the data rate expression.
- We assumed in Chapter 4 that the receiver decodes sample per sample, so the time and frequency correlations between the linear part and the nonlinear part are neglected. Actually, joint decoding by taking into account the whole process could improve the performance for each symbol detection.

Resource allocation

- In this thesis, we focused on power allocation. An extension has been proposed with the joint optimization of subband assignment and power allocation, under the assumption of a

linear [HPA](#). It would be interesting to extend it to the nonlinear case, which would lead to *Mixed-Integer Signomial Programming* [\[49\]](#).

- In [\[50\]](#), the authors perform resource allocation when the satellites belong to different operators under the assumption of a linear [HPA](#), leading to distributed optimization. It would be interesting to adapt their method in the presence of nonlinear effects.

Bibliography

- [1] R. Blasco-Serrano, J. Lv, R. Thobaben, E. Jorswieck, A. Kliks, and M. Skoglund, "Comparison of underlay and overlay spectrum sharing strategies in miso cognitive channels," in *2012 7th International ICST Conference on Cognitive Radio Oriented Wireless Networks and Communications (CROWNCOM)*, 2012, pp. 224–229.
- [2] S. Maleki, S. Chatzinotas, B. Evans, K. Liolis, J. Grotz, A. Vanelli-Coralli, and N. Chuberre, "Cognitive spectrum utilization in Ka band multibeam satellite communications," *IEEE Communications Magazine*, vol. 53, no. 3, pp. 24–29, 2015.
- [3] E. Lagunas, S. Maleki, S. Chatzinotas, S. K. Sharma, and B. Ottersten, "Resource Allocation for Cognitive Satellite Communications With Incumbent Terrestrial Networks," *IEEE Transactions on Cognitive Communications and Networking*, vol. 1, no. 3, pp. 305–317, 2015.
- [4] D. Tarchi, A. Guidotti, V. Icolari, A. Vanelli-Coralli, S. K. Sharma, S. Chatzinotas, S. Malekil, B. Evans, P. Thompson, W. Tang, and J. Grotz, "Technical challenges for cognitive radio application in satellite communications," in *2014 9th International Conference on Cognitive Radio Oriented Wireless Networks and Communications (CROWNCOM)*, 2014, pp. 136–142.
- [5] K. Liolis, G. Schlueter, J. Krause, F. Zimmer, L. Combelles, J. Grotz, S. Chatzinotas, B. Evans, A. Guidotti, D. Tarchi, and A. Vanelli-Coralli, "Cognitive radio scenarios for satellite communications: The corasat approach," in *2013 Future Network Mobile Summit*, 2013, pp. 1–10.
- [6] S. K. Sharma, E. Lagunas, S. Maleki, S. Chatzinotas, J. Grotz, J. Krause, and B. Ottersten, "Resource allocation for cognitive satellite communications in ka-band (17.7–19.7 ghz)," in *2015 IEEE International Conference on Communication Workshop (ICCW)*, 2015, pp. 1646–1651.
- [7] S. K. Sharma, S. Maleki, S. Chatzinotas, J. Grotz, J. Krause, and B. Ottersten, "Joint carrier allocation and beamforming for cognitive satcoms in ka-band (17.3–18.1 ghz)," in *2015 IEEE International Conference on Communications (ICC)*, 2015, pp. 873–878.
- [8] E. Lagunas, S. Maleki, S. Chatzinotas, M. Soltanalian, A. I. Pérez-Neira, and B. Ottersten, "Power and rate allocation in cognitive satellite uplink networks," *IEEE International Conference on Communications*, 2016.

- [9] B. Evans, P. Thompson, E. Lagunas, S. K. Sharma, D. Tarchi, and V. Icolari, "Extending the usable Ka band spectrum for satellite communications: The CoRaSat project," in *Wireless and Satellite Systems (WiSATS)*, Bradford, UK, 2015, pp. 119–132.
- [10] B. F. Beidas, "Intermodulation distortion in multicarrier satellite systems: Analysis and turbo volterra equalization," *IEEE Transactions on Communications*, vol. 59, no. 6, pp. 1580–1590, 2011.
- [11] S. Benedetto, E. Biglieri, and R. Daffara, "Modeling and performance evaluation of nonlinear satellite links-a volterra series approach," *IEEE Transactions on Aerospace and Electronic Systems*, vol. AES-15, no. 4, pp. 494–507, 1979.
- [12] K. An, T. Liang, G. Zheng, X. Yan, Y. Li, and S. Chatzinotas, "Performance limits of cognitive-uplink fss and terrestrial fs for ka-band," *IEEE Transactions on Aerospace and Electronic Systems*, vol. 55, no. 5, pp. 2604–2611, 2019.
- [13] Z. Chen, D. Guo, K. An, B. Zhang, X. Zhang, and B. Zhao, "Efficient and fair resource allocation scheme for cognitive satellite-terrestrial networks," *IEEE Access*, vol. 7, pp. 145 124–145 133, 2019.
- [14] G. Maral, M. Bousquet, and Z. Sun, *Satellite Communications Systems: Systems, Techniques and Technology*, ser. Wiley Series in Communication and Distributed Systems. Wiley, 2011.
- [15] C. Caini, G. E. Corazza, G. Falciasecca, M. Ruggieri, and F. Vatalaro, "A spectrum- and power-efficient EHF mobile satellite system to be integrated with terrestrial cellular systems," *IEEE Journal on Selected Areas in Communications*, vol. 10, no. 8, pp. 1315–1325, Oct 1992.
- [16] M. Chiang, C. W. Tan, D. P. Palomar, D. O'neill, and D. Julian, "Power control by geometric programming," *IEEE Transactions on Wireless Communications*, vol. 6, no. 7, pp. 2640–2651, Jul. 2007.
- [17] M. Chiang, "Geometric programming for communication systems," *Foundations and Trends in Communications and Information Theory*, vol. 2, January 2005.
- [18] M. Avriel and A. C. Williams, "Complementary geometric programming," *SIAM J. Appl. Math.*, vol. 19, no. 1, pp. 125–141, 1970.
- [19] S. Boyd and L. Vandenberghe, *Convex Optimization*. Cambridge University Press, 2004.
- [20] S. Boyd, S.-J. Kim, L. Vandenberghe, and A. Hassibi, "A tutorial on geometric programming," *Optimization and Engineering*, vol. 8, pp. 67–127, May 2007.
- [21] Y. Nesterov and A. Nemirovski, *Interior-Point Polynomial Algorithms in Convex Programming*. Society for Industrial and Applied Mathematics, 1994.
- [22] B. R. Marks and G. P. Wright, "A general inner approximation algorithm for nonconvex mathematical programs," *Operations Research*, vol. 26, no. 4, pp. 681–683, 1978.

- [23] J. C. Bezdek and R. J. Hathaway, "Some notes on alternating optimization," in *Proceedings of the 2002 AFSS International Conference on Fuzzy Systems. Calcutta: Advances in Soft Computing*, ser. AFSS '02. Berlin, Heidelberg: Springer-Verlag, 2002, p. 288–300.
- [24] D. P. Palomar, "Convex primal decomposition for multicarrier linear MIMO transceivers," *IEEE Transactions on Signal Processing*, vol. 53, no. 12, pp. 4661–4674, Dec. 2005.
- [25] A. Abdelnasser and E. Hossain, "Resource allocation for an OFDMA cloud-RAN of small cells underlying a macrocell," *IEEE Transactions on Mobile Computing*, vol. 15, no. 11, pp. 2837–2850, Nov. 2016.
- [26] K. Shen and W. Yu, "A coordinated uplink scheduling and power control algorithm for multicell networks," *Asilomar Conference on Signals, Systems and Computers*, pp. 1305–1309, 2015.
- [27] J. S. Pang, G. Scutari, D. P. Palomar, and F. Facchinei, "Design of cognitive radio systems under temperature-interference constraints: A variational inequality approach," *IEEE Transactions on Signal Processing*, vol. 58, no. 6, pp. 3251 – 3271, Jul. 2010.
- [28] J. Huang, V. Subramanian, R. Agrawal, and R. Berry, "Joint scheduling and resource allocation in uplink OFDM systems for broadband wireless access networks," *IEEE Journal on Selected Areas in Communications*, vol. 27, no. 2, pp. 226–234, Nov. 2009.
- [29] R. Masmoudi, E. V. Belmega, and I. Fijalkow, "Efficient spectrum scheduling and power management for opportunistic users," *EURASIP Journal on Wireless Communications and Networking*, vol. 2016, no. 1, Apr. 2016.
- [30] L. Zhang, Y. C. Liang, and Y. Xin, "Joint beamforming and power allocation for multiple access channels in cognitive radio networks," *IEEE Journal on Selected Areas in Communications*, vol. 26, no. 1, pp. 38–51, Jan. 2008.
- [31] O. Ozel, K. Tutuncuoglu, J. Yang, S. Ulukus, and A. Yener, "Transmission with energy harvesting nodes in fading wireless channels: Optimal policies," *IEEE Journal on Selected Areas in Communications*, vol. 29, no. 8, pp. 1732–1743, Sep. 2011.
- [32] S. Gault, W. Hachem, and P. Ciblat, "Performance analysis of an OFDMA transmission system in a multicell environment," *IEEE Transactions on Communications*, vol. 55, no. 4, pp. 740–751, Apr. 2007.
- [33] M. Grant and S. Boyd, "CVX: Matlab software for disciplined convex programming, version 2.2," <http://cvxr.com/cvx>, Mar. 2014.
- [34] A. Ben-Tal and A. Nemirovski, "Lectures On Modern Convex Optimization," 2000.
- [35] T. Lan, D. Kao, M. Chiang, and A. Sabharwal, "An axiomatic theory of fairness in network resource allocation," in *2010 Proceedings IEEE INFOCOM*, 2010, pp. 1–9.
- [36] F. Kelly, "Charging and rate control for elastic traffic," *European Transactions on Telecommunications*, vol. 8, 02 1997.

- [37] R. Jain, D. M. Chiu, and H. W. R., “A quantitative measure of fairness and discrimination for resource allocation in shared computer systems,” *CoRR*, vol. cs.NI/9809099, 01 1998.
- [38] T. Deleu, M. Dervin, and F. Horlin, “Low complexity block pre-distortion of a multi-carrier non-linear satellite channel,” in *2014 IEEE International Conference on Communications (ICC)*, 2014, pp. 4325–4330.
- [39] N. J. Beaudry and R. Renner, “An intuitive proof of the data processing inequality,” *Quantum Inf. Comput.*, vol. 12, pp. 432–441, 2012.
- [40] R. A. Ince, B. L. Giordano, C. Kayser, G. A. Rousselet, J. Gross, and P. G. Schyns, “A statistical framework for neuroimaging data analysis based on mutual information estimated via a gaussian copula,” *Human Brain Mapping*, vol. 38, no. 3, pp. 1541–1573, 2017.
- [41] O. T. Demir and E. Bjornson, “The bussgang decomposition of nonlinear systems: Basic theory and mimo extensions [lecture notes],” *IEEE Signal Processing Magazine*, vol. 38, no. 1, pp. 131–136, 2021.
- [42] P. Delesques, “Analyses of transmission and switching capacities in optical networks,” Ph.D. dissertation, Telecom Paris, December 2012.
- [43] I. Reed, “On a moment theorem for complex gaussian processes,” *IRE Transactions on Information Theory*, vol. 8, no. 3, pp. 194–195, 1962.
- [44] S. Stanczak, M. Wiczanowski, and H. Boche, *Fundamentals of Resource Allocation in Wireless Networks: Theory and Algorithms*. Springer Berlin Heidelberg, 2008.
- [45] D. Tse and P. Viswanath, *Fundamentals of Wireless Communication*. USA: Cambridge University Press, 2005.
- [46] P. Mary, I. Fijalkow, and C. Poulliat, “Multi-rate resource allocations for th-uwb wireless communications,” *IEEE Transactions on Wireless Communications*, vol. 11, no. 12, pp. 4470–4481, 2012.
- [47] C. Weeraddana, M. Codreanu, and M. Latva-aho, “Cross-layer resource allocation for wireless networks via signomial programming,” in *GLOBECOM 2009 - 2009 IEEE Global Telecommunications Conference*, 2009, pp. 1–6.
- [48] D. Morgan, Z. Ma, J. Kim, M. Zierdt, and J. Pastalan, “A generalized memory polynomial model for digital predistortion of rf power amplifiers,” *IEEE Transactions on Signal Processing*, vol. 54, no. 10, pp. 3852–3860, 2006.
- [49] A. Lundell and T. Westerlund, *Global Optimization of Mixed-Integer Signomial Programming Problems*. Springer, 11 2012, pp. 349–369.
- [50] E. Tohidi, D. Gesbert, and P. Ciblat, “Distributed resource allocation algorithms for multi-operator cognitive communication systems,” in *2020 28th European Signal Processing Conference (EUSIPCO)*, 2021, pp. 1737–1741.

Titre : Allocation de ressources adaptées aux défauts de nonlinéarité des systèmes cognitifs par satellite

Mots clés : allocation de ressources, optimisation non convexe, système non linéaire, séries de Volterra

Résumé : Cette thèse traite le problème de l'allocation de ressources pour les communications cognitives par satellite. Dans un contexte de demandes grandissantes en terme de débit, les systèmes de communication par satellite sont amenés à utiliser des fréquences déjà employées par des systèmes terrestres. Le paradigme de la radio cognitive de type sous couche permet à un réseau secondaire d'utiliser la même bande de fréquence qu'un réseau primaire. Cependant, l'interférence créée par le réseau secondaire ne doit pas excéder une certaine limite, fixée par le réseau primaire. Nous considérons un système de communication cognitif par satellite, où des utilisateurs terrestres transmettent des informations à un satellite, ce dernier les renvoyant à une passerelle terrestre à la manière d'un relais. De cette façon, les utilisateurs terrestres du réseau secondaire satellitaire génèrent des interférences sur le réseau primaire, qui sont dues aux lobes secon-

dares des antennes d'émission. La gestion de la puissance de transmission des utilisateurs satellitaires secondaires devient primordiale pour limiter les interférences sur le réseau primaire terrestre et, en même temps, atteindre le débit maximal du système. De plus, la prise en compte des non-linéarités provenant du satellite, notamment l'amplificateur de haute puissance, devient cruciale lorsque celui-ci est utilisé au maximum de ses capacités. Car les effets non linéaires produits par l'amplificateur, modélisé par des séries de Volterra, dégradent les débits du système. Dans ce contexte, la thèse consiste à proposer des algorithmes d'allocation de ressources afin d'optimiser la somme des débits du système satellitaire, tout en respectant les limites d'interférence fixées par le réseau terrestre primaire, avec la prise en compte des effets non linéaires générées par les composants du satellite.

Title : Nonlinear impairments aware resource allocation for cognitive satellite systems

Keywords : resource allocation, nonconvex optimization, nonlinear system, Volterra series

Abstract : This thesis addresses the problem of resource allocation for cognitive satellite communications. In a context of increasing throughput demands, satellite communication systems are required to use frequencies already used by terrestrial systems. The underlay cognitive radio paradigm allows a secondary network to use the same frequency band that a primary network uses. However, the interference created by the secondary network must not exceed a certain limit, which is set by the primary network. We consider a cognitive satellite communication system, where terrestrial users transmit information to a satellite, and that satellite sends it back to a terrestrial gateway in a relay-like fashion. In this way, the terrestrial users of the satellite secondary network generate interference on the primary network, which is due to the secondary lobes

of the transmitting antennas. The management of the transmission power of the secondary satellite users becomes essential to limit the interference on the primary terrestrial network and, at the same time, to reach the maximum throughput of the system. Moreover, taking into account the nonlinearities coming from the satellite, especially the high-power amplifier, becomes crucial when the satellite is used at its maximum capabilities. This is because the non-linear effects produced by the amplifier, modeled by Volterra series, degrade the system throughput. In this context, the thesis consists in proposing resource allocation algorithms in order to optimize the sum-rate of the satellite system, while respecting the interference limits set by the primary terrestrial network, taking into account the nonlinear effects generated by the satellite components.